IDENTIFICATION OF *RALSTONIA SOLANACEARUM* EXOPROTEINS SECRETED BY THE TYPE TWO SECRETION SYSTEM USING PROTEOMIC TECHNIQUES

by

MARIA CAROLINA ZULETA

(Under the Direction of Timothy P. Denny)

ABSTRACT

Ralstonia solanacearum, the causal agent of bacterial wilt, has a functional type II secretion system (T2SS), which uses a pore formed by SdpD1 to secret cell wall degrading enzymes and other proteins. Deletion of *sdpD*1 in *R. solanacearum* GMI1000 produced a mutant reduced in virulence, colonization and secretion of many proteins. However, some proteins are still secreted by the *sdpD*1 mutant. GMI1000 is predicted to have three incomplete T2SS that include SdpD-related proteins that could be partially functional. To identify proteins secreted via the principle T2SS and alternative T2SS, all *sdpD* genes were deleted using unmarked mutagenesis. Proteomic techniques such as two-dimensional gel electrophoresis and peptide labeling with isobaric tags followed by mass spectrometry allowed the identification of proteins secreted through the principle T2SS. Although candidates for the alternative T2SS were not identified, functionality of the SdpD-related proteins was not ruled out.

INDEX WORDS: *Ralstonia solanacearum*, type II secretion system, mass spectrometry, 2-D gel electrophoresis, iTRAQ

IDENTIFICATION OF *RALSTONIA SOLANACEARUM* EXOPROTEINS SECRETED BY THE TYPE TWO SECRETION SYSTEM USING PROTEOMIC TECHNIQUES

by

MARIA CAROLINA ZULETA

B.S., Universidad del Tolima, Ibagué, Colombia, 2001

A Thesis Submitted to the Graduate Faculty of The University of Georgia in Partial Fulfillment of the Requirements for the Degree

MASTER OF SCIENCE

ATHENS, GEORGIA

2007

IDENTIFICATION OF *RALSTONIA SOLANACEARUM* EXOPROTEINS SECRETED BY THE TYPE TWO SECRETION SYSTEM USING PROTEOMIC TECHNIQUES

by

MARIA CAROLINA ZULETA

Major Professor: Timothy P. Denny

Committee: Mark A. Schell
Ronald Walcott

Electronic Version Approved:

Maureen Grasso
Dean of the Graduate School
The University of Georgia
May 2007

DEDICATION

To my husband Ivan, my parents and siblings

ACKNOWLEDGEMENTS

First, I would like to thank my advisor, Dr. Timothy Denny for his support and great encouragement to research. Special thanks to Dr. Huanli Liu for offering his experience and expert advice. My appreciation also goes to Marla Popov and, Jeremy Wolff who helped me in different steps of my project. Finally, thanks to my fellow students fot the support received during these years at the Plant Pathology Department.

TABLE OF CONTENTS

Page

LIST OF TABLES

Page

CHAPTER 3

LIST OF FIGURES

Page

CHAPTER 1

INTRODUCTION AND LITERATURE REVIEW

Introduction

Ralstonia solanacearum is a Gram-negative, aerobic rod in the β-subdivision of Proteobacteria (Stackebrandt et al. 1988) and has been the subject of numerous studies on host-pathogen interactions. The pathogen initiates root infection through wounds caused by machinery or soil inhabitants such as nematodes and insects. Invasion is also possible through the colonization of unwounded roots starting at exudation sites in the extremities and axils of secondary roots. Infection of the inner cortex and the vascular parenchyma ensues, and bacteria soon invade the protoxylem vessels by degrading cell walls. Bacteria then move throughout the xylem and accumulate to high cell densities. This condition stimulates the production of a high molecular weight exopolysaccharide that mechanically plugs the vessels, producing wilt symptoms in susceptible plants (Vasse et al. 1995).

The type II secretion system (T2SS) is an important mechanism for the transport of virulence-associated proteins including endopectate lyases, pectin acetylesterases, pectin methylesterase and polygalacturonase in *Erwinia chrysanthemi* (Kazemi-Pour et al. 2004), pectate lyase, polygalacturonase and cellulase in *E carotovora* subspecies (Barras et al. 1994), and xylanase and cellulases in *Xanthomonas oryzae* pv. oryzae (Sun et al. 2005). It is known that some Gram$^-$negative pathogenic bacteria can have more than one T2SS (Preston et al. 2005) and that some of these systems are functional. In *P. aeruginosa* PAK the alternative T2SS secretes small amounts of lipase, alkaline phosphatase and elastase (Martinez et al. 1998), In *P. putida* strain GB-1 the principle and alternative T2SS transport Mn^{2+}-oxidizing factor (de Vrind et al. 2003). In *Xanthomonas campestris* pv. campestris, *X. axonopodis* pv. citri and *X. campestris* pv. vesicatoria the presence of a second complete set of T2SS orthologs suggests that these systems might be functional.

Liu et al. (2005) showed that exoproteins secreted by the *R. solanacearum* T2SS contribute to disease. These exoproteins include cell wall degrading enzymes (CWDE's) most of which had previously been identified as virulence factors. However, results indicated that additional unidentified proteins are important for virulence (Liu et al. 2005). Genomic DNA sequence analysis revealed that, in addition to the typical T2SS, strain GMI1000 has three incomplete T2SS-related clusters with *sdpD-G* homologues (Genin and Boucher 2004). One of these clusters is located in the chromosome and the other two clusters are located on the megaplasmid.

In *R. solanacearum*, the confinement sensing system establishes a regulatory network for positively or negatively control the expression many genes, including those for virulence and plant colonization factors. At the heart of this system is PhcA, a LysR-type transcriptional regulator. This system allows *R. solanacearum* to switch from one phenotypical state to another in response to nutrient availability and cell density (Denny 2006), allowing the pathogen to adapt itself for survival in the soil as a saprophyte or to maximize its ability to colonize plant tissues that normally resist bacterial infection.

In this study, I used proteomic techniques to identify proteins that probably exit cells via T2SS and other extracellular proteins that may be associated with the colonization process. The first part of the project, involved the creation of mutants lacking from one to four SdpD proteins, protein identification using 2-dimensional gel electrophoresis and iTRAQ labeling followed by mass spectrometry techniques such as fourier transform ion cyclotron resonance mass spectrometry (FTICR-MS) and liquid chromatography tandem mass spectrometry (LC-MS/MS). The second part of the project, focused in the identification of exoproteins associated with colonization using iTRAQ labeling combined with LC-MS/MS. To accomplish this objective I

compared the GMI1000 wild type with colonization deficient mutants' a mutant lacking the global regulator *phcA* and the two-component system *vsrD* wich are part of the phenotype conversion system in *R. solanacearum* regulating numerous traits associated with colonization and thus virulence.

Literature review

Bacterial wilt caused by *Ralstonia solanacearum*, is responsible for incalculable yield losses every year, affecting principally banana, groundnut, potato, tomato, tobacco and ginger crops in tropical and subtropical regions worldwide (Hayward 1994). The pathogen is a Gram-negative, aerobic rod in the β-subdivision of Proteobacteria (Stackebrandt et al. 1988) and has been the subject of numerous studies on host-pathogen interactions in the infection process. Recent work revealed the genomic organization of *R. solanacearum* GMI1000, indicating the existence of two replicons: a chromosome of 3.7 Mb and a megaplasmid of 2.1 Mb, which constitute a bipartite genome (Salanoubat et al. 2002). These replicons have a very similar %GC base content, which can be explained by their long coevolution. However, their local variations indicate different functions for each replicon, making it evident that both are important for efficient bacterial growth and survival (Genin and Boucher 2004). Analysis of the megaplasmid suggests that it is involved in environmental adaptation processes, as it carries all of the *hrp* genes required for the type III secretion system (T3SS). It also encodes the components of the flagellum and the genes responsible for exopolysacharide production (Salanoubat et al. 2002). Identification of more than fifteen genes related to pathogenicity, and the pathogen's currently available genomic sequence, increase the possibilities for deep exploration of gene functions constituting the pathogenic pathways.

Virulence Factors: *R. solanacearum* needs a series of virulence factors that allow plant colonization and symptom development. These factors include extracellular polysaccharide (EPS), lipopolysaccharide (LPS), plant cell wall degrading enzymes (CWDE) secreted by the T2SS, and the Hrp-encoded T3SS and secreted effectors.

Exopolysacharide (EPS): EPS is a long polymer with an acidic trimeric repeat unit of N-acetyl galactosamine, 2-N-acetyl-2-deoxy-L-galacturonic acid, and 2-N-acetyl-4-N-(3-hydroxy butanoyl)-2-4-6-trideoxy-D-glucose (Schell 2000). The proteins comprising the EPS biosynthetic pathway are encoded by the 16-kb *eps* operon containing more than 12 genes (Schell 2000). EPS causes wilt by vascular occlusion or rupture of vessel elements due to excess of hydrostatic pressure. EPS also promotes rapid systemic colonization of tomato plants because mutants lacking EPS rarely wilt or kill plants, mostly colonizing the roots and lower stem of susceptible plants even when introduced directly into stem wounds (Saile et al. 1997).

Lipopolysaccharide (LPS): LPS is a main component of the outer leaflet of the outer membrane in Gram-negative bacteria. It is composed of lipid A, a non-repeating core polysaccharide and a distal oligosaccharide, the O-antigen. In *R. solanacearum*, the O-antigen is the most variable moiety of the LPS molecule, containing different proportions of rhamnose, glucose, xylose and acetylglucosamine (Varbanets et al. 2003). Synthesis of the O-antigen side chain is blocked by inactivating the gene in GMI1000 that appears to encode the lipid A core:O-antigen ligase, an enzyme that couples the O-antigen oligosaccharide subunits to the core polysaccharide. The resulting mutant exhibits normal EPS production, but lacks the O-antigen and is less virulent than its wild-type parent (Denny 2006).

Plant Cell Wall-Degrading Enzymes: Some exoproteins move through the outer membrane by the T2SS, an extension of the general secretion pathway (Gsp) (Voulhoux et al.

2001). Secreted proteins move from the cytosol to the extracellular medium in a two-step process. *R. solanacearum* CWDEs known to transit the T2S system include a β-1-4-endoglucanase (Egl), an exoglucanase (CbhA), an endopolygalacturonase (PehA or PglA), two exopolygalacturonases (PehB and PehC), and a pectin methylesterease (Pme). Experimentation with mutants lacking one to three enzymes indicated that, although not essential for virulence, they contribute more or less to virulence depending on the pathogen strain. In K60 PehA and PehB contribute to pathogen colonization and wilt severity, and the K60 double mutant PehA-PehB is less virulent that either single mutants. Unexpectedly a triple mutant also lacking PehC is more virulent than the double mutant, possibly due to the absence of pectic breakdown products that stimulate plant defenses (Tans-Kersten et al. 1998).

In contrast to K60, Liu et al. (2005) reported that GMI1000 mutants lacking one pectic enzyme (PehA, PehB or PehC) are slightly less virulent than GMI1000, but mutants lacking two (PehA and PehB) or three pectic enzymes (PehA, PehB or PehC) are at least as virulent as wild-type GMI1000. Deletion of one or two cellulolytic enzymes (Egl and CbhA) produced mutants significantly less virulent than GMI1000 and in combination this effect increased. Plants inoculated with the mutant lacking all six enzymes (PehA, PehB, PehC, Egl, CbhA and Pme) showed delayed symptom development, but was more virulent than the Egl/CbhA double mutant. Although significantly less virulent than GMI1000, the 6-fold mutant still wilted more than 80% of the inoculated plants.

Type II Secretion System

This system, which is highly conserved in Gram-negative bacteria, is one of the ways bacteria export proteins to the extracellular space. Proteins secreted by this system are translocated across the cytoplasmatic membrane using either the Sec-dependent pathway or the twin-arginine (tat)

pathway. Then, they move from the periplasm across the outer membrane into the extracellular medium through a pore formed by the T2SS secretin (Jha et al. 2005).

The Sec protein-translocation pathway is responsible for the translocation of unfolded, recently-formed proteins from the cytoplasm to the periplasm (Mori and Ito 2001). The mechanism is composed of SecB, a chaperone related to protein export, SecA, an ATPase that drives protein movement across the membrane, the integral membrane proteins SecY, SecE, SecG, SecD, SecF, YajC, and SecYEG, a heterotrimeric complex that forms a channel for protein transport across the inner membrane. This complex requires the presence of SecA and ATP to form the translocase. SecD and SecF function as protein export enhancers. After signal sequence recognition by SecB, the protein is directed to the Sec-mechanism channel, where it is attracted to SecA and then to the membrane. After energy is provided by ATP, hydrolysis and/or proton motive force, translocation is completed by separation of the signal peptide by a signal peptidase, releasing the protein into the periplasmic space (Mori and Ito 2001).

Studies in *Escherichia coli* showed that the Tat pathway is encoded by an operon containing three Tat genes *(tatABC*) and the *tatE* gene that seems to encode a *tatA* paralog of minor importance. Inactivating any of these *tatABC* results in the inability to export certain proteins from the cytoplasm to the periplasm (Oates et al. 2003). Tat substrates are folded proteins up to 70 Å in diameter, so a channel is required to move them across the membrane. It is assumed that this protein-conducting channel is formed primarily by TatA because it acts once signal-peptide recognition by TatBC has occurred (Berks et al. 2005).

The T2SS requires 12 to 16 genes encoding proteins named Sdp for secreton-dependent pathway, a current term to describe the components of this system (Desvaux et al. 2004), using *Pseudomonas aeruginosa* as the model to identify the functions of each protein encoded by the

T2SS (Table 1.1 and Fig. 1.1) (Filloux et al. 1997). The SdpE, F, L and M proteins form the inner membrane platform. Five Sdp proteins (SdpG-K) have an N-terminus similar to type IV pilins, so they are sometimes called pseudopilins. The SdpO protein, which is not present in all bacteria, is a specialized prepilin peptidase. The SdpC protein is proposed to, connect the two sub-secreton complexes, the inner membrane (IM) platform and the outer membrane (OM) complex. The SdpN protein is a bitopic IM protein that seems to interact with the secretin pore (see below) and with the SdpL-M complex. SdpA and SdpB form a complex within the cytoplasmic membrane, probably for energy transduction, stabilization or increased expression of the Sdp complex and piloting the secretin protein to the OM (Filloux et al. 1997).

Mature folded proteins are secreted from the periplasm to the extracellular space through a pore formed by the integral OM SdpD secretin protein (Fig. 1.1). Electron microscopy of *Pseudomonas aeruginosa* XcpQ (an SdpD homolog), confirmed that this member of the secretin family can adopt a ring structure with a cavity of 95 Å (Filloux 2004). Mutation of the *sdpD* gene causes exoprotein accumulation in the periplasm. The conserved C-terminal part of SdpD is predicted to be embedded in the membrane, whereas a more variable N-terminus extends into the periplasm with a recognized roles in substrate identification, interaction with cytoplasmic components, protein multimerization and possibly as a receptacle in the formed pore (Kostakioti et al. 2005).

Type II secretion system-related gene clusters

Pseudomonas aeruginosa: The typical T2SS in *Pseudomonas aeruginosa* is encoded by the *xpc* genes (extracellular protein-deficient) (Wretlind and Pavlovskis 1984). In *P. aeruginosa* PAO1 there also is a cluster of *hxc* genes homologous to all *xcp* genes (Table 1.2) (Ball et al. 2002). The organization of the *xcp* cluster is different from the *hxc* cluster; the *xcp* cluster is

divided in two operons and the *hxc* cluster is organized in at least four transcriptional units. The Xcp system is known to secrete exotoxin A, lipases, phospholipase C, alkaline phosphatase, elastase (LasB) (Filloux et al. 1997), staphylotopic protease (Kessler et al. 1993) aminopeptidase (Braun et al. 1998), alkaline ceramidase (Okino et al. 1999), chitin-binding protein (Folders et al. 2000) and protease IV (Wilderman et al. 2001). However, the Hxc system seems to be dedicated to the secretion of low-molecular mass alkaline phosphatases (Ball et al. 2002). It has also been demonstrated that HxcT, the XcpT pseudopilin homologue, is processed by the XcpA prepilin peptidase, which is required for the functionality of at least three different pathways: Pil, Xcp and Hxc (Filloux 2004).

In a mutant of strain PAO1 lacking the *xcp* cluster (*xcpP–Z*), a 40-kDa protein is observed in its supernatant when bacteria grow under phosphate limiting conditions. In a mutant lacking *hxcR* the 40-kDa protein is not present. The protein identified as LapA is a low-molecular-mass alkaline phosphatase encoded by a gene is located downstream of the *hxc* gene cluster. Therefore, LapA seems to be a substrate for the *hxc* system (Ball et al., 2002). Alkaline phosphatase activity in the individual *hxc* and *xcp* mutants is only 20% and 25%, respectively, of the total activity for the wild-type PAO1 strain. However, the double *xcp/hxc* mutant lacks all alkaline phosphatase activity in the supernatant, indicating that both the Hxc and the Xcp T2S systems contribute to the release of alkaline phosphatases (Ball et al. 2002).

Pseudomonas aeruginosa strain PAK with an inactivated *sdpD* ortholog (*xcpQ*) unexpectedly still secretes small amounts of at least four proteins (Martinez et al. 1998). The residual protein secretion depends on another *sdpD* homologue, *xqhA* (XcpQ homologue A) (Table 1.2). XcpQ and XqhA are 59% identical and differ mostly at their N- and C-termini. Although inactivation of *xqhA* alone has little effect on secretion of lipase, alkaline phosphatase,

elastase or exotoxin A, the residual protein secretion by the *xcpQ* mutant is completely abolished in the *xcpQ-xqhA* double mutant (Martinez et al. 1998). XqhA and HxcQ (the alternative secretin in PAO1) are 32% identical and 48% similar to each other, meaning that there is large variation between isolates.

Pseudomonas putida: In addition to its conserved T2SS, *P. putida* strain GB-1 has a second, incomplete T2S system (Table 1.2). Brouwers et al. (1998) used transposon mutagenesis to identify two mutants unable to transport the Mn^{2+}-oxidizing factor across the outer membrane. DNA sequencing of the disrupted genes of these mutants determined that the affected genes are very similar to those in the *P. aeruginosa xcp* gene cluster. In one of the two mutants, the disruption occurs in the *xcpT*-like gene that encodes a typical pseudopilin (Brouwers et al. 1998). In the other mutant the disruption occurs in the *xcpA (sdpO)* gene (Brouwers et al. 1998). The Xcm system was first reported in *P. putida* GB-1 with genes located in two loci on the chromosome (de Vrind et al. 2003). One locus contains two genes, *xcmT1* and *xcmS*, which encode proteins homologous to the pseudopilin XcpT and the integral membrane protein XcpS, respectively. The second locus contains a large operon including the genes *xcmR* (traffic ATPase), *xcmQ* (secretin), *xcmT2*, *xcmT3* and *xcmX*. Mutations in *xcmT1* or *xcmX* genes encoding pseudopilin-like proteins inhibited the secretion of manganese-oxidizing activity (de Vrind et al. 2003). These results indicate the involvement of both T2S systems in the transport of the Mn^{2+} -oxidizing factor of *P. putida* strain GB-1.

Pseudomonas fluorescens PFO-1: There are genes for two T2S-related systems in its genome. The first system is similar to the Xcm system in *P. putida* and the second one is most related to the Hxc system of *P. aeruginosa* for the secretion of low-molecular weight alkaline

phosphatase (Filloux et al. 2004). The absence of a conserved Xps-like gene cluster for T2S makes this strain very unusual.

Plant pathogenic xanthomonads: Available genomic sequences revealed genes for two potential T2S systems in *Xanthomonas campestris* pv. campestris (Xcc), *Xanthomonas axonopodis* pv. citri (Xac), and *Xanthomonas campestris* pv. vesicatoria (Xcv) (Table 1.3). The typical T2S system was first described for Xcc by Dums et al. (1991), who characterized mutants in *sdp* orthologs that greatly reduced secretion of endoglucanase, α-amylase and polygalacturonate lyase. The mutants also exhibited reduced virulence. The *xcs* gene cluster, which might encode an alternative T2S system, was discovered in the genome sequence of Xcc strain 33913 (da Silva et al. 2002). The same two gene clusters are also present in Xcc strain 8004 (Qian et al. 2005). Remarkably, inmunoblot analysis of XpsN in Xcc strain 1701 revealed that this protein associates with XpsL-XpsM complex located at the cytoplasmic membrane, stabilizing it and preparing XpsN to interact with the XpsD; this last interaction could serve as an activator to open the SdpD pore (Lee et al. 2004). In addition, due to its molecular mass, localization and membrane topology, XpsN is proposed to be an ortholog of the SdpC protein in *Klebsiella oxytoca* (Lee et al. 2004), which is essential for function of the T2S system, because it establishes a signal for channel opening after interacting with the SdpD protein (Lee et al. 2001; Lee et al. 2005b). The function of the potential T2S system encoded by the *xcs* gene cluster in Xcc has not been addressed directly. However, among the many random transposon mutants that are reduced in virulence studied by Qian et al. (2005) six mutations were found in the *xps* genes and no mutants were found in the *xcs* genes. These results confirm that the typical T2S encoded by the *xps* genes contributes to virulence and suggest that the *xcs* genes do not. However, they

provide no insight as to whether the *xcs* genes encode a functional T2S system not involved in virulence.

Two transcriptional units, one with two genes (*xpsE* and *xpsF*) and the other with 10 genes (*xpsG-xpsN* and a conserved hypothetical gene similar to glycosyltransferase genes) form the *xps* cluster in Xac Table 1.3). The *xcs* cluster comprises one transcriptional unit with 13 genes *xcsC-xcsN* and a gene similar to a TonB-dependent receptor gene (Brunings and Gabriel 2003). In Xcv strain 85-10 the *xps* and *xcs* clusters are very similar to those in Xac (Table 1.3). It is likely that for both Xac and Xcv one or both systems are involved in the secretion of the encoded CWDE's (da Silva et al. 2002; Thieme et al. 2005).

Xanthomonas oryzae pv. oryzae (Xoo) is different from the other xanthomonads because it has only a typical T2SS. The predicted proteins of the *xps* homologs in Xoo are >79% identical to their counterparts in other *Xanthomonas* strains (Lee et al. 2005b). There are twenty-seven enzymes as possible substrates in Xoo, including cellulases, proteases, a polygalacturonase, pectin degrading enzymes, xylanases, xylosidases, and a 1,4-ß-cellobiosidase (Lee et al. 2005a). Mutants lacking the *sdpD, sdpE* and *sdpF* orthologs are pathogenicity-deficient and cause xylanase and protease accumulation in the periplasm, indicating a role for the T2S system in *Xoo* pathogenesis (Ray 2000; Sun et al. 2005).

Ralstonia solanacearum GMI1000: DNA sequence analysis revealed that, in addition to a typical T2S system, this pathogen contains three incomplete T2S-related clusters with *sdpD-G* homologues (Table 1.4) (Genin and Boucher 2004). One of these three clusters is located in the chromosome and the other two clusters are located on the megaplasmid. Inactivation of the T2SS in GMI1000 strongly reduces virulence, with the mutant wilting just 15% of the inoculated plants (Liu et al. 2005). Analysis of mutant culture supernatant by sodium dodecyl sulfate-

polyacrylamide gel electrophoresis (SDS-PAGE) shows that most of the plentiful EXPs are not secreted by this mutant. However, in addition to many less plentiful proteins, at least two lower-molecular-mass proteins (≈ 11 and 17 kDa) are still secreted in large amounts (Liu et al. 2005). The T2S-related gene clusters could be playing an important role for secretion of specific substrates as in *P. aeruginosa*, but the proteins secreted (if any) are unknown.

The Phenotype Conversion (Phc) System

This system establishes a regulatory network for controlling the expression of virulence and pathogenicity factors positively or negatively regulated by PhcA, a LysR-type transcriptional regulator (Fig 1.2).

PhcA: This protein allows *R. solanacearum* to switch from one phenotypical state to another in response to nutrient availability and cell density. In AW, positively regulated characteristics include production of EPS, Egl and Pme. PhcA also upregulates *xpsR* expression, competence for natural transformation by DNA and the acyl-homoserine lactone quorum sensing system. PhcA negatively regulates production of PehA, staphyloferrin B siderophore, type IV pili (necessary for twitching motility), autoaggregation and biofilm formation, flagellar motility at high density, salt tolerance and activity of the HrpG transcriptional regulator (Denny 2006). Levels of active PhcA are controlled in response to cell density or confinement by the products of the *phcBSR* operon.

PhcB: PhcB is predicted to be a small-molecule methyltransferase that synthesizes 3-OH palmitic acid methyl ester (3-OH PAME), which accumulates extracellularly when bacteria grow rapidly in confining conditions, but diffuses away when growing slowly or in an open environment (Schell 2000).

PhcS and PhcR: These two proteins form a two-component regulatory system that activates PhcA in response to elevated levels of 3-OH PAME. Once PhcA is produced and activated it stimulates transcription of *xpsR* and other genes (Schell 2000).

XpsR: This is a basic 33-kDa protein that regulates EPS production in response to PhcA and VsrD. Expression of *xpsR* is controlled by PhcA and the VsrA/VsrD two-component system. XpsR interacts with VsrC, a component of another two-component system (VsrB/VsrC) to activate *eps* transcription (Schell 2000). Inactivation of either *vsrB* or *vsrC* also increases the production of PehA (Denny 2006).

VsrA/VsrD: The *vsrA* gene encodes a sensor kinase and has a corresponding response regulator known as *vsrD* (Schell et al. 1994). Inactivation of either *vsrA* or *vsrD* drastically reduces virulence and EPS production, the ability to cause disease, and the ability to grow *in planta* but not in culture media. Confirming Dr. C. Allen's observations (personal communication), I found that an AW *vsrD* mutant is more swimming motile than its wild-type parent. I also found that a GMI1000 *vsrD* mutant is more swimming motile than GMI1000 wild-type, an AW *vsrD* mutant and AW wild-type strains. The AW and AW1 *vsrA* mutants also are twitching and swimming hypermotile. The AW and AW1 *vsrB* mutants are EPS reduced, twitching motile but not swimming motile. In both cases (i.e., *vsrA* and *vsrB*), EPS production is recovered after complementation by *vsrAD* and *vsrBC* genes.

A *vsrAD* mutant colonizes plants poorly and it therefore exhibits greatly reduced virulence. This reduction of symptoms is not due to the low production of EPS, but rather to other traits affected by the inactivation of *vsrAD* (McGarvey 1999b). This was demonstrated by integrating a plasmid containing *xpsR* under the control of the constitutively expressed *lacZ* promoter into the chromosome of a *vsrD* mutant. The resulting strain produces wild-type levels

of EPS *in vitro* and when stem-inoculated into tomato plants, produces wild-type levels of EPS on a per cell basis, However, it still is unable to grow rapidly *in planta* and does not cause any disease symptoms. These data strongly suggest that other, unidentified VsrD-regulated genes are required for wild-type growth *in planta* and production of disease symptoms (McGarvey 1999b). Two additional genes are known to be regulated by VsrD. McGarvey (1999) surveyed random Tn*5*-*lacZ* mutants of strain AWD (*vsrD*) for promoters regulated by a plasmid-borne copy of *vsrD*. One of the two genes found that are negatively regulated by VsrD is homologous to nfrB in *E. coli*, which encodes an IM protein of unknown function. The other negatively-regulated gene appeared to be unique and not function was assigned. No positively-regulated *lacZ* fusions were recovered. However, some genes are positively regulated by VsrD, because the extracellular protein profile of AWD lacks several major proteins that are secreted by the wild type (Huang et al. 1995). The N-terminal amino acid sequence of one of these proteins (with a mass of 47 kDa) was determined and, when the GMI1000 genomic sequence became available, identified as belonging to the CbhA exoglucanase (McGarvey and Schell, personal communication).

Hrp-encoded Type III Secretion System (T3SS)

The T3SS allows the translocation of effector proteins from the pathogen cytoplasm directly into the cytoplasm of plant cells. At least some of these effectors suppress plant host defense responses, which makes it easier for pathogens to multiply during colonization (Collmer et al. 2000). The T3SS pathway is encoded by *hrp* and *hrc* genes. The Hrc proteins direct secretion of T3SS substrates across the bacterial envelope while a subset of Hrp proteins is secreted by the T3SS and direct the translocation of effectors through host cell barriers (Alfano and Collmer 2004). Inactivation of any of the *hrc* genes makes pathogens incapable of causing disease on

susceptible plants and the hypersensitive response on resistant plants (Arlat et al. 1992). *R. solanacearum* T3SS mutants reduce the pathogen's ability to colonize the upper section of the plant after either leaf infiltration or soil drench. However, they are still able to colonize the main root and lower section of the stem (Denny 2006).

The *R. solanacearum* T3SS *hrp/hrc* gene cluster has more than 20 genes in a 23-kb region of the megaplasmid. Nine conserved *hrc* genes (*hrcC, hrcT, hrcN, hrcJ, hrcU, hrcV, hrcQ, hrcR and hrcS*) encode proteins essential for the type III secretion machinery with most of the Hrc proteins located at the inner membrane (excluding the HrcN ATPase, which is cytoplasmic, and the HrcC secretin that creates a pore in the outer membrane). On the other hand, the *hrp* genes encode proteins with species-specific roles in translocation of effector proteins. That is the case of *hrpB, hrpF, hrpK, hrpW, hrpX* and *hrpY* in GMI1000, which are essential genes for HR in tobacco and virulence in tomato, for the secretion of the PopA protein, and for production of Hrp pili, used as a conduit for proteins exported by the Hrp system (Denny 2006). The other genes, *hrpD, hrpH, hpaP, hrpV* and *hrpJ* contribute to enhancing the efficiency effector protein translocation (Denny 2006).

The AraC-type transcriptional regulator protein HrpB is responsible for activating other transcriptional units in the *hrp/hrc* gene cluster and genes for most of the known and putative effector proteins. HrpY constitutes the principal subunit of the Hrp pilus. HrpX is essential for Hrp pilus assembly and HrpV for display of Hrp pili. Other proteins such as HrpJ, HrpV and HpaB can play a role in protein translocation (Denny 2006).

Regulation of *hrpB* expression in GMI1000 is complex (Denny 2006). HrpG (a member of the OmpR subclass of two component response regulators), activates expression of *hrpB* and downstream *hrp/hrc* operons in minimal medium and in co-cultivation with *Arabidopsis* and

tomato cells. *HrpG* mutants are non-pathogenic on tomato and are HR negative on tobacco. Also, *hrpG* mutants are less aggressive for colonization than *hrpB* mutants. *In planta* expression of *hrpG* is controlled by the PrhARIJ signal cascade that responds to contact with plant cell walls (Fig. 1.3). However, in minimal medium expression of *hrpG* occurs independently of Prh pathway.

The expression of *hrpB* is also controlled by PhcA, because inactivation of *phcA* increases *hrpB* expression by 60 fold in rich medium. In addition, GMI1000 constitutively expressing *phcA* elicits partial and delayed HR on tobacco, due to reduced functionality of the T3SS (Genin et al. 2005). PhcA-dependent control of the Hrp regulatory pathway occurs at the level of HrpG function, probably via a post-transcriptional mechanism that integrates environmental and plant-derived signals required for activation of HrpB. The PhcA-dependent repression of *hrp* genes is best observed during growth in complex nitrogen sources. Therefore, HrpG appears to be the convergence point of two 'input' signal pathways: the Prh plant-responsive pathway and an unidentified 'minimal medium' pathway that associates *hrp* gene regulation by HrpB with the global virulence regulator, PhcA.

Proteomics approaches

Protein separation: One-dimensional SDS-PAGE allows protein separation based on the molecular masse and a protein's ability to penetrate the pore matrix of the gel. Before electrophoresis, samples are exposed to SDS for denaturation and acquisition of negative charge from the SDS sulfate group. As a result, the charge density of all proteins is about the same. In addition, samples are heat denaturated in presence of a reducing agent (DTT) that cleaves inter and intra-chain disulfide linkages between cysteine residues, overcoming tertiary and quaternary

protein folding (Liebler 2002). Once resolved in a gel, the bands can contain more than one protein making this approach more appropriate for simple protein samples and proteins 10 to100 kDa.

Two-dimensional polyacrylamide gel electrophoresis (2-D PAGE) separates complex protein mixtures by using two independent steps. The first step separates the proteins according to their isoelectric point (pI) on a pH gradient. The second step separates proteins by mass using SDS-PAGE as noted above, but using a slab gel. Gels can have different polyacrylamide gradients and size formats, offering diverse alternatives for protein profile studies. After separation, the proteins are detected by staining (e.g., with Coomassie Blue or silver nitrate) (Bernot 2004).

The ability of 2-D-PAGE to resolve intact proteins has made it the long-standing method of choice to initiate a proteomics analysis of complex samples. Once protein spots are revealed, they can be excised, the stain removed, the protein digested with trypsin, and the peptides eluted for analysis, usually on a mass spectrometer. However, 2-D-PAGE has several disadvantages. Proteins with very acidic or basic pIs are difficult to separate during isoelectric focusing, and very large or very small proteins are, respectively, difficult to resolve or to retain on polyacrylamide gels. Consequently, a substantial percentage of proteins present in a complex sample may not be observed. In addition, proteins present at low concentrations can be difficult to visualize on the 2-D gel when there are more abundant proteins (Liebler 2002). Detection of low abundance proteins can be enhanced by using silver staining, which is substantially more sensitive than the standard Coomassie Blue dye. However, the low peptide concentration recovered from such spots and the inherent incompatibility of silver-stained peptides with subsequent mass spectrometry (MS) analysis reduces the likelihood of successful protein

identification. Fortunately, colloidal Coomassie Blue and fluorescent stains, such as Sypro Ruby, exhibit intermediate sensitivities, and are compatible with MS analysis.

Mass spectral analysis: The introduction of soft ionization methods like matrix-assisted laser desorption/ionization (MALDI) and electrospray ionization (ESI) made MS a useful tool for proteome analysis, because these techniques ionize biological molecules such as peptides and proteins without inducing fragmentation (Witt et al. 2003). Selected proteins can be identified by digestion using an endoprotease (trypsin or chymotrypsin) to create peptides whose mass-to-charge ratio (m/z) can be determined by MS (Speicher 2004). The resulting mass spectrograph of a protein's peptides (referred to as a peptide mass fingerprint) is then matched to theoretical digests of individual proteins in a database.

MALDI provides molecular information on intact peptides, a feature useful for protein identification and characterization. A sample submitted to a MALDI source needs to be mixed with a matrix containing a organic compound, commonly either sinapinic acid, 2,5-dihydroxybenzoic (DHB) or α-cyano-4-hydroxycinnamic acid (HCCA). The matrix protects the sample from UV light by absorbing some of the energy from the laser while the sample is vaporized. The peptides are then ionized and injected into the mass analyzer to measure their m/z (Siuzdak 2003).

Unlike MALDI, ESI produces the gaseous phase from a liquid solution. The process starts with a highly-charged drop that is sprayed into an electric field by means of a high voltage needle. The resulting droplets, when in contact with a dry gas or heat, increase the charge density of multiple charged ions that are ejected through a Taylor cone into a mass analyzer (Siuzdak 2003).

Many mass spectrometers employ a linear time of flight analyzer (TOF) to measure the time required for ions to travel from one end of the analyzer to the detector (Liebler 2002). Lighter ions travel faster than the heavy ones and reach the ion detector sooner. That means that the measured TOF depends on the mass, charge and kinetic energy of the ions (Siuzdak 2003). A TOF-reflecton mass analyzer improves ion resolution by increasing the length of the flight path and because the reflecton focuses ions of the same *m/z* values, allowing them to reach the detector more at the same time (Liebler 2002).

Determining peptide structure and amino acid sequence require a tandem mass spectrometer capable of fragmenting peptides into smaller ions prior to analysis. Tandem MS can occur in time by using the same mass analyzer consecutively, or in space by using two different mass analyzers (Siuzdak 2003). Tandem MS produces partial amino acid sequence information that is more specific than the just the peptide mass, because two different peptides with identical amino acid composition (and thus mass) will produce different fragmentation patterns.

Tandem MS can be performed on triple quadrupole mass analyzer. A quadrupole uses radio frequency voltages applied alternately to opposing pairs of metal rods and a direct current voltage to direct ions down the length of the quadrupole (Siuzdak 2003). The first quadrupole makes an initial scan of the ions, filtering them by their *m/z* and allowing only those desired to pass through. The second quadrupole is a collision cell on which the peptide ions are fragmented by interaction with neutral gas atoms. The *m/z* of the resulting daughter ions are then analyzed in the third quadrupole (Siuzdak 2003).

In an ion-trap mass analyzer, which is very similar to the triple quadrupole analyzer, the peptide ions are stored in the ion trap prior to a second fractionation during an MS/MS analysis. The ion trap is surrounded by electrodes that, with a combination of DC and radio frequency

voltages, keeps the ions in orbit. Ions can be analyzed according their *m/z* by application of different voltages that allow the ejection of ions of different *m/z* into the second mass analyzer. The ion trap also can be used to induce further fragmentation of selected peptides, and the resulting daughter ions are then analyzed to deduce a peptide sequence with high mass resolution (Liebler 2002).

Fourier Transform-Ion Cyclotron Resonance MS uses a powerful magnetic field to keep ions orbiting while a radio frequency is used to excite them, creating a current that is transformed into a frequency. Each frequency represents a specific *m/z* value. This method offers high resolution and can be used in multiple collision experiments yielding highly accurate fragment masses (Siuzdak 2003).

Protein quantification: Cell processes can be affected by small changes in protein production. Quantifying such changes has traditionally been achieved through visual comparison of 2-D gels and, more recently, using differential in gel electrophoresis (DIGE). Alternatively, gel-free proteomic methodologies have been developed that separate peptides generated by enzymatic digestion of previously labeled complex protein samples by liquid chromatography (LC) and tandem MS (MS/MS).

DIGE was initially proposed by Schena et al. (1995), for quantification of mRNA expression, but has been adapted for use with proteins (Unlu et al. 1997). The technique requires labeling proteins on their lysine ε-amino groups with one of two different fluorescent cyanide dyes. Two samples are then mixed prior to electrofocusing and 2-D-PAGE. The gel is then scanned to measure the fluorescence intensity of each dye in every protein spot (Wittmann-Liebold et al. 2006). The two dyes commonly used are Cy3 (λ_{em}= 569 nm) and Cy5 (λ_{em}= 645). A gradient in color is observed when the two dyes are present, allowing the identification of the

predominant one (Wittmann-Liebold et al. 2006) using software that interprets the signals of the samples being compared (Hamdan and Righetti 2002). This method has some disadvantages, namely its lack of reproducibility and the fact that more than one protein can be present in the same spot, causing interference with the signal emitted (Yan and Chen 2005). Identification of the desired proteins requires gel staining after fluorescent imaging, spot selection and digestion for peptide elution prior to peptide mass fingerprint analysis. Consequently, the disadvantages of standard 2-D-PAGE noted above also apply to DIGE.

Gel-free techniques for quantification involve the use of proteins or peptides labeled with stable isotopes or isobaric tags that provide a tool for data normalization. Labeling can occur *in vivo* and *in vitro*. *In vivo* labeling involves adding an isotopically labeled molecule to the media in which one of two samples is cultured so that new proteins will incorporate it. In addition to using labeled amino acids (e.g., ^{12}C and ^{13}C arginine), prototrophic organisms can be labeled with ^{14}N and ^{15}N ammonium sulfate. Only databases with annotated peptide sequences can be quantified using this method, which represents a disadvantage in protein identification. Additionally, this method often requires modifications to reduce the sample complexity to make the results more reliable (Yan and Chen 2005).

In the case of the *in vitro* labeling, isotopic tags are incorporated by a chemical reaction to specific sites in peptides. One commercial method is known as isotope-coded affinity tags (ICAT). The labeling reagent has a biotin affinity tag, which includes a linker with nine molecules of a ^{1}H or ^{2}H and an iodoacetamide reactive group that interacts with cysteine thiols of peptides (Yan and Chen 2005). After independent labeling, two samples are pooled, subjected to affinity chromatography to enrich the biotin-labeled peptides (which also reduces sample complexity), and then analyzed by LC-MS/MS. The same peptide from the two samples will

differ in mass by 9 Da, and the signal intensity of these two peptides provides quantitative data on their relative abundance. This method has a broader range of applications than the *in vivo* methods (Yan and Chen 2005). A disadvantage, however, is that ICAT is not applicable to cysteine-free proteins, which are relatively frequent. This problem was addressed with isotope-coded protein label ICPL (^{12}C and ^{13}C), which labels proteins with lysine residues that are usually plentiful, increasing MS sensitivity (Wiese et al. 2007).

A second commercial *in vitro* labeling method is isobaric tags for relative and absolute quantification (iTRAQ). This method uses tags that initially have equal mass to label the N-terminus of peptides. Since virtually all peptides will be labeled, this eliminates one of the shortcomings of ICAT. Isobaric tags consist of a reporter group with one of four masses (114.1, 115.1, 116.1 or 117.1 Da), a balance group that ensures the overall mass of each tag is 145 Da, and a reactive group that interacts with amino groups (Yan and Chen 2005). Up to four separately labeled peptide samples can be mixed prior to cation-exchange chromatography to create fractions with reduced peptide complexity, and subsequent analysis of the fractions by LC-MS/MS. The reporter groups and balance groups are liberated from the peptides (and each other) during the collision-induced dissociation step, and the resulting diagnostic ions (114-117 Da) are used for relative quantification of the peptide in the samples, while the peptide daughter ions are used for identification (Yan and Chen 2005). One advantage of iTRAQ is improved ionization of labeled peptides, which results in higher signal intensity that enhances detection of non-abundant proteins. iTRAQ-labeled peptides also generate better sets of daughter ions, which improves protein identification. Another advantage is the possibility of performing a multiplexed test with up to four samples that can represent different treatments or sample states. One

disadvantage is the preference for quantifying abundant peptides in high complexity samples (Wiese et al. 2007).

Data analysis involves the use of databases SWISS-PROT, OWL, UniProt and NCBInr. Software uses the *m/z* values along with parameters such as the enzyme used during digestion, the number of missed cleavages allowed, possible peptide modifications and the expected mass range. The resulting candidates are scored using programs such as Protein Pilot, ProQUANT, FindPept, MS-Fit, MOWSE and MASCOT, some of which aid selection using a statistical approach (Liebler 2002).

Previous work by Dr. Tim Denny during 2004 with *R. solanacearum* strain GMI1272 identified a number of exoproteins. This mutant does not produce the EPS polysaccharide that under normal conditions can interfere with isoelectric focusing. Proteins were visualized on 2-D-PAGE, selected spots were digested and their peptide mass fingerprints determined using FTICR-MS analysis. Twenty-three proteins were indentified, including PglB, PglC, ChbA, Tek, Egl, Pme, PopW, VirK and other proteins classified as conserved hypotetical proteins. Besides, probable signal peptide proteins, a putative antibiotic hydrolase signal peptide protein, a hydrolase transmembrane protein, a putative hemolysin type protein, a putative serine protease protein and a putative transglycosylase protein were identified. These results constituted the beginning of the proteomics research with *R. solanacearum* in Dr. Denny's lab and the foundation on which I developed my thesis research.

References

Alfano, J. R., and Collmer, A. 2004. Type III secretion system effector proteins: Double agents in bacterial disease and plant defense. Annu. Rev. Phytopathol. 42:385-414.

Arlat, M., Gough, C. L., Zischek, C., Barberis, P. A., Trigalet, A., and Boucher, C. A. 1992. Transcriptional organization and expression of the large *hrp* gene cluster of *Pseudomonas solanacearum*. Mol. Plant-Microbe Interact. 5:187-193.

Ball, G., Durand, E., Lazdunski, A., and Filloux, A. 2002. A novel type II secretion system in *Pseudomonas aeruginosa*. Mol. Microbiol. 43:475-485.

Barras, F., Gijsegem, F., and Chatterjee, A. 1994. Extracellular enzymes and pathogenesis of soft-rot Erwinia. Annu. Rev. Phytopathol. 32:201-234.

Berks, B. C., Palmer, T., and Sargent, F. 2005. Protein targeting by the bacterial twin-arginine translocation (Tat) pathway. Curr. Opin. Microbiol. 8:174-181.

Bernot, A. 2004. Genome, transcriptome and proteome analysis. John Wiley & Sons, Ltd, Chichester, England.

Braun, P., de Groot, A., Bitter, W., and Tommassen, J. 1998. Secretion of elastinolytic enzymes and their propeptides by *Pseudomonas aeruginosa*. J. Bacteriol. 180:3467-3469.

Brouwers, G. J., De Vrind-De Jong, E., Corstjens, P. L. A. M., and Jong, E. W. V. 1998. Involvement of genes of the two-step protein secretion pathway in the transport of the manganese-oxidizing factor across the outer membrane of *Pseudomonas putida* strain GB-I. American Mineralogist 83:1573-1582.

Brunings, A. M., and Gabriel, D. W. 2003. *Xanthomonas citri*: breaking the surface. Mol. Plant Pathol. 4:141-157.

Collmer, A., Badel, J. L., Charkowski, A. O., Deng, W. L., Fouts, D. E., Ramos, A. R., Rehm, A. H., Anderson, D. M., Schneewind, O., van Dijk, K., and Alfano, J. R. 2000. *Pseudomonas syringae* Hrp type III secretion system and effector proteins. Proc. Natl. Acad. Sci. USA 97:8770-8777.

da Silva, A. C. R., Ferro, J. A., Reinach, F. C., Farah, C. S., Furlan, L. R., Quaggio, R. B., Monteiro-Vitorello, C. B., Van Sluys, M. A., Almeida, N. F., Alves, L. M., do Amaral, A. M., Bertolini, M. C., Camargo, L. E., Camarotte, G., Cannavan, F., Cardozo, J., Chambergo, F., Ciapina, L. P., Cicarelli, R. M., Coutinho, L. L., Cursino-Santos, J. R., El Dorry, H., Faria, J. B., Ferreira, A. J., Ferreira, R. C., Ferro, M. I., Formighieri, E. F., Franco, M. C., Greggio, C. C., Gruber, A., Katsuyama, A. M., Kishi, L. T., Leite, R. P., Lemos, E. G., Lemos, M. V., Locali, E. C., Machado, M. A., Madeira, A. M., Martinez-Rossi, N. M., Martins, E. C., Meidanis, J., Menck, C. F., Miyaki, C. Y., Moon, D. H., Moreira, L. M., Novo, M. T., Okura, V. K., Oliveira, M. C., Oliveira, V. R., Pereira, H. A., Rossi, A., Sena, J. A., Silva, C., de Souza, R. F., Spinola, L. A., Takita, M. A., Tamura, R. E., Teixeira, E. C., Tezza, R. I., Trindade dos, S. M., Truffi, D., Tsai, S. M., White, F. F., Setubal, J. C., and Kitajima, J. P. 2002. Comparison of the genomes of two *Xanthomonas* pathogens with differing host specificities. Nature 417:459-463.

de Vrind, J., de Groot, A., Brouwers, G. J., Tommassen, J., and Vrind-de Jong, E. 2003. Identification of a novel Gsp-related pathway required for secretion of the manganese-oxidizing factor of *Pseudomonas putida* strain GB-1. Mol. Microbiol. 47:993-1006.

Denny, T. P. 2006. Plant pathogenic *Ralstonia* species. Pages 573-644 in: Plant-Associated Bacteria. S. S. Gnanamanickam, ed. Springer, Dordrecht, The Netherlands.

Desvaux, M., Parham, N. J., Scott-Tucker, A., and Henderson, I. R. 2004. The general secretory pathway: a general misnomer? Trends Microbiol. 12:306-309.

Dums, F., Dow, J. M., and Daniels, M. J. 1991. Structural characterization of protein secretion genes of the bacterial phytopathogen *Xanthomonas campestris* pathovar *campestris* - relatedness to secretion systems of other Gram-negative bacteria. Mol. Gen. Genet. 229:357-364.

Filloux, A., Bleves, S., van Ulsen, P., and Tommassen, J. 2004. Protein secretion mechanisms in *Pseudomonas*. Pages 749-791 in: Pseudomonas, Vol 1: Genomics, Life Style and Molecular Architecture. J. L. Ramos, ed. Kluwer academic/plenum publ, New York, NY USA.

Filloux, A. 2004. The underlying mechanisms of type II protein secretion. Biochem. Biophys. Acta 1694:163-179.

Filloux, A., Michel, G., and Bally, M. 1997. GSP-dependent protein secretion in Gram-negative bacteria: the Xcp system of *Pseudomonas aeruginosa*. FEMS Microbiol. Rev. 22:177-198.

Folders, J., Tommassen, J., Van Loon, L. C., and Bitter, W. 2000. Identification of a chitin-binding protein secreted by *Pseudomonas aeruginosa*. J. Bacteriol. 182:1257-1263.

Genin, S., and Boucher, C. 2004. Lessons learned from the genome analysis of *Ralstonia solanacearum*. Annu. Rev. Phytopathol. 42:107-134.

Genin, S., Brito, B., Denny, T. P., and Boucher, C. 2005. Control of the *Ralstonia solanacearum* type III secretion system (Hrp) genes by the global virulence regulator PhcA. FEBS Lett. 579:2077-2081.

Hamdan, M., and Righetti, P. G. 2002. Modern strategies for protein quantification in proteome analysis: Advantages and limitations. Mass Spectrometry Reviews 21:287-302.

Hayward, A. C. 1994. The hosts of *Pseudomonas solanacearum*. Pages 9-24 in: Bacterial Wilt: The Disease and its Causative Agent, *Pseudomonas solanacearum*. A. C. Hayward and G. L. Hartman, eds. CAB International, Wallingford, UK.

Huang, J., Carney, B. F., Denny, T. P., Weissinger, A. K., and Schell, M. A. 1995. A complex network regulates expression of *eps* and other virulence genes of *Pseudomonas solanacearum*. J. Bacteriol. 177:1259-1267.

Jha, G., Rajeshwari, R., and Sonti, R. V. 2005. Bacterial type two secretion system secreted proteins: Double-edged swords for plant pathogens. Mol. Plant-Microbe Interact. 18:891-898.

Kazemi-Pour, N., Condemine, G., and Hugouvieux-Cotte-Pattat, N. 2004. The secretome of the plant pathogenic bacterium *Erwinia chrysanthemi*. Proteomics 4:3177-3186.

Kessler, E., Safrin, M., Olson, J. C., and Ohman, D. E. 1993. Secreted LasA of *Pseudomonas-aeruginosa* is a staphylolytic protease. J. Biol. Chem. 268:7503-7508.

Kostakioti, M., Newman, C. L., Thanassi, D. G., and Stathopoulos, C. 2005. Mechanisms of protein export across the bacterial outer membrane. J. Bacteriol. 187:4306-4314.

Lee, B. M., Park, Y. J., Park, D. S., Kang, H. W., Kim, J. G., Song, E. S., Park, I. C., Yoon, U. H., Hahn, J. H., Koo, B. S., Lee, G. B., Kim, H., Park, H. S., Yoon, K. O., Kim, J. H., Jung, C., Koh, N. H., Seo, J. S., and Go, S. J. 2005a. The genome sequence of *Xanthomonas oryzae* pathovar oryzae KACC10331, the bacterial blight pathogen of rice. Nucleic Acids Res. 33:577-586.

Lee, H. M., Chen, J. R., Lee, H. L., Leu, W. M., Chen, L. Y., and Hu, N. T. 2004. Functional dissection of the XpsN (GspC) protein of the *Xanthomonas campestris* pv. campestris type II secretion machinery. J. Bacteriol. 186:2946-2955.

Lee, H. M., Tyan, S. W., Leu, W. M., Chen, L. Y., Chen, D. C., and Hu, N. T. 2001. Involvement of the XpsN protein in formation of the XpsL-XpsM complex in *Xanthomonas campestris* pv. campestris type II secretion apparatus. J. Bacteriol. 183:528-535.

Lee, M. S., Chen, L. Y., Leu, W. M., Shiau, R. J., and Hu, N. T. 2005b. Associations of the major pseudopilin XpsG with XpsN (GspC) and secretin XpsD of *Xanthomonas campestris* pv. campestris type II secretion apparatus revealed by cross-linking analysis. J. Biol. Chem. 280:4585-4591.

Liebler, D. C. 2002. Introduction to Proteomics: Tools for the New Biology. Humana Press, Totowa, NJ.

Liu, H., Zhang, S., Schell, M. A., and Denny, T. P. 2005. Pyramiding unmarked mutations in *Ralstonia solanacearum* shows that secreted proteins in addition to plant cell wall degrading enzymes contribute to virulence. Mol. Plant-Microbe Interact. 18:1296-1305.

Martinez, A., Ostrovsky, P., and Nunn, D. N. 1998. Identification of an additional member of the secretin superfamily of proteins in *Pseudomonas aeruginosa* that is able to function in type II protein secretion. Mol. Microbiol. 28:1235-1246.

McGarvey, J. A. (1999). In vivo and in vitro growth and virulence factor production by *Ralstonia solanacearum*. (Abstract)

Mori, H., and Ito, K. 2001. The Sec protein-translocation pathway. Trends Microbiol. 9:494-500.

Oates, J., Mathers, J., Mangels, D., Kuhlbrandt, W., Robinson, C., and Model, K. 2003. Consensus structural features of purified bacterial TatABC complexes. J. Mol. Biol. 330:277-286.

Okino, N., Ichinose, S., Omori, A., Imayama, S., Nakamura, T., and Ito, M. 1999. Molecular cloning, sequencing, and expression of the gene encoding alkaline ceramidase from *Pseudomonas aeruginosa* - Cloning of a ceramidase homologue from Mycobacterium tuberculosis. J. Biol. Chem. 274:36616-36622.

Preston, G. M., Studholme, D. J., and Caldelari, I. 2005. Profiling the secretomes of plant pathogenic Proteobacteria. FEMS Microbiol. Rev. 29:331-360.

Qian, W., Jia, Y. T., Ren, S. X., He, Y. Q., Feng, J. X., Lu, L. F., Sun, Q. H., Ying, G., Tang, D. J., Tang, H., Wu, W., Hao, P., Wang, L. F., Jiang, B. L., Zeng, S. Y., Gu, W. Y., Lu, G., Rong, L., Tian, Y. C., Yao, Z. J., Fu, G., Chen, B. S., Fang, R. X., Qiang, B. Q., Chen, Z., Zhao, G. P., Tang, J. L., and He, C. Z. 2005. Comparative and functional genomic analyses of the pathogenicity of phytopathogen *Xanthomonas campestris* pv. campestris. Genome Res. 15:757-767.

Ray, S. K. 2000. Mutants of *Xanthomonas oryzae* pv. *oryzae* deficient in general secretory pathway are virulence deficient and unable to secrete xylanase. Mol. Plant-Microbe Interact. 13:394-401.

Saile, E., Schell, M. A., and Denny, T. P. 1997. Role of extracellular polysaccharide and endoglucanase in root invasion and colonization of tomato plants by *Ralstonia solanacearum*. Phytopathology 87:1264-1271.

Salanoubat, M., Genin, S., Artiguenave, F., Gouzy, J., Mangenot, S., Arlat, M., Billault, A., Brottier, P., Camus, J. C., Cattolico, L., Chandler, M., Choisne, N., Claudel-Renard, C., Cunnac, S., Demange, N., Gaspin, C., Lavie, M., Moisan, A., Robert, C., Saurin, W., Thébault, P., Schiex, T., Siguier, P., Whalen, M., Wincker, P., Levy, M., Weissenbach, J., and Boucher, C. A. 2002. The genome sequence of the wide host-range plant pathogen *Ralstonia solanacearum*. Nature 415:497-502.

Schell, M. A. 2000. Control of virulence and pathogenicity genes of *Ralstonia solanacearum* by an elaborate sensory array. Annu. Rev. Phytopathol. 38:263-292.

Schell, M. A., Denny, T. P., and Huang, J. 1994. VsrA, a second two-component system regulating virulence genes of *Pseudomonas solanacearum*. Mol. Microbiol. 11:489-500.

Schena, M., Shalon, D., Davis, R. W., and Brown, P. O. 1995. Quantitative monitoring of gene-expression patterns with a complementary-DNA microarray. Science 270:467-470.

Siuzdak, G. 2003. The expanding role of mass spectrometry in biotechnology. MCC Press, San Diego, CA.

Speicher, D. W. 2004. Pages 1-18 in: Proteome analysis: Interpreting the genome. Elsevier Science, Amsterdam ; San Diego.

Stackebrandt, E., Murray, R. G. E., and Trüper, H. G. 1988. *Proteobacteria* classis nov., a name for the phylogenetic taxon that includes the "Purple Bacteria and their relatives". Int. J. Syst. Bacteriol. 38:321-325.

Sun, Q. H., Hu, J., Huang, G. X., Ge, C., Fang, R. X., and He, C. Z. 2005. Type-II secretion pathway structural gene *xpsE*, xylanase- and cellulase secretion and virulence in *Xanthomonas oryzae* pv. oryzae. Plant Pathol. 54:15-21.

Tans-Kersten, J., Guan, Y. F., and Allen, C. 1998. *Ralstonia solanacearum* pectin methylesterase is required for growth on methylated pectin but not for bacterial wilt virulence. Appl. Environ. Microbiol. 64:4918-4923.

Thieme, F., Koebnik, R., Bekel, T., Berger, C., Boch, J., Buttner, D., Caldana, C., Gaigalat, L., Goesmann, A., Kay, S., Kirchner, O., Lanz, C., Linke, B., McHardy, A. C., Meyer, F., Mittenhuber, G., Nies, D. H., Niesbach-Klosgen, U., Patschkowski, T., Ruckert, C., Rupp, O., Schneiker, S., Schuster, S. C., Vorholter, F. J., Weber, E., Puhler, A., Bonas, U., Bartels, D., and Kaiser, O. 2005. Insights into genome plasticity and pathogenicity of the plant pathogenic bacterium *Xanthomonas campestris* pv. vesicatoria revealed by the complete genome sequence. J. Bacteriol. 187:7254-7266.

Unlu, M., Morgan, M. E., and Minden, J. S. 1997. Difference gel electrophoresis: a single gel method for detecting changes in protein extracts. Electrophoresis 18:2071-2077.

Varbanets, L. D., Vasil'ev, V. N., and Brovarskaya, O. S. 2003. Characterization of lipopolysaccharides from *Ralstonia solanacearum*. Microbiology 72:12-17.

Vasse, J., Frey, P., and Trigalet, A. 1995. Microscopic studies of intercellular infection and protoxylem invasion of tomato roots by *Pseudomonas solanacearum*. Mol. Plant-Microbe Interact. 8:241-251.

Voulhoux, R., Ball, G., Ize, B., Vasil, M. L., Lazdunski, A., Wu, L. F., and Filloux, A. 2001. Involvement of the twin-arginine translocation system in protein secretion via the type II pathway. EMBO J. 20:6735-6741.

Wiese, S., Reidegeld, K. A., Meyer, H. E., and Warscheid, B. 2007. Protein labeling by iTRAQ: A new tool for quantitative mass spectrometry in proteome research. Proteomics 7:340-350.

Wilderman, P. J., Vasil, A. I., Johnson, Z., Wilson, M. J., Cunliffe, H. E., Lamont, I. L., and Vasil, M. L. 2001. Characterization of an endoprotease (PrpL) encoded by a PvdS-regulated gene in *Pseudomonas aeruginosa*. Infection. Immunity 69:5385-5394.

Witt, M., Fuchser, J., and Baykut, G. 2003. Fourier transform ion cyclotron resonance mass spectrometry with NanoLC/microelectrospray ionization and matrix-assisted laser desorption/ionization: Analytical performance in peptide mass fingerprint analysis. J. Am. Soc. Mass Spectrom. 14:553-561.

Wittmann-Liebold, B., Graack, H. R., and Pohl, T. 2006. Two-dimensional gel electrophoresis as tool for proteomics studies in combination with protein identification by mass spectrometry. Proteomics 6:4688-4703.

Wretlind, B., and Pavlovskis, O. R. 1984. Genetic-mapping and characterization of *Pseudomonas aeruginosa* mutants defective in the formation of extracellular proteins. J. Bacteriol. 158:801-808.

Yan, W., and Chen, S. S. 2005. Mass spectrometry-based quantitative proteomic profiling. Brief. Funct. Genomic. Proteomic. 4:27-38.

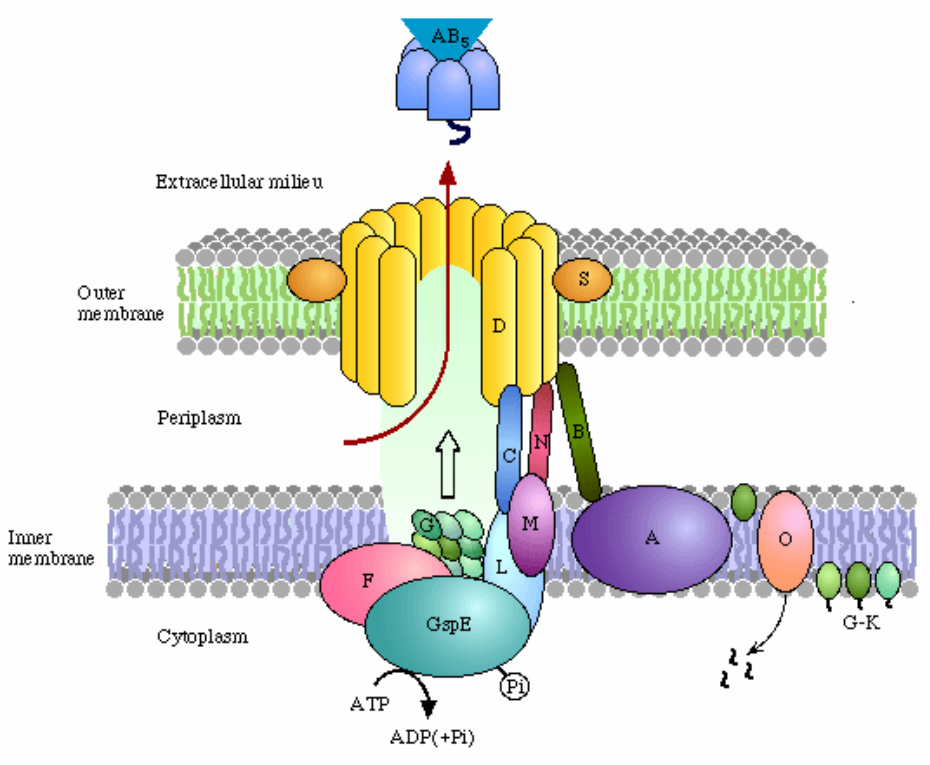

Fig 1.1. Type II secretion system structure. http://www.genome.jp/kegg/pathway/pcu/pcu03090.gif

Table 1.1. Sdp proteins found in *Pseudomonas aeruginosa*

Sdp	Location	Function
A*	Integral IM	Assistance in translocation of protein D to the OM
B*	IM	Assistance in translocation of protein D to the OM
C	Bitopic IM	Connector between the OM complex and the IM complex
D	Integral OM	Pore for translocation of secreted proteins to the extracellular space.
E	Peripheral IM	Traffic ATPase, provides energy for translocation of pseudopilus across IM
F	Polytopic IM	Formation of platform for pseudopilus building
G	IM	Prepilin-like protein. Can form a pseudopilus with proteins H, I and J.
H	IM	Pseudopilin subunits
I	IM	Pseudopilin subunits
J	IM	Pseudopilin subunits
K	IM	Prepilin subunit whose inclusion in the complex arrests pilus elongation
L	Bitopic IM	Formation of platform for pseudopilus building
M	Bitopic IM	Formation of platform for pseudopilus building
N*	Bitopic IM	Connector between the OM complex and the IM complex
O	Inner IM	Prepilin peptidase. Methylation of N-terminus after cleavage of the prepilin
S	Peripheral OM	Small lipoprotein. May stabilize and promote protein D insertion into the OM

* not in *P. aeruginosa* but included to show gene function. IM = inner membrane, OM= outer membrane

Table 1.2. Proteins of the typical *(xcp)* and alternative *(hxc, xqh, xcm*) T2SS in different pseudomonads.

	***P. aeruginosa* PAO1**		***P. aeruginosa* PAK**		***P. putida* GB-1**	
Cluster / Gene	*xcp*	*hxc*	*xcp*	*xqh*	*xcp*	*xcm*
sdpA						
sdpB						
sdpC	*P*	*P*	*P*		*P*	
sdpD	*Q*	*Q*	*Q*	*A*	*Q*	*Q*
sdpE	*R*	*R*	*R*		*R*	*R*
sdpF	*S*	*S*	*S*		*S1-S2*	*S*
sdpG	*T*	*T*	*T*		*T1-T2*	*T1-T2-T3*
sdpH	*U*	*U*	*U*		*U*	
sdpI	*V*	*V*	*V*		*V*	
sdpJ	*W*	*W*	*W*		*W*	
sdpK	*X*	*X*	*X*		*X*	*X*
sdpL	*Y*	*Y*	*Y*		*Y*	
sdpM	*Z*	*Z*	*Z*		*Z*	
sdpN						
sdpO	*A*		*A*		*A*	
sdpS						

Table 1.3. Proteins of the typical and alternative T2S systems in different xanthomonads.

	***Xcc*[1]**		***Xcv*[2], *Xac*[3]**		***Xoo*[4]**
Cluster / **Gene**	*xps*	*xcs*	*xps*	*xcs*	*xps*
sdpA					
sdpB					
sdpC	*N*	*C*		*C*	
sdpD	*D*	*D*	*D*	*D*	*D*
sdpE	*E*	*E*	*E*	*E*	*E*
sdpF	*F*	*F*	*F*	*F*	*F*
sdpG	*G*	*G*	*G*	*G*	*G*
gspH	*H*	*H*	*H*	*H*	*H*
sdpI	*I*	*I*	*I*	*I*	*I*
sdpJ	*J*	*J*	*J*	*J*	*J*
sdpK	*K*	*K*	*K*	*K*	*K*
sdpL	*L*	*L*	*L*	*L*	*L*
sdpM	*M*	*M*	*M*	*M*	*M*
sdpN		*N*	*N*	*N*	*N*
sdpO					
gspS					

1. *Xanthomonas campestris* pv. campestris strains 33913 and 8004
2. *Xanthomonas campestris* pv. vesicatoria strain 85-10
3. *Xanthomonas axonopodis* pv. citri strain 306
4. *Xanthomonas oryzae pv*. oryzae strain KACC10331

Table 1.4. Components and location of the T2S and T2S-related gene clusters in *R. solanacearum* GMI1000. Numbers are the locus tags assigned during genome sequencing.

	T2S	**T2S-related**		
Gene	**Chromosome**	**Cluster 2 * Chromosome**	**Cluster 3 * Megaplasmid**	**Cluster 4 Megaplasmid**
sdpA				
sdpB				
sdpC	3105			
sdpD	3114	2303	0143	474
sdpE	3115	2308	0148	464
sdpF	3116	2309	0149	467
sdpG	3106	2300-2301-2302-2310	0140-0141-0142-0150	0468-0470-0471
sdpH	3107			
sdpI	3108			
sdpJ	3109			
sdpK	3110			
sdpL	3111			
sdpM	3112			
sdpN	3113			
sdpO				
sdpS				

* Clusters 2 and 3 are co-linear.

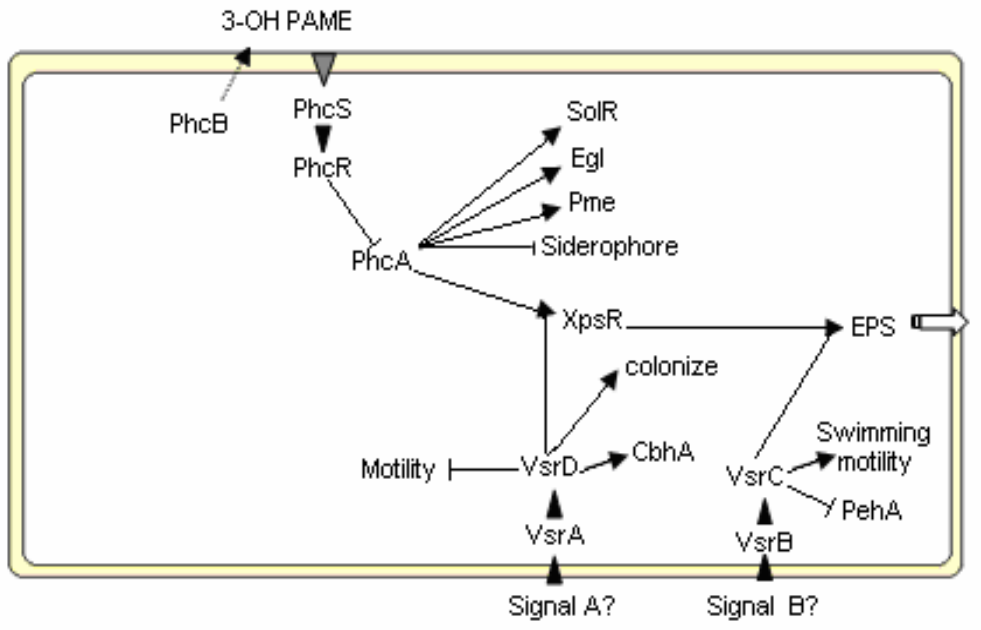

Fig 1.2. Phc regulatory network in *R. solanacearum* (Adapted from Denny, 2006)

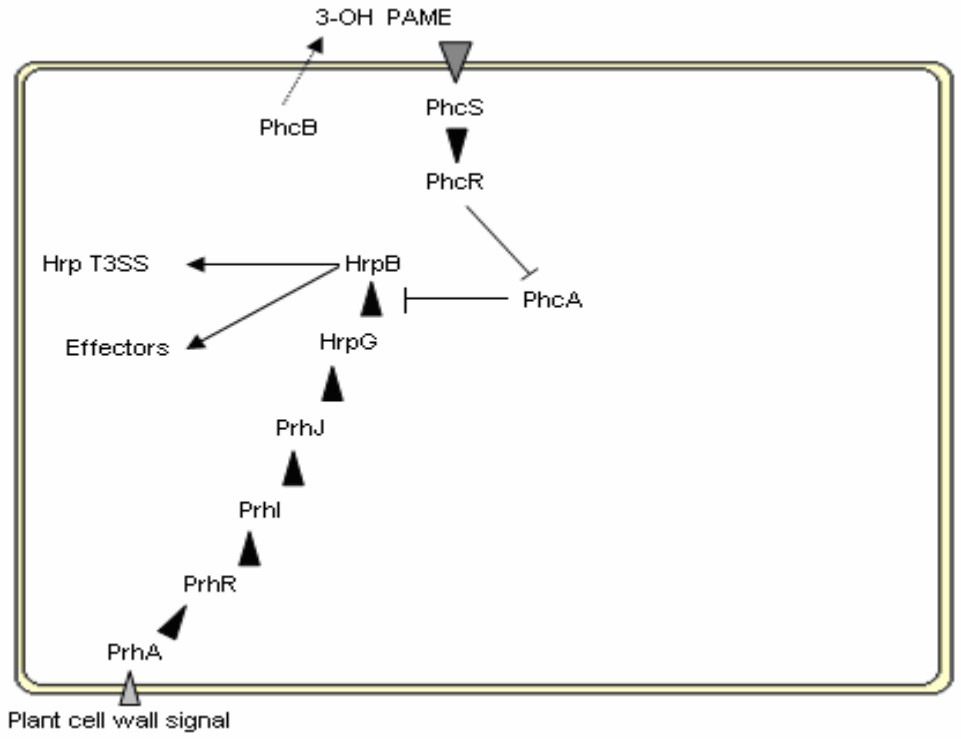

Fig. 1.3. Hrp-encoded Type III Secretion System (T3SS) network in *R. solanacearum.* (Adapted from Denny, 2006).

CHAPTER 2

IDENTIFICATION OF *RALSTONIA SOLANACEARUM* EXOPROTEINS SECRETED BY THE TYPE TWO SECRETION SYSTEM USING PROTEOMIC TECHNIQUES[1]

[1] Zuleta, M. C., Wolff, J., Liu, H., Schell, M. and Denny, T. P. To be submitted to *Molecular Plant-Microbe Interaction.*

Introduction

The type II secretion system (T2SS), which is highly conserved in many Gram-negative bacteria, is one of the ways bacteria export proteins to the extracellular space. The T2SS requires the secreton-dependent pathway (Sdp) proteins encoded by 12 to 16 genes (Desvaux et al. 2004), using *Pseudomonas aeruginosa* as the model to identify the functions of each protein encoded by the T2SS (Filloux et al. 1997). Once proteins reach the periplasm via the Sec-dependent pathway (Mori and Ito 2001) or the Tat pathway (Oates et al. 2003), mature folded proteins are secreted from the periplasm to the extracellular space through a pore formed by SdpD, the integral outer membrane (OM) protein that is a member of the larger secretin family (Kostakioti et al. 2005). The other essential Sdp proteins are SdpF, L and M that form the inner membrane (IM) platform, SdpG, H, I, J and K that are pseudopilins associated with the IM, SdpC and N that connect the IM and OM components, and SdpE that is an ATPase to power protein secretion. The Sdp gene clusters in some bacteria also encode SdpA and SdpB that are required for energy transduction, SdpO, a prepilin peptidase, and SdpS, a small lipoprotein in the OM that stabilizes SdpD pore formation.

R. solanacearum has a conserved and functional T2SS comprising 12 Sdp proteins (Guidot et al. 2007). Like some other bacteria, the essential prepilin peptidase is encoded by *pilD*, which also processes components of the type IV pilus system (Liu et al. 2001). To date the most detailed research on T2SS in *R. solanacearum* was presented by Liu et al. (2005), who found that inactivating *sdpD* (and presumably *sdpE* and *sdpF* due to polar effects of the inserted DNA) prevented secretion of many exoproteins and greatly reduced the pathogen's ability to colonize tomato plants and cause. Among the exoproteins that transit the T2SS are multiple plant cell wall degrading enzymes (CWDE), most of which had previously been identified as

contributing to virulence and colonization (Kang et al. 1994; Denny 2006). However, the loss of virulence could not be attributed solely to the absence of the CWDE, which indicated that additional unidentified proteins are important for virulence (Liu et al. 2005).

Some Gram-negative pathogenic bacteria can have more than one T2SS (Preston et al. 2005) and that some of these systems are functional. In *P. aeruginosa* PAK the alternative T2SS secretes small amounts of lipase, alkaline phosphatase and elastase (Martinez et al. 1998), in *P. aeruginosa* PA01 the Xcp system is required for secretion of exotoxin A, lipases, phospholipases C, alkaline phosphatase, or elastase (LasB) (Filloux et al. 1997)whereas the Hxc system is required for secretion of the low-molecular-weight alkaline phosphatase LapA(Ball et al. 2002). In *P. putida* strain GB-1 the principle and alternative T2SS transport Mn^{2+}-oxidizing factor (de Vrind et al. 2003). In *Xanthomonas campestris* pv. campestris, *X. axonopodis* pv. citri and *X. campestris* pv. vesicatoria the presence of a second complete set of T2SS orthologs suggests that these systems might be functional.

DNA sequence analysis of the GMI1000 genome revealed that, in addition to the typical T2SS, it also has three incomplete T2SS-related clusters with *sdpD-G* homologues (Genin and Boucher 2004). One of these clusters is located in the chromosome and the other two clusters are located on the megaplasmid. Recently, Guidot et al (Guidot et al. 2007) used comparative genomic hybridization (CGH) with microarrays to explore the genomic diversity among four *R. solanacearum* phylotypes. Analysis of the genes encoding alternative T2SS showed high diversity in the distribution of these genes. Phylotype I biovar 3 which was the reference group, conserved the complete three alternative T2SS, among alternative T2SS, the number 3 was the most conserved among strains tested.

This study investigated the role of the primary and alternative SdpD proteins in the *R. solanacearum* T2SS. Mutants lacking either individual *sdpD* genes or combinations of three or four *sdpD* genes were created by introducing unmarked deletions that should have had no effect on expression of downstream genes. The effects on extracellular proteins were examined first using standard 2-D gel electrophoresis and peptide mass fingerprinting of selected gel spots. We also used a shotgun approach employing iTRAQ labeling and liquid chromatography-tandem mass spectrometry (LC-MS/MS) analysis to identify a larger number of proteins and provide quantitative data on relative protein production. Inactivation of the *sdpD* genes and analysis of the exoprotein profile revealed that more proteins than the previously studied are secreted through this system, increasing the number of candidates to 44. Among these proteins are the one(s) responsible for the virulence observed in the *sdpD*1 mutants. Functionality of the alternative T2SS still to be determined. This study is an example of how modern proteomics approaches can help to identify proteins that exit cells via the T2SS and thus provide insight into this system and its role in pathogenicity.

Results

Creation of mutants lacking *sdpD* and *sdpD*-related genes in *R. solanacearum*

R. solanacearum GMI1000 genome sequencing revealed the presence of three incomplete T2SS: one located in the chromosome and the other two located in the megaplasmid. In contrast to the typical T2SS gene cluster comprising at least 12 genes, these incomplete T2SS have of 8 or 9 genes potentially encoding proteins involved in the translocation of a pseudopilus across the inner membrane, pseudopilus platform formation, pseudopilus-like structure formation and the outer membrane secretin pore for protein export (Fig. 2.1). The three incomplete T2SS lack the

proteins that connect the outer and inner membranes, one pseudopilin subunit and the proteins associated with pilus elongation (Fig. 2.1). Homology between the typical SdpD1 secretin and the SdpD-related proteins ranged from a low 27% identity to a high 50% similarity (Table 2.1). Homology was higher among the SdpD-related proteins, ranging from 56% to 63% similarity, indicating that SdpD-related proteins are more related to each other than they are to SdpD1.

Site directed mutagenesis was used to delete each of the *sdpD* genes individually (creating strains GMI1367, GMI1369, GMI1370 and GMI1415) so that expression of downstream genes should not be affected. GMI1367 (*sdpD*2) was used as the background strain to create a triple mutant (GMI1374) lacking all three SdpD-related proteins; this mutant genotype will be referred as 3x*sdpD*. Then *sdpD*1 was deleted from GMI1374 to make a four-fold mutant (GMI1423) lacking all of the potential T2SS secretins; this mutant genotype will be referred as 4x*sdpD*. GMI1374 was also used as the background strain for another four-fold mutant (GMI1388) created by genomic transformation with DNA from GMI1266 (*sdpD*1') (Liu et al. 2005). Disruption of *sdpD*1 in GMI1388 by insertion of pTOK2 should have a polar effect on expression of *sdpE* and *sdpF* genes located downstream and thereby eliminate all T2SS functions (Liu et al. 2005). This mutant genotype will be referred as 4x*sdpD*'. Diagnostic PCR confirmed the unmarked mutations in strain GMI1423 (Fig. 2.2).

β,1-4 endoglucanase (Egl) is one of the enzymes retained in the periplasm by inactivation of the T2SS in GMI1266 (Liu et al. 2005). To assess T2SS function, Egl activity of the *sdpD* mutants was checked using a plate assay containing carboxymethylcellulose as substrate. No Egl activity was observed for the GMI1266 (*sdpD1'*), GMI1415 (Δ*sdpD*1), GMI1423 (4x*sdpD*) and GMI1388 (4x*sdpD'*) (Fig. 2.3). However, the enzymatic activity of GMI1367 (Δ*sdpD*2), GMI1369 (Δ*sdpD*3) and GMI1370 (Δ*sdpD*4) and GMI1374 (3x*sdpD*) mutants, was comparable

to the wild type. These results indicate that inactivation of SdpD1, either with polar or non-polar effects on downstream genes is the principal factor limiting the secretion of this known T2SS exoprotein. This does not exclude the possibility that the SdpD-related proteins function for exporting other proteins.

Virulence assays in tomato plants revealed that deletion of *sdpD*3 in GMI1369 reduced symptom development by an average of 12% in three assays. However, in one assay with more succulent plants, it wilted 100% of the leaves as rapidly as the wild type. In one assay, GMI1367 (Δ*sdpD*2) wilted 94% of the leaves, but in other assays it wilted 100% of the leaves. GMI1370 (Δ*sdpD*4) caused symptoms at wild-type level in all assays. In two assays, GMI1374, the triple mutant lacking all the SdpD-related proteins, wilted 82% of the leaves on average,in assays 1 and 2 but in assays 3, 4 and 5 it caused 100% wilt. GMI1415 (Δ*sdpD*1) wilted 2% of the leaves in contrast to the GMI1266 (*sdpD*1'), which wilted between 7 and 37% of the leaves. GMI1388 (4x*sdpD'*) wilted 2% of the tested leaves, whereas GMI1423 (4x*sdpD*) wilted 7% of the leaves (Fig 2.4). These results indicate that mutating only *sdpD1* is enough to reduce symptom development in tomato as much or more than the polar *sdpD*1' mutant used previously (Liu et al. 2005). The SdpD-related proteins, either alone or in the triple mutant, have little or no effect on symptom development. Symptom reduction in plants inoculated with GMI1369 (Δ*sdpD*3) suggests that this protein may have a role in exporting virulence-related proteins, since a symptom reduction was observed in three of four assays (Fig. 2.4).

Symptom development depended on susceptibility of the plants to *R. solanacearum* as well as the growth stage of the plants inoculated. In assay 5 (Fig 2.4e), the plants were more susceptible because they were less lignified than plants used in other assays. Consequently, plants died in less than 8 days and more symptoms developed in all of the plants inoculated with

the mutants lacking SdpD-related proteins. During this assay, GMI1415 (Δ*sdpD*1) and GMI1423 (4x*sdpD*) behaved as in previous assays, whereas the GMI1266 (*sdpD*1') and the GMI1388 (4x*sdpD'*) wilted up to almost 40% of the leaves. These results showed that even when the inoculated plants were more susceptible, SdpD1 inactivation contributed to major reductions in symptom development.

Colonization tests revealed that mutants lacking one or all three SdpD-related proteins colonized 100% of the inoculated plants, even though not all of the plants were completely wilted. Inactivation of *sdpD*1 (either polar or non-polar) resulted in colonization of 13 to 40% of the plants, which explains the strong symptom reduction when tomato plants were inoculated with these mutants. The four-fold mutants colonized only 30% of the inoculated plants.

***sdpD* mutants protein profile**

2-D gel electrophoresis was performed for each of the mutants generated during this study (Appendix 1). The pI range used was either 3 to 10 or 3 to 11 NL (non-linear) and the polyacrylamide percentage was 10% or 10 t0 20%. Mutants lacking SdpD1 (GMI1266, GMI1415, GMI1388 and GMI1423) had many fewer exoproteins relative to the GMI1000 wild type (Appendix 1). Protein profiles of mutants lacking SdpD-related proteins (GMI1367, GMI1369, GMI1370 and GMI1374) were not noticeably different from the profile observed for the GMI1000 (Appendix 1), indicating that the bulk of the exoproteins require the SdpD1 protein for secretion and the related proteins could be non-functional or secreting few proteins.

If proteins are secreted through the alternative T2SS, the best way to identify them would be to compare the protein profiles of the SdpD1 mutant and the four-fold SdpD mutants. Overlapping false-color, reverse images of the 2-D gels simplified comparison of the SdpD mutants to detect differences in protein secretion (Figs. 2.5 to 2.10). Proteins located in thirty-

two areas were secreted in different amounts when the GMI1266 (*sdpD*1'), GMI1415 (Δ*sdpD*1), GMI1388 (4x*sdpD*') and GMI1423 (4x*sdpD*) were compared (Tables 2.2 and 2.3). Comparing GMI1266 and GMI1388 showed eight regions with more protein secreted by GMI1266 and 17 regions with more proteins secreted by GMI1388. Regions 11, 14 and 20 were remarkably more intense in GMI1266 (*sdpD*1') and absent in the GMI1388 (4x*sdpD*') (Fig. 2.5, Table 2.3). However, similar protein samples run on 10% acrylamide gels (rather than 10-20% acrylamide gradient gels) did not have these three protein spots, so regions 11, 14 and 20 could be gel artifacts. These regions also were not present in 2-D gels of either GMI1415 (Δ*sdpD*1) or GMI1423 (4x*sdpD*).

Comparison of the protein profile between GMI1266 (*sdpD*1') and GMI1415 (Δ*sdpD*1) mutant (Fig. 2.6) showed six regions where more proteins were secreted by GMI1266, whereas there were 11 regions with more protein secreted by GMI1415 (Table 2.3). Comparison of GMI1266 (*sdpD*1') and GMI1423 (4x*sdpD*) mutants, showed 5 regions with more protein secreted by GMI1266 (Fig. 2.7, Table 2.3), whereas 14 regions had more proteins in GMI1423. These results suggest that the insertions mutation that inactivated *sdpD*1' in GMI1266 could affect the number of proteins secreted due to a polar effect that eliminates *sdpE* and *sdpF* expression.

Gel comparison between GMI1415 (Δ*sdpD*1) and GMI1423 (4x*sdpD*) showed that region 31 was only present in GMI1415 (Fig. 2.8, Table 2.3). In contrast, regions 24, 25 and two big regions identified as 6 and 9 were over-secreted in GMI1423. Otherwise, these two mutant produced protein profiles very similar to each other.

Gel comparison between GMI1415 (Δ*sdpD*1) and GMI1388 (4x*sdpD*') revealed 2 areas where protein secretion was more abundant in the non-polar mutant (Fig. 2.9, Table 2.3). On the

other hand, 10 areas were more plentiful in GMI1388, most of them located in the region between pI 6 and 11. Contrary to the results, more proteins were expected for GMI1415 mutant due to the polar effect expected in GMI1388. GMI1423 (4x*sdpD*) showed higher protein secretion than the GMI1388 (4x*sdpD*') polar mutant (Fig. 2.10, Table 2.3). This could be an indication of the effect of the polar mutation in protein secretion.

Protein identification from 2-D gels

To identify the proteins secreted though the typical and alternative T2SS, mass spectrometry was performed on selected protein spots after 2-D gel electrophoresis. Two *R. solanacearum* strains were used: GMI-7 (a strain lacking seven exoproteins that include six CWDEs and Tek) and the GMI1266 (*sdpD*1') mutant. The elimination of seven major exoproteins in GMI-7 facilitated the identification of less abundant proteins that might be secreted through the alternative T2SS.

Proteins precipitated from the GMI-7 supernatant were run in a large 2-D format gel system using an 18 cm, 3-11 IPG strip, and an 8-16% polyacrylamide gel. The gel was stained with Sypro Ruby and protein plugs were harvested robotically. After protein digestion of 49 selected gel spots and FTICR-MS analysis, 12 proteins were identified (Fig. 2.11 and Table 2.4). A second GMI-7 sample was run on a smaller format gel of similar characteristics but using colloidal Coomassie Blue staining (Fig. 2.12). Fifty-six protein spots were processed and 18 proteins were identified; 12 of them had already been identified in the first gel (Table 2.6). A third gel analyzed the exoproteins from GMI1266 using an 11 cm 3-11NL IPG strip and a 10% polyacrylamide gel followed by staining with colloidal Coomassie Blue. GMI1266 secreted many fewer proteins than GMI-7 (Fig. 2.13). Protein spot digestion and FTICR-MS analysis of 29 spots identified 10 proteins, with only one previously identified in GMI-7 (Table 2.4). The low efficiency in protein identification was due to protein plugs producing few peptide mass

peaks and the observed mass of the protein disagreeing with the predicted mass. One protein had a good peptide mass fingerprint, but no match was found in the annotated database (see box in figures 2.12 and 2.13). We suspect that sequence analysis of the genomic DNA missed the open reading frame for this protein. In all, 28 proteins were identified using this method, 13 of which are candidates for substrates of the T2SS (Table 2.4)

The proteins identified on the 2-D gels of GMI-7 and GMI1266 correspond to regions 5, 8, 19, 23, and 26 identified in 2-D gel comparisons of the *sdpD* mutants (Figs. 2.5 to 2.10). Either the other proteins were not selected for identification, they did not have good image alignment, or produced a weak signal in mass spectrometry. A possible explanation for the deviation of protein spots from their predicted pI is that posttranslational modifications, such as hydroxylation and/or phosphorylation in the amino-terminal domain, occurred during protein processing before MS analysis.

Protein identification using iTRAQ and LC-MS/MS

To identify additional candidate proteins as substrates for the T2SS, iTRAQ technology was implemented for *R. solanacearum*. iTRAQ labeling and LC-MS/MS identified 80 proteins in the *sdpD* strains (Table 2.5): 76 in the GMI1266 (*sdpD*1')/GMI1388 (4x*sdpD*') pair and 34 in the GMI1415 (Δ*sdpD*1)/GMI1423 (4x*sdpD*) pair. Thirty proteins were produced by both the polar and non-polar *sdpD* mutants, whereas 46 proteins were present just in the GMI1266 (*sdpD*1')/GMI1388 (4x*sdpD*') pair (Table 2.5 and Fig. 2.14). The four proteins unique to the GMI1415 (Δ*sdpD*1)/GMI1423 (4x*sdpD*) pair were identified as a probable thiol:disulfide interchange signal peptide protein (RSc0285), a putative RHS-related transmembrane protein (RSp1137), a conserved hypothetical protein (RSc0824) and a putative transmembrane protein (RSc1707).

iTRAQ analysis also was used to identify 126 proteins from the pairs of GMI1000 (wild type)/GMI1390 (*vsrD*::pCR2.1) and GMI1277 (*phcA*::Ω)/GMI1272 (*epsB*::pCR2.1) (see Table 3.1). Comparison of results for these four strains, all of which have a functional T2SS, to those for the *sdpD* mutants, revealed 72 proteins that were absent in the *sdpD* mutants (Fig. 2.15). Based on previous results (Liu et al. 2007) and database searches, 44 proteins were classified as T2SS candidates, 10 with known function, 17 with a putative or hypothetical function and 17 with unknown function. Table 2.6 presents these proteins organized according the secretion systems, structural functions and hypothetical or putative functions.

Protein quantification

Every iTRAQ data pair that had a 95% probability of having a relative abundance ratio ≠ 1 and a standard deviation of that ratio of <20% was included to study quantitative differences in protein production among the *sdpD* mutants (Table 2.5). However, we used a 2-fold change in expression as the threshold for biological significance. In the GMI1266 (*sdpD*1')/GMI1388 (4x*sdpD*') pair a total of 70 proteins were quantified out of 76 identified, and 19 had statistically significant differences. There was a ≥2-fold increase in three proteins and a reduction in five proteins secreted by this pair of strains (Fig. 2.16). Proteins secreted in greater abundance by GMI1266 (*sdpD*1') were Rsp0876 (PopB), Rsc0293 (hypothetical signal peptide) and Rsp1415 (hypothetical protein). Proteins under produced by GMI1266 were Rsp0877 (PopA), Rsp0295 (putative hemolysin), Rsc2775 (PopW), Rsp1130 (hypothetical protein) and Rsp0294 (putative hemolysin-type calcium-binding protein). None of these proteins is likely to be secreted by the T2SS.

Two independently produced and labeled samples of GMI1415 (Δ*sdpD*1) and GMI1423 (4x*sdpD)* were analyzed. In the first replicate, 34 proteins were identified, 28 were quantified

and four showed a statistically significant difference. The maximum values were a 30% increase and a 47% decrease in the single mutant compared to the four-fold mutant (Fig. 2.13). The second replicate was very similar: from 34 proteins identified, 29 were quantified and eight were statistically significant. There was a maximum of a 36% increase and a 53% decrease in protein production. None of the quantified proteins exceeded a 2-fold change in expression that we used as the threshold for biological significance. However, the unexpectedly low number of proteins identified in the supernatants of these samples hampered this analysis.

Discussion

Proteomic methods have been used only a few times to study extracellular proteins made by plant pathogenic bacteria. To date, protein visualization techniques like 1-dimensional sodium dodecyl sulfate polyacrylamide gel electrophoresis (SDS-PAGE), 2-dimensional PAGE, and fluorescence 2-D difference gel electrophoresis (DIGE) combined with protein identification using mass spectrometry have been used. In the case of *Xylella fastidiosa*, proteases, antioxidant enzymes, and proteins potentially involved in adhesion and toxicity were identified(Smolka et al. 2003). Watt et al.(Watt et al. 2005), identified many proteins in the supernatant from *Xanthomonas campestris* pv. campestris, among them CWDE and other degradative enzymes; they also found many proteins expected to be cell-associated. The *Erwinia carotovora* pv. atroseptica supernatant contained some of the previously reported pectate lyases, cellulases and proteases, besides flagella structures and a AvrXca homologue (Corbett et al. 2005) and *Erwinia chrysanthemi* produced proteins secreted by the type I system, many CWDE secreted by the T2SS, membrane proteins and some cytoplasmic proteins(Kazemi-Pour et al. 2004).

Many aspects of the conserved T2SS have been studied to determine how the secreton transports folded proteins across the OM(Filloux 2004; Kostakioti et al. 2005). However, despite the fact that bioinformatics cannot predict which periplasmic proteins will be secreted, we found very few reports where a proteomic approach was used to study the T2SS. In *Erwinia carotovora* pv. atroseptica, DIGE was used to compare a wild-type strain with a T2SS (Out) mutant, and detected changes only in four previously characterized extracellular CWDE and an AvrXca homologue that has a role as virulence factor(Corbett et al. 2005). In *Xanthomonas oryzae* pv oryzae, standard 2-D PAGE revealed that a T2SS mutant does not secrete or is reduced in the secretion of several exoproteins, causing strong reduction in extracellular xylanase and cellulose activity.(Furutani et al. 2004). Studies in the non-plant pathogen *Legionella pneumophila*, a human pathogen, identified 20 proteins that are T2SS-dependent, including proteases, peptidases, a phospholipase, a chitinase, and a phosphatase (DebRoy et al. 2006). Unusually, the supernatant from the T2SS mutant lacked all the major proteins produced by the wild type when analyzed by 2-D PAGE, including six proteins not secreted by the T2SS. iTRAQ labeling and LC-MS/MS analysis were used to profile the secretome of *Pseudoalteromonas tunicata,* a bacterium that inhibits different marine organisms(Evans et al. 2007). Among the 182 proteins identified, most of which were released from the cytoplasm by cell lysis, only five appear to be dependent on the T2SSs, among which are several for iron transport and acquisition.

Earlier studies with *R. solanacearum* used 1-D SDS-PAGE to observe a marked reduction in the number or abundance of exoproteins produced by two different T2SS mutants(Kang et al. 1994; Liu et al. 2005). Those mutants resulted from insertions expected to have polar effects on downstream genes that encode “core” components of the type II secreton and, therefore, their T2SS should have been completely inactive. In addition to reexamining

mutant GMI1266 (*sdpD*1') created by Liu et al.(2005), we created and examined mutants with non-polar deletions that should have eliminated only SdpD1, the major secretin, and one to three different SdpD-like proteins. These mutations should have left the core secreton in tact (although complementation tests are still required to prove this).

We found that, as expected, deleting *sdpD*1 in GMI1415 or inactivating the T2SS in GMI1266 greatly reduced the number of exoproteins observed on 2-D gels, confirming and extending the results of Liu et al. (2005). However, the 2-D gels of exoproteins made by the SdpD-related single mutants or the triple mutant lacking all three SdpD-related proteins were essentially identical to those of their wild type parent, making it difficult to identify any proteins affected by eliminating these secretin-like proteins. Consequently, it seems that SdpD1 is required for functionality of the principle T2SS and that the SdpD-like proteins cannot replace it.

Overlapping false-color, reverse images of the 2-D gels helped to detect differences in protein profiles between pairs of SdpD mutants. If the SdpD-like proteins or the alternative T2SS are functional, then mutants lacking only SdpD1 (Δ*sdpD*1) or the conserved T2SS (*sdpD*1') should have secreted more proteins than mutants lacking all four secretins (4x*sdpD*) or lacking the T2SS and the SdpD-like secretins (4x*sdpD*'). However, in almost all cases, we observed the reverse (Figs. 2.5 and 2.7 to 2.10). These unexpected differences may be due to gel artifacts or side-effects of eliminating all the SdpD proteins (e.g., causing greater leakage of periplasmic proteins). The one pair of mutants that behaved as predicted was that of GMI1266 (*sdpD*1') and GMI1415 (Δ*sdpD*1), because the supernatant of the latter mutant, which retained its wild-type SdpD-like proteins and a potentially functional T2SS core secreton, had more proteins than the former (Fig. 2.6). Further work is required to identify if this difference is real and whether any of the proteins over produced by GMI1415 are secreted by the alternative T2SS.

Recently, Guidot et al. (2007) used comparative genomic hybridization with microarrays to explore the genetic diversity of the *R. solanacearum* species complex by compare the gene content in GMI1000 (phylotype I, biovar 3) to that in 16 additional strains. As expected, all the strains have the gene cluster encoding the conserved T2SS, but other than GMI1000 only one additional phylotype I, biovar 3 strain encodes all three alternative T2SS. Two phylotype I biovar 4 strains encode the alternative #2- and #3-T2SS, but they have few genes for the #4-T2SS. Four of five phylotype II strains have #3-T2SS genes, but not the other two alternative T2SS. The exception is strain IPO1609, the only race 3 biovar 2 strain examined, which has not complete alternative T2SS gene clusters. All five phylotype III strains have #2-T2SS genes but lack some of the #4-T2SS genes; three strains also have #3-T2SS genes. One of three phylotype IV strains has #2-T2SS genes, but the other clusters are incomplete in this and the other two strains. It is clear from these results that the alternative T2SS in *R. solanacearum* are not highly conserved, which suggests that they are not essential for pathogenesis. Although we did not conclusively detect any proteins secreted by the alternative type II systems, we think that the presence of these alternative T2SS may still be important for this strain under certain circumstances.

Although 2-D gels were useful for detecting changes in protein profiles, this was an inefficient method for protein identification. Determining peptide mass fingerprints using MS identified just 30% of the selected 2-D gel spots, resulting in the identification of only13 T2SS candidates. This low yield was partly due to our using strain GMI-7, which does not produce most of the plentiful exoproteins (because they had previously been identified using 2-D gels). We also had problems with apparent gel artifacts, because spots that were present in a 10-20% polyacrylamide gel were not present when using a 10% polyacrylamide gel. However, we

detected on our 2-D gels a major protein spot that does not appear to be in the annotated database of open reading frames, something a gel-free method could not do so easily.

To identify a larger number of candidate substrates for the *R. solanacearum* T2SS, we used iTRAQ labeling and LC-MS/MS. We identified a total of 152 proteins, among which are 44 T2SS candidates including 10 characterized T2SS proteins, 17 hypothetical proteins with putative function, and 17 proteins with unknown function. Out of these, five proteins were identified only by iTRAQ LC-MS/MS. The remaining 39 proteins were identified previously from 2-D gels and regular LC-MS/MS. This indicates that *R. solanacearum* secretes more than the known CWDEs through its T2SS, and that its T2SS appears to secrete substantially more proteins than observed for any other bacterium to date. It remains to be determined which protein, or more likely groups of proteins, that transit the T2SS is responsible for the ability of *R. solanacearum* to systemically colonize tomato plants.

Materials and Methods

Bacterial strains and gene targets

Strains and plasmids used in this study are listed in Table 2.7. *R. solanacearum* mutants and *E. coli* DH5α strains containing plasmids with the deletion alleles were stored in glycerol at -80^{o}C after PCR and enzyme digestion confirmation of the constructs.

Media and growth conditions: *R. solanacearum* strains were grown routinely in BG broth (1% Bacto peptone, 0.1% casamino acids, 0.1% yeast extract and 0.5% glucose) or BG agar (BG broth + 1.6% agar) at 30^{o}C. Minimal medium (Clough et al. 1994) plus 0.5%, 1.0% or 1.5% sucrose was used in the unmarked mutagenesis procedure. 3x MM plus 0.5% glucose were used to prepare the inoculum for virulence assays. MMP (10 mM K_2HPO_4, 5 mM NaH_2PO_4, 5 mM

$(NH_4)_2SO_4$, 1 mM $MgSO_4$, 0.1 mM $CaCl_2$, non Fe trace elements, 0.01 mM $FeCl_3$, 55 mM sodium citrate and 0.1% glycerol, pH 7.0) was used to grow bacteria in preparation for exoprotein precipitation. *E. coli* DH5α strains were grown in Luria–Bertani broth or Luria–Bertani agar at 30–37°C (Maniatis et al. 1982).

DNA manipulation and transformation

Cloning followed standard protocols. *E. coli* heat-shock competent cells were prepared using $CaCl_2$ and *R. solanacearum* electroporation-competent cells were prepared using 10% glycerol (Sambrook et al. 1989). Electroporation was performed as described elsewhere (Ausubel et al. 1989), except that cells were shaken in BG broth for one hour before plating on BG agar containing antibiotic. *R. solanacearum* genomic DNA isolation used the method described by Chen and Kuo (1993) modified to include proteinase K (0.2mg ml^{-1}) for 5 min prior to lysis and Phase Lock Gel tubes (Eppendorf) during the separation of the organic and aqueous phases. Natural transformation of *R. solanacearum* was done as described elsewhere (Liu et al. 2001).

PCR conditions: PCR primers were synthesized by IDT (Coralville, IA, U.S.A). The MasterAmp *Tfl* DNA polymerase kit (Epicentre Technologies, Madison, WI) was used for splice overlap extension (SOE) PCR and diagnostic PCR amplification. SOE and diagnostic PCR reactions contained 1x MasterAmp *Tfl* PCR buffer, 2.5 mM $MgCl_2$, 3X MasterAmp PCR Enhancer, 200 µM dNTP, 1 µM forward primer, 1 µM reverse primer, 0.5 Unit MasterAmp *Tfl* DNA Polymerase. The standard PCR program included initial denaturation at 94°C for 4 min, followed by 30 cycles of 94°C for 40 s, 62°C for 2 min and 72°C for 3 min, and a final elongation at 72°C for 10 min. KOD hot start polymerase (Novagen, San Diego, CA, U.S.A) was used to amplify wild-type fragments during unmarked mutant confirmation. Table 2.8 contains a list of primers used in SOE PCR.

Plasmid construction and unmarked mutants creation

The technique described by (Horton et al. 1993) and successfully applied in *R. solanacearum* (Liu et al. 2005) allows the deletion of a region using SOE PCR. Briefly, two pairs of primers were used to amplify two approximately 500- to 1000-bp regions flanking the gene targeted for deletion. These fragments were then joined during the SOE reaction to create a deletion allele that was cloned into pEX18Tc. The deletion was then introduced into the genome by a two-step, SacB-assisted homologous recombination process. Pools containing 10 tetracycline-sensitive and sucrose resistant colonies were screened by colony PCR, after mixing in 50µl water and heating to 100^{o}C for 9 min prior to amplification using SOE1 and SOE4 primers or SOE4 and DIAG primers. Colonies in pools that produced an amplicon of approximately 1 kb (SOE1-SOE4) or 500 bp (SOE4-DIAG) were tested individually to find the positive colonies. Deletion of the target region was confirmed by PCR amplification from the wild type and the putative mutant using SOE1 and SOE4 primers.

Virulence assays

Tomato (*Lycopersicum sculentum*, cultivar Bonnie Best) plants were inoculated using the soil drench method previously described by Liu et al. (2001). Briefly, tomato plants with six to seven leaves were inoculated by pouring 40 ml of a 1 x 10^{7} c.f.u. ml^{-1} cell suspension into each pot. Plants were evaluated daily until day 15 to determine the average number of wilted leaves. At the end of the assay, pathogen colonization of asymptomatic plants was determined by excising a 0.5-cm stem section at the cotyledon level, incubating each section for one hour in 1 mL sterile distilled water, and then spotting 20 µL drops on BG agar. Mucoid morphology of 48-hours old colonies indicated *R. solanacearum* colonization.

Protein precipitation

R. solanacearum cells were grown in MMP at 30°C with shaking (250 rpm) until reaching OD_{600} = 1.0. Cells were removed by centrifugation (4°C, 25 min, 8,800 *g*) and filtration (0.20 μm pore size; Supor® 200, Pall). Cell-free filtrates were stored immediately at –20°C. To remove polysaccharides, cetyl trimethyl ammonium bromide (CTAB) was added to filtrates of EPS^+ strains to a final concentration of 0.1% and sodium deoxycholate (DOC) was added to filtrates of EPS^- strains to a final concentration of 1%. Samples were incubated on ice for 10 min and then centrifuged (4°C, 30 min, 8,000 *g)*. The supernatant was recovered and proteins precipitated by adding 100% trichloroacetic acid to a final concentration of 10%, incubating on ice for 30 min and centrifuging as above. The supernatant was discarded and the protein pellet was suspended (0.1X original volume) in absolute EtOH or 100% acetone for EPS^+ or EPS^- samples, respectively. After the insoluble protein was evenly distributed among 2.0–mL microcentrifuge tubes it was pelleted (4°C, 10 min, 11,000 *g*) and then washed two more times. A representative protein pellet was dissolved in 10 μL 0.1 M NaOH and quantified using the enhanced BCA assay according to the manufacturer's protocol (Pierce Biotechnology, Inc. Rockford, IL. USA).

2-D gel electrophoresis

Protein pellets with ≈ 50 μg protein were solubilized in 200 μL of a buffer containing 9 M UREA, 2% CHAPS (3-[(3-cholamidopropyl)dimethyl-ammonio] propane sulfonate), a trace of bromophenol blue, 20 mM DTT (dithiothreitol), 2 mM TCEP (Tris-(-2-carboxyethyl) phosphine) and 0.4% Bio-lyte 3/10 Ampholyte (Bio-Rad) in Milli-Q water, pH 5.0. Protein was applied to IPG strips (Immobiline Drystrip, GE Healthcare) that were hydrated overnight at room temperature. Electrofocusing was performed in a PROTEAN IEF Cell (Bio-Rad) at 20°C constant temperature and a 3-step program. Focusing started with 250 V for 20 min, and then the

voltage increased to 4500 V following a linear slope. This voltage was maintained for a total of 27,000 to 28,000 volt-hours, and then the voltage was reduced to 500 V until the run was terminated (within 2 hours). The strips were stored at -80^{o}C. IPG strips were thawed at room temperature and then "refocused" for an additional 1000 volt-hours immediately prior to subsequent steps. Proteins were reduced by incubating an IPG strip in equilibration buffer (0.375 M Tris HCl, 6 M urea, 20% glycerol, 2% SDS, pH 9.0) containing 1% DTT for 20 min with gentle agitation. Proteins were alkylated by repeating the process using an equilibration buffer containing 2.5% iodoacetamide (IAA) rather than DTT. The IPG strip was embedded in molten low-temperature agarose dissolved in 1X TGS with a trace of bromophenol blue (Overlay agarose, Bio-Rad) on top of an SDS slab gel (Criterion gel, Bio-Rad). Electrophoresis proceeded in 1X TBG buffer (25 mM Tris, 192 mM glycine and 0.1% SDS (w/v), pH 8.3) at 165 V for approximately 75 min.

Gels to be photographed were stained with silver using the procedure of Blum et al. (1987) with slight modifications. Proteins were fixed with a solution of 50% EtOH, 12% acetic acid and 0.05% formaldehyde for 1 to 3 hours with gentle agitation and rinsed with 50% EtOH. The gel was then incubated in sensitizer solution (0.02% sodium thiosulfate) for 1 minute and washed three times with Milli-Q water. The gel was incubated in 0.2% silver nitrate plus 0.075% formaldehyde for 20 min, washed two times with Milli-Q water, and treated with the developer solution (6% sodium carbonate, 0.02% sodium thiosulfate, 0.05% formaldehyde) for 2 to 4 min. The reaction was stopped by transferring the gel to 1% glycine for 10 min before washing with water and storing at 4^{o}C. Gels to be used for protein identification were stained with colloidal Coomassie Blue (Bio-Safe, Bio-Rad) or Sypro Ruby.

Protein identification from 2-D gels

Proteins in gel plugs were digested as previously described (Shevchenko et al. 1996) with some modifications. Stain was removed by soaking gel plugs in 50 mM ammonium bicarbonate (ABC)/50% methanol for 30 min at 37°C. The plugs were then dehydrated in 100% acetonitrile (ACN) and dried in a vacuum centrifuge (SpeedVac). Proteins in the plugs were reduced with 10 mM DTT (in 20 mM ABC) for 30 min at room temperature and alkylated with IAA (100 mM IAA in 20 mM ABC) for 30 min at room temperature in the dark. Plugs were washed with 50 mM ABC in 50% methanol, dehydrated in ACN and dried a second time, and then rehydrated in 20 mM ABC, 10% ACN, containing 15-20 μg ml^{-1} trypsin (Sigma). Digestion proceeded for one hour at 37°C and then overnight at room temperature. The supernatant was transferred to Eppendorf Protein LoBind tubes that were pre-washed with 50% ACN/0.1% TFA. Peptides remaining in the gel plug were recovered by incubation for 30 min in 50% ACN/0.1% TFA and repeating the process. These supernatants were pooled with the initial supernatant, and samples were then dried in a SpeedVac at room temperature and stored at -20°C until MS analysis.

Dried samples were dissolved in 80% ACN prior to MALDI-FTICR-MS using a Bruker BioApex 7 Tesla mass spectrometer in the Chemistry Department at the University of Georgia. The matrix used for sample analysis was 2, 5-dihydroxybenzoic acid (DHB). Data were interpreted with the MS-Fit program (http://prospector.ucsf.edu/prospector/4.0.8/html/msfit.htm) using a *R. solanacearum* mass peptide database. The molecular weight and pI of the mature proteins were calculated using SignalP http://www.cbs.dtu.dk/services/SignalP/ and ExPASy http://www.expasy.org/tools/pi_tool.html servers. These values were matched with the 2-D gel images to assess the accuracy of the identified protein.

Protein identification using iTRAQ and LC-MS/MS.

Exoproteins were precipitated as indicated for 2-D-gel preparation, but 100% acetone was used instead of EtOH to remove any CTAB or DOC reagents. The initial protein concentration was 100 μg for each sample. Proteins were digested and peptides were labeled according to the manufacturer's protocols (Applied Biosystems). Samples were then acidified by adding phosphoric acid and loaded on a 0.2 ml cation-exchange cartridge (Applied Biosystems). Labeling reagents were washed out and peptides were recovered by step-wise elution with 1 mL each of 50, 100, 150, 250 and 500 mM KCl. Selected fractions were pooled (fraction 1 = 50 mM KCl, fraction 2 = 100 and 150 mM KCl, and fraction 3 = 250 and 500 mM KCl) and dried in a SpeedVac. Each fraction was dissolved in 1 mL of 2% acetonitrile (ACN) containing 1% formic acid and desalted using a C18 Sep-Pak cartridge (Waters; 1 cc cartridge with a pore size of 125 Å and 80 μm particle size) using 1 mL of 2% ACN and 1% formic acid. Peptides were recovered in 650 μL of 70% ACN and 1% formic acid in Eppendorf LoBind Protein tubes previously washed with the same solution. Samples were dried in a SpeedVac and stored at -20^{o}C prior to LC-MS/MS.

LC-MS/MS was performed by the Cornell University Biotechnology Resource Center Proteomics and Mass Spectrometry Core Facility. Peptide samples were reconstituted in 45 μL of 0.1% formic acid with 2% ACN prior to mass spectrometry. Peptides (6.4 μL) were injected using a Famous auto-sampler onto a PepMap C-18 trap column (5 μm, 300 μm × 5 mm, Dionex) for on-line desalting and then separated on a PepMap C-18 reversed phase nano column, eluted in a 90-minute gradient of 5% to 40% acetonitrile in 0.1% formic acid at 250 nL/min. The nanoLC was connected in-line to a hybrid triple quadrupole linear ion trap mass spectrometer (4000 Q Trap, ABI/MDS Sciex) equipped with Micro Ion Spray Head ion source. MS data

acquisition was performed using Analyst 1.4.1 software (Applied Biosystems) in the positive ion mode for information-dependant acquisition analysis. The nanospray voltage was 2.0 kV in positive ion mode. Nitrogen was used as the curtain (value of 10) and collision gas (set to high) with heated interface at 150°C. The declustering potential was set at 50 eV and Gas1 was 15 psi. During information-dependent acquisition analysis, after each survey scan from *m/z*=400 to *m/z*=1550 and an enhanced resolution scan, the three highest intensity ions with multiple charge states were selected for tandem MS (MS/MS) with rolling collision energy applied for detected ions based on different charge states and *m/z* values.

MS/MS spectra generated from nanoLC/ESI-based IDA analyses were interrogated using ProteinPilot™ software 1.0 (Applied Biosystems) for database search against the MS-Fit database by Paragon method. The default setting for trypsin with methyl methanethiosulfonate modification of cysteine and a methionine oxidation was used for quantitative processing and rapid ID. The protein identifications are reported with total ProtScore >1.3 for each protein representing > 95% statistical significance in ProteinPilot. Quantification data was considered statistically significant when the error factor (EF) was < 2 and the confidence score was 95% (P values $\leq$ 0.05).

References

Ausubel, F. M., Brent, R., Kingston, R. E., More, D. D., Seidman, J. G., Smith, J. A., and Struhl, K. 1989. Short Protocols in Molecular Biology. Green Publishing Assoc. and Wiley-Interscience, New York.

Ball, G., Durand, E., Lazdunski, A., and Filloux, A. 2002. A novel type II secretion system in *Pseudomonas aeruginosa*. Mol. Microbiol. 43:475-485.

Blum, H., Beier, H., and Gross, H. J. 1987. Improved silver staining of plant proteins, RNA and DNA in polyacrylamide gels. Electrophoresis 8:93-99.

Chen, W. P., and Kuo, T. T. 1993. A simple and rapid method for the preparation of gram-negative bacterial genomic DNA. Nucleic Acids Res. 21:2260

Clough, S. J., Schell, M. A., and Denny, T. P. 1994. Evidence for involvement of a volatile extracellular factor in *Pseudomonas solanacearum* virulence gene expression. Mol. Plant-Microbe Interact. 7:621-630.

Corbett, M., Virtue, S., Bell, K., Birch, P., Burr, T., Hyman, L., Lilley, K., Poock, S., Toth, I., and Salmond, G. 2005. Identification of a new quorum-sensing-controlled virulence factor in *Erwinia carotovora* subsp. *atroseptica* secreted via the type II targeting pathway. Mol. Plant-Microbe Interact. 18:334-342.

de Vrind, J., de Groot, A., Brouwers, G. J., Tommassen, J., and Vrind-de Jong, E. 2003. Identification of a novel Gsp-related pathway required for secretion of the manganese-oxidizing factor of *Pseudomonas putida* strain GB-1. Mol. Microbiol. 47:993-1006.

DebRoy, S., Dao, J., Soderberg, M., Rossier, O., and Cianciotto, N. P. 2006. *Legionella pneumophila* type II secretome reveals unique exoproteins and a chitinase that promotes bacterial persistence in the lung. Proc. Natl. Acad. Sci. U. S. A 103:19146-19151.

Denny, T. P. 2006. Plant pathogenic *Ralstonia* species. Pages 573-644 in: Plant-Associated Bacteria. S. S. Gnanamanickam, ed. Springer, Dordrecht, The Netherlands.

Desvaux, M., Parham, N. J., Scott-Tucker, A., and Henderson, I. R. 2004. The general secretory pathway: a general misnomer? Trends Microbiol. 12:306-309.

Filloux, A. 2004. The underlying mechanisms of type II protein secretion. Biochem. Biophys. Acta 1694:163-179.

Filloux, A., Michel, G., and Bally, M. 1997. GSP-dependent protein secretion in Gram-negative bacteria: the Xcp system of *Pseudomonas aeruginosa*. FEMS Microbiol. Rev. 22:177-198.

Furutani, A., Tsuge, S., Ohnishi, K., Hikichi, Y., Oku, T., Tsuno, K., Inoue, Y., Ochiai, H., Kaku, H., and Kubo, Y. 2004. Evidence for HrpXo-dependent expression of type II secretory proteins in *Xanthomonas oryzae* pv. oryzae. J. Bacteriol. 186:1374-1380.

Genin, S., and Boucher, C. 2004. Lessons learned from the genome analysis of *Ralstonia solanacearum*. Annu. Rev. Phytopathol. 42:107-134.

Guidot, A., Prior, P., Schoenfeld, J., Carrere, S., Genin, S., and Boucher, C. 2007. Genomic structure and phylogeny of the plant pathogen *Ralstonia solanacearum* inferred from gene distribution analysis. J. Bacteriol. 189:377-387.

Hoang, T. T., Karkhoff-Schweizer, R. R., Kutchma, A. J., and Schweizer, H. P. 1998. A broad-host-range Flp-FRT recombination system for site-specific excision of chromosomally-located DNA sequences: application for isolation of unmarked *Pseudomonas aeruginosa* mutants. Gene 212:77-86.

Horton, R. M., Ho, S. N., Pullen, J. K., Hunt, H. D., Cai, Z. L., and Pease, L. R. 1993. Gene-splicing by overlap extension. Methods Enzymol. 217:270-279.

Kang, Y., Huang, J. Z., Mao, G. Z., He, L. Y., and Schell, M. A. 1994. Dramatically reduced virulence of mutants of *Pseudomonas solanacearum* defective in export of extracellular proteins across the outer membrane. Mol. Plant-Microbe Interact. 7:370-377.

Kazemi-Pour, N., Condemine, G., and Hugouvieux-Cotte-Pattat, N. 2004. The secretome of the plant pathogenic bacterium *Erwinia chrysanthemi*. Proteomics 4:3177-3186.

Kostakioti, M., Newman, C. L., Thanassi, D. G., and Stathopoulos, C. 2005. Mechanisms of protein export across the bacterial outer membrane. J. Bacteriol. 187:4306-4314.

Liu, H., Kang, Y., Genin, S., Schell, M. A., and Denny, T. P. 2001. Twitching motility of *Ralstonia solanacearum* requires a type IV pilus system. Microbiology-UK 147:3215-3229.

Liu, H., Sherling, C. M., Zuleta, M. C., Wolff, J. J., Wells, L., Amster, I. J., Schell, M. A., and Denny, T. P. (2007). Exploring the secretome of *Ralstonia solanacearum*: mass spectral analysis to identify proteins secreted through the type II system. unknown (Abstract)

Liu, H., Zhang, S., Schell, M. A., and Denny, T. P. 2005. Pyramiding unmarked mutations in *Ralstonia solanacearum* shows that secreted proteins in addition to plant cell wall degrading enzymes contribute to virulence. Mol. Plant-Microbe Interact. 18:1296-1305.

Malhotra, S., Silo-Suh, L. A., Mathee, K., and Ohman, D. E. 2000. Proteome analysis of the effect of mucoid conversion on global protein expression in *Pseudomonas aeruginosa* strain PAO1 shows induction of the disulfide bond isomerase, DsbA. J. Bacteriol. 182:6999-7006.

Maniatis, T., Fritsch, E. F., and Sambrook, J. 1982. Molecular cloning: a laboratory manual. Cold Spring Harbor Laboratory, Cold Spring Harbor, NY.

Martinez, A., Ostrovsky, P., and Nunn, D. N. 1998. Identification of an additional member of the secretin superfamily of proteins in *Pseudomonas aeruginosa* that is able to function in type II protein secretion. Mol. Microbiol. 28:1235-1246.

Mori, H., and Ito, K. 2001. The Sec protein-translocation pathway. Trends Microbiol. 9:494-500.

Oates, J., Mathers, J., Mangels, D., Kuhlbrandt, W., Robinson, C., and Model, K. 2003. Consensus structural features of purified bacterial TatABC complexes. J. Mol. Biol. 330:277-286.

Pappin, D. J. C., Hojrup, P., and Bleasby, A. J. 1993. Rapid identification of proteins by peptide-mass fingerprinting. Curr. Biol. 3:327-332.

Preston, G. M., Studholme, D. J., and Caldelari, I. 2005. Profiling the secretomes of plant pathogenic Proteobacteria. FEMS Microbiol. Rev. 29:331-360.

Salanoubat, M., Genin, S., Artiguenave, F., Gouzy, J., Mangenot, S., Arlat, M., Billault, A., Brottier, P., Camus, J. C., Cattolico, L., Chandler, M., Choisne, N., Claudel-Renard, C., Cunnac, S., Demange, N., Gaspin, C., Lavie, M., Moisan, A., Robert, C., Saurin, W., Thébault, P., Schiex, T., Siguier, P., Whalen, M., Wincker, P., Levy, M., Weissenbach, J., and Boucher, C. A. 2002. The genome sequence of the wide host-range plant pathogen *Ralstonia solanacearum*. Nature 415:497-502.

Sambrook, J., Fritsch, E. F., and Maniatis, T. 1989. Molecular Cloning, A Laboratory Manual. Cold Spring Harbor Laboratory Press, Plainview, NY.

Shevchenko, A., Wilm, M., Vorm, O., and Mann, M. 1996. Mass spectrometric sequencing of proteins from silver stained polyacrylamide gels. Anal. Chem. 68:850-858.

Smolka, M. B., Martins, D., Winck, F. V., Santoro, C. E., Castellari, R. R., Ferrari, F., Brum, I. J., Galembeck, E., Coletta, H. D., Machado, M. A., Marangoni, S., and Novello, J. C. 2003. Proteome analysis of the plant pathogen *Xylella fastidiosa* reveals major cellular and extracellular proteins and a peculiar codon bias distribution. Proteomics 3:224-237.

Watt, S. A., Wilke, A., Patschkowski, T., and Niehaus, K. 2005. Comprehensive analysis of the extracellular proteins from *Xanthomonas campestris* pv. campestris B100. Proteomics 5:153-167.

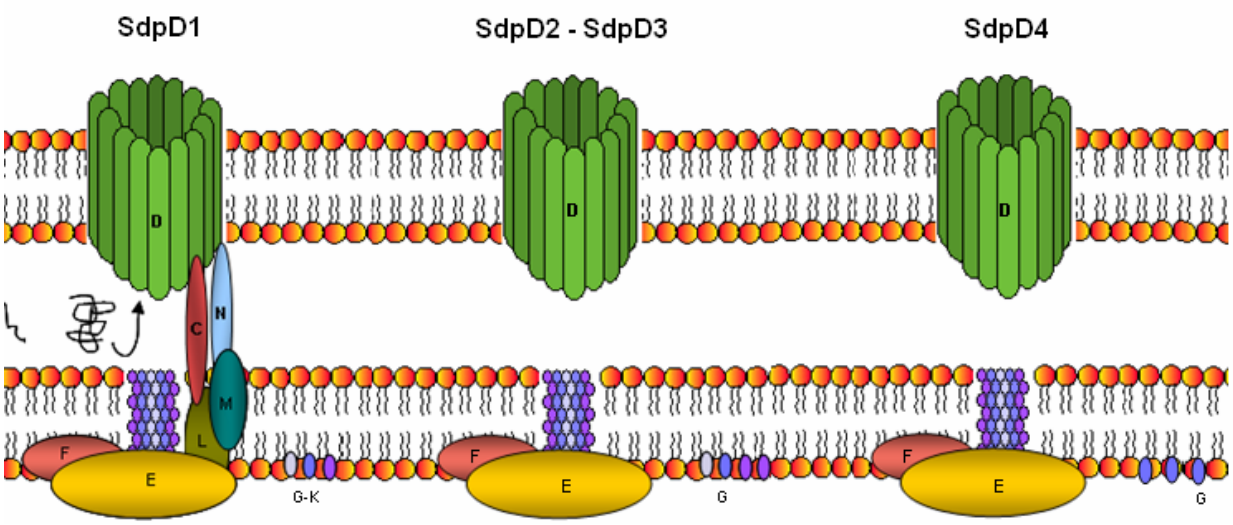

Cluster 1
Chromosome

Cluster 2
Chromosome

Cluster 3
Megaplasmid

Cluster 4
Megaplasmid

Fig 2.1. Cellular organization of the type II secreton dependent proteins in *R. solanacearum* GMI1000.

Table 2.1. Protein sequence comparison of SdpD1 (the T2SS secretin) with SdpD-related proteins from the incomplete T2SS in *R. solanacearum* GMI1000.

	% Sequence homology [a]		
	SdpD1	SdpD2	SdpD3
SdpD2	27 (42)		
SdpD3	28 (50)	42 (61)	
SdpD4	27 (47)	38 (56)	42 (63)

[a] Percentage amino acid identity (similarity).

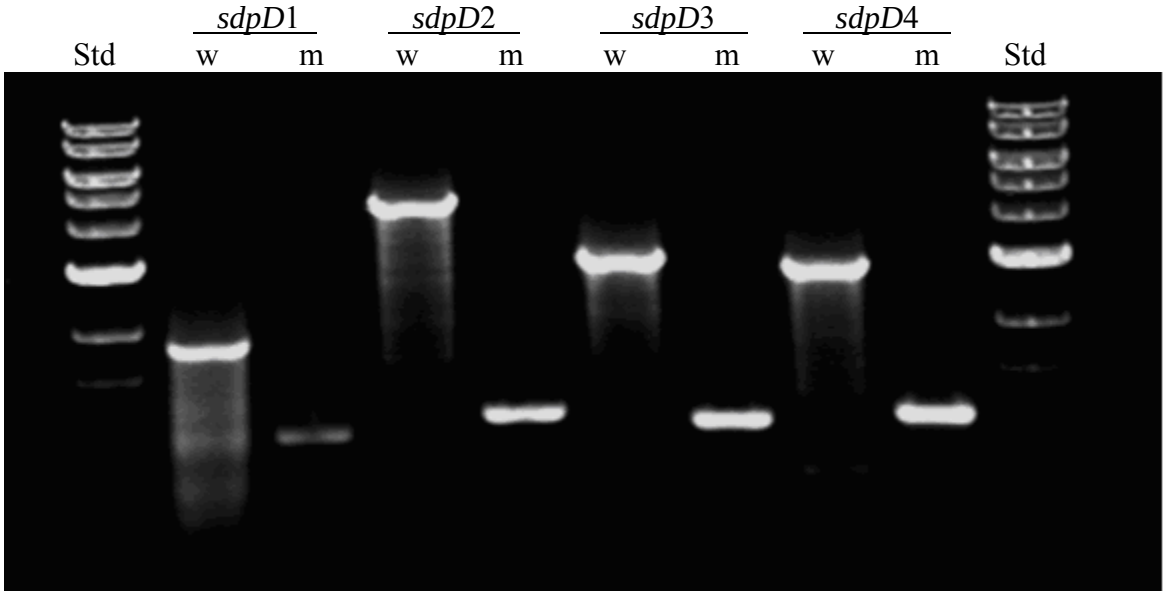

Fig 2.2. PCR confirmation of the deletions in *sdpD*1 and *sdpD*-related genes in *R. solanacearum* strain GMI1423 (4x*sdpD*). The four SOE1 and SOE4 primer pairs were used in four PCR reactions with genomic DNA templates from either GMI1000 (w) or the GMI1423 mutant (m). The DNA size standard (Std) was the 1-kb ladder from New England Biolabs.

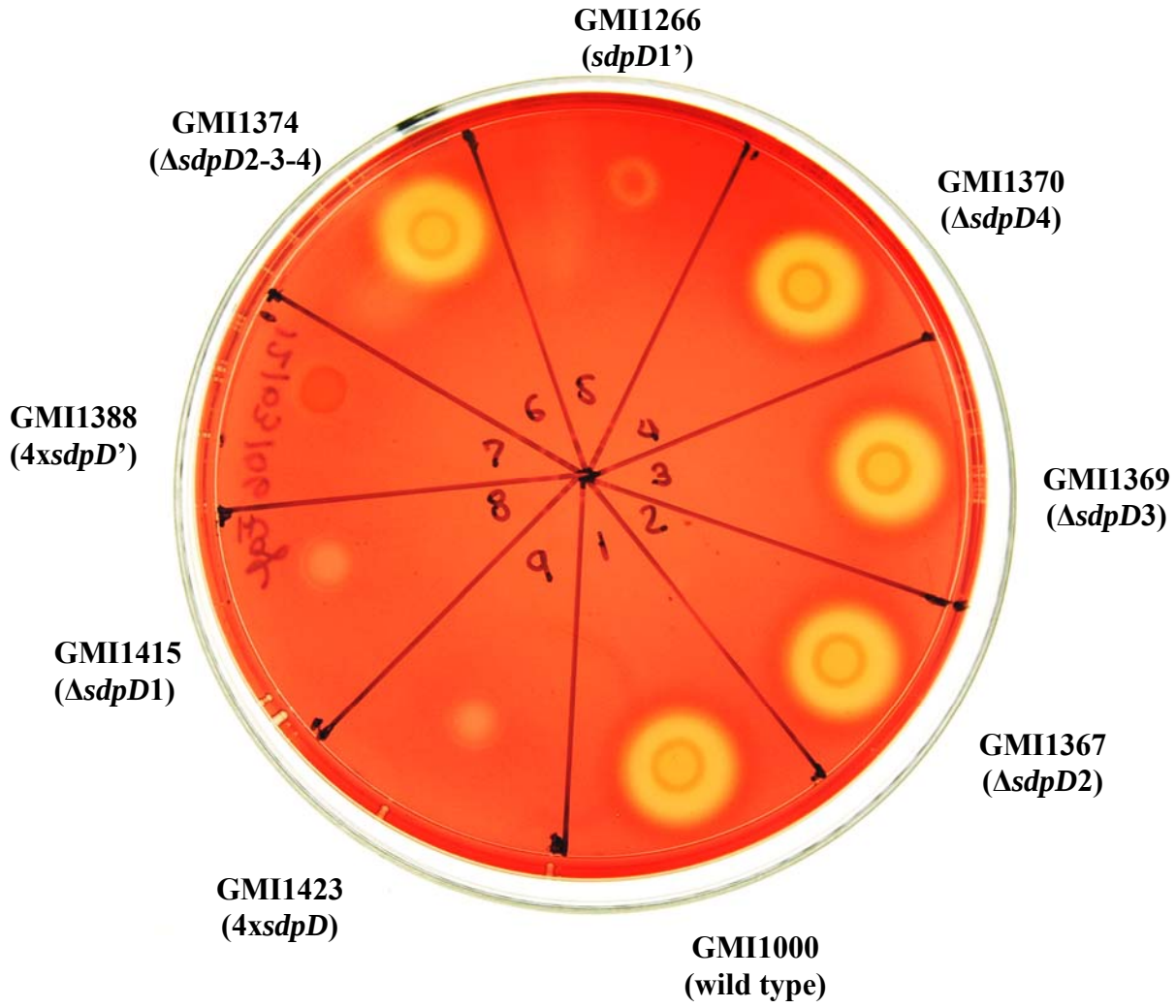

Fig 2.3. Endoglucanase activity of *sdpD* mutants. The assay plate was developed after 24 hours incubation. Yellow halos show where the carboxymethylcellulose substrate had been degraded by Egl activity.

a) Assay 1

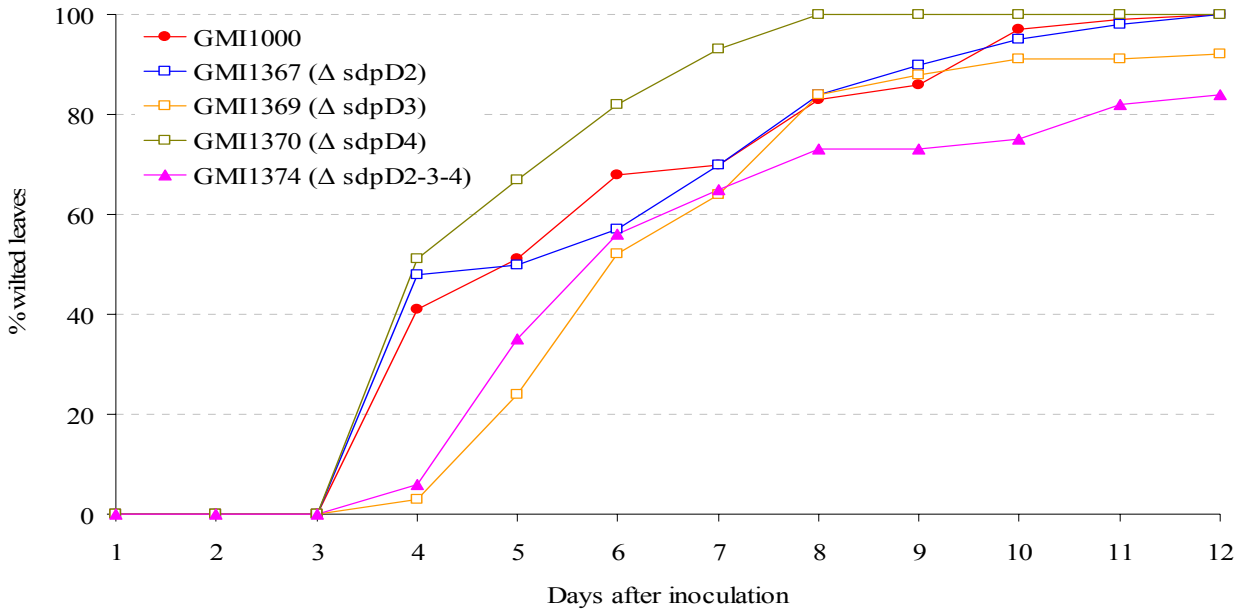

b) Assay 2

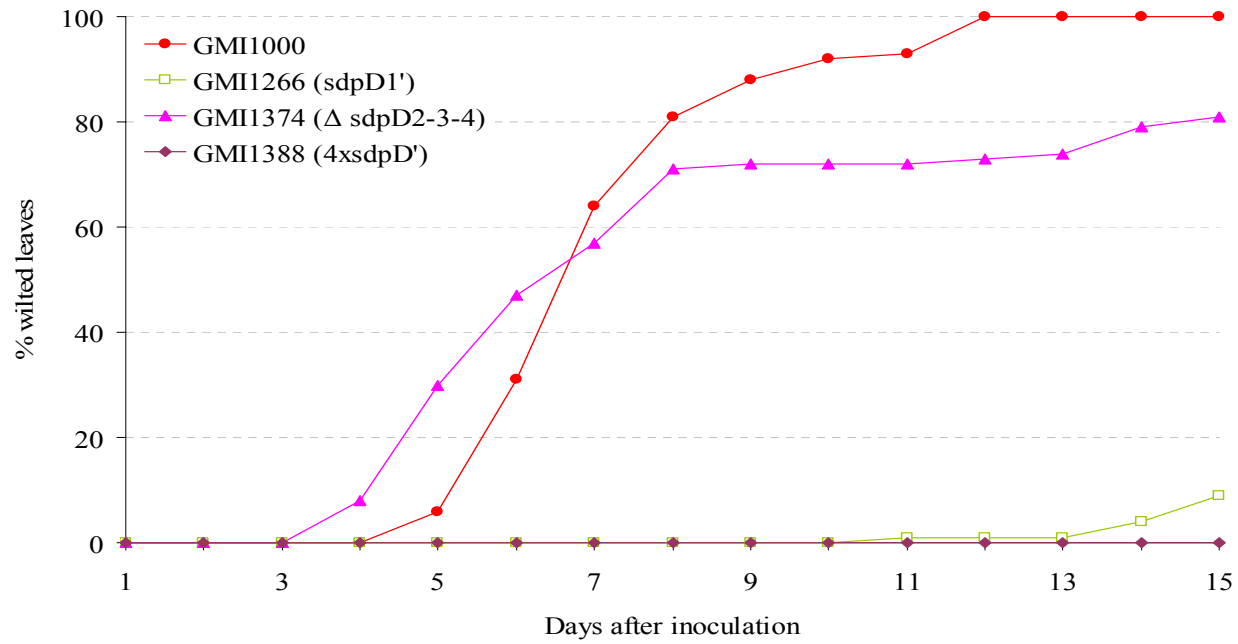

Fig 2.4. Virulence assays testing the *sdpD* mutants using the soil-drench method for inoculation of tomato plants.

Fig. 2.4. Continued

c) Assay 3

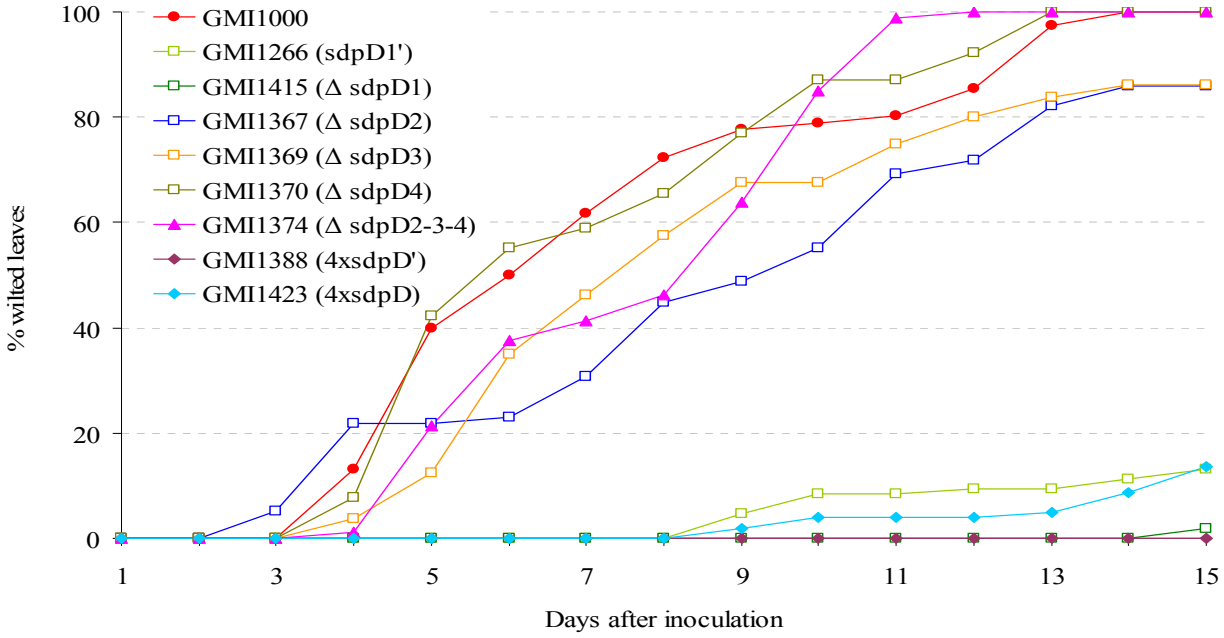

d) Assay 4

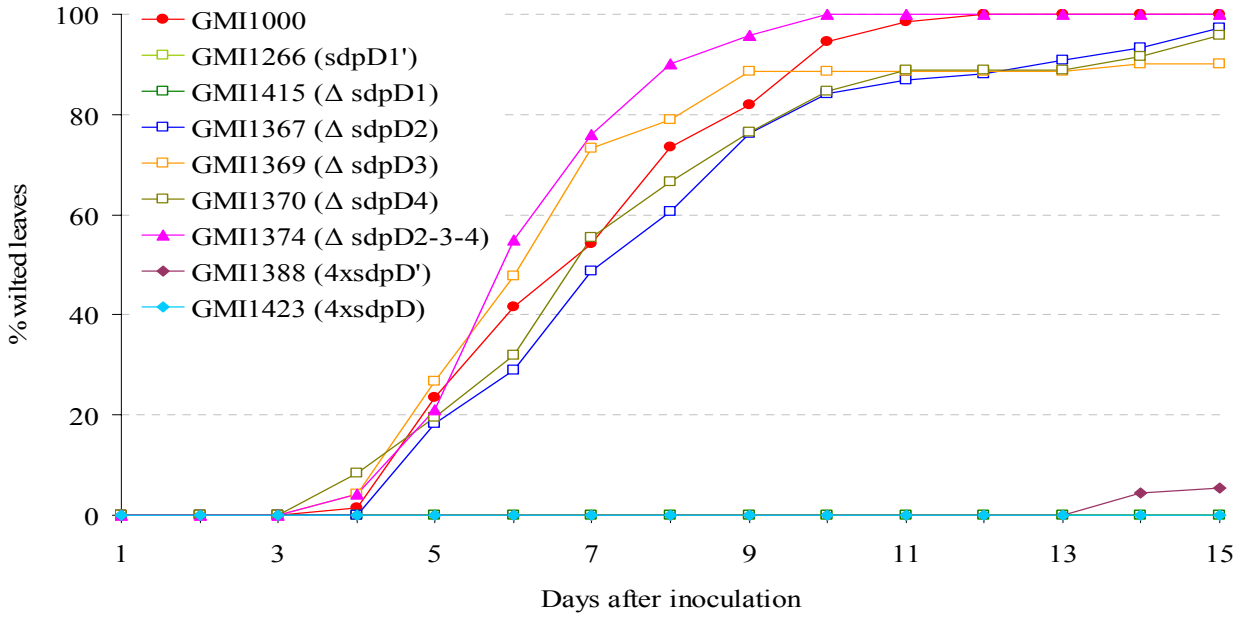

Fig. 2.4. Continued

e) Assay 5

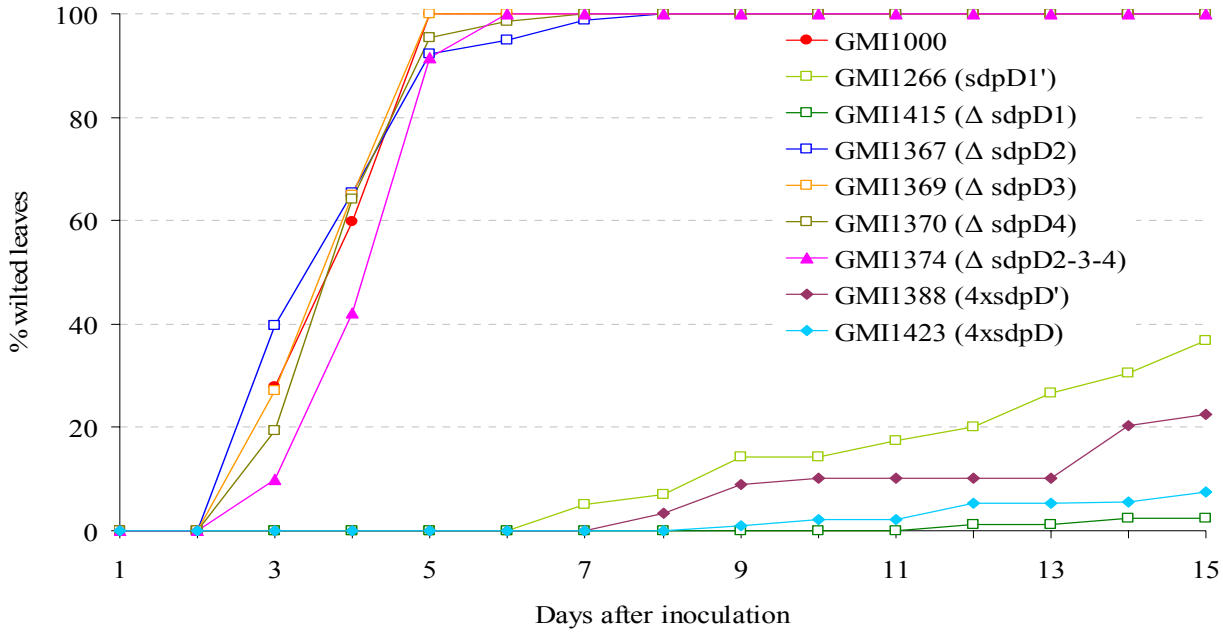

a)

b)

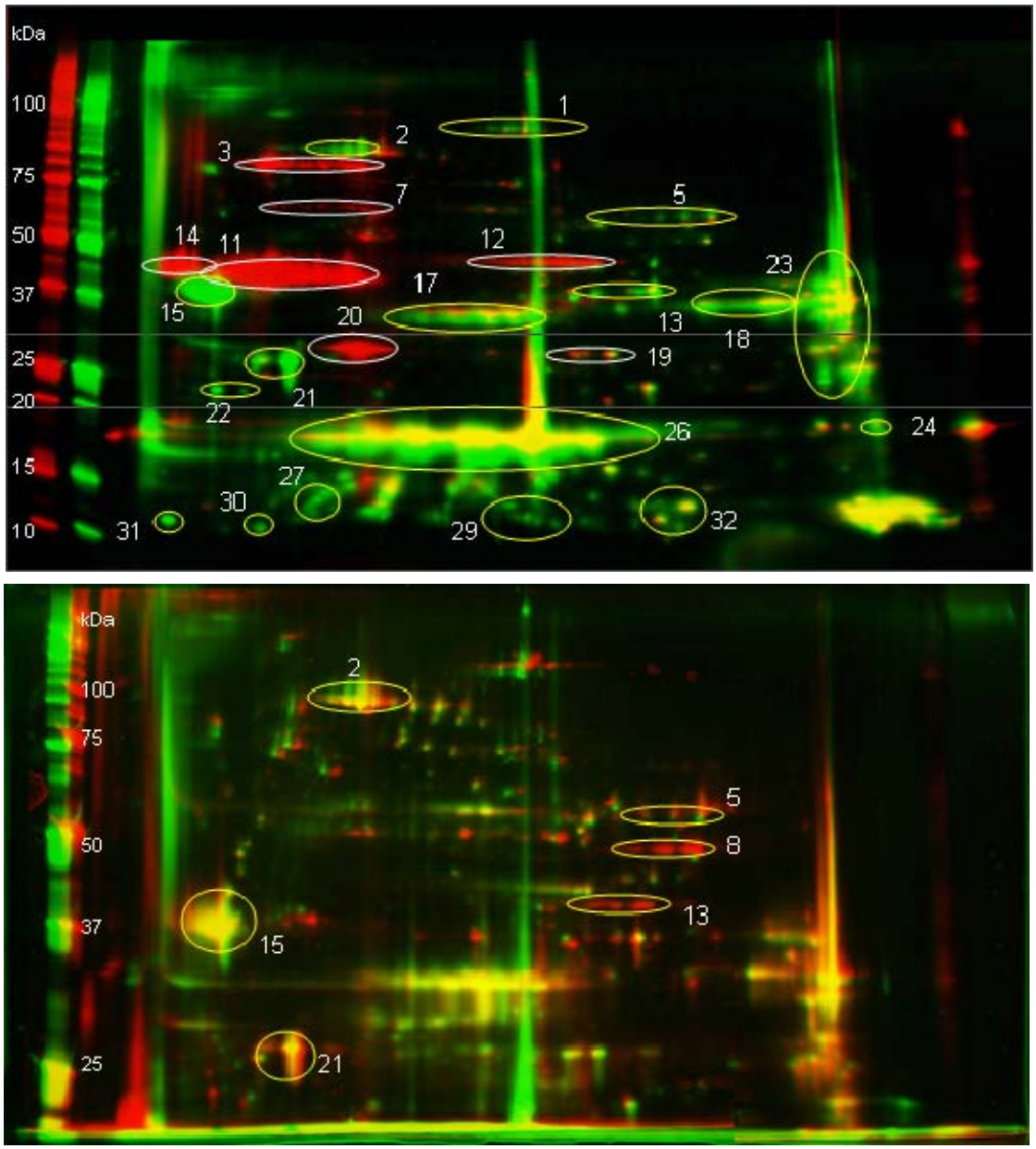

Fig 2.5. Image comparison of 2-D gels of extracellular proteins from GMI1266 (*sdpD*1') (red) and GMI1388 (4x*sdpD*') (green). a) pI 3-11NL and 10-20% PAGE, white ovals indicate proteins that were more plentiful in GMI1266 than in GMI1388, whereas yellow ovals are the reverse. b) pI 3-11NL and 10% PAGE, ovals indicate some common areas to Fig. 2.5a. Note that areas 11, 14 and 20 are not present in Fig. 2.5b. Numbers identifying these regions correspond to the list in Table 2.2. Gray horizontal lines indicate points where images where digitally aligned.

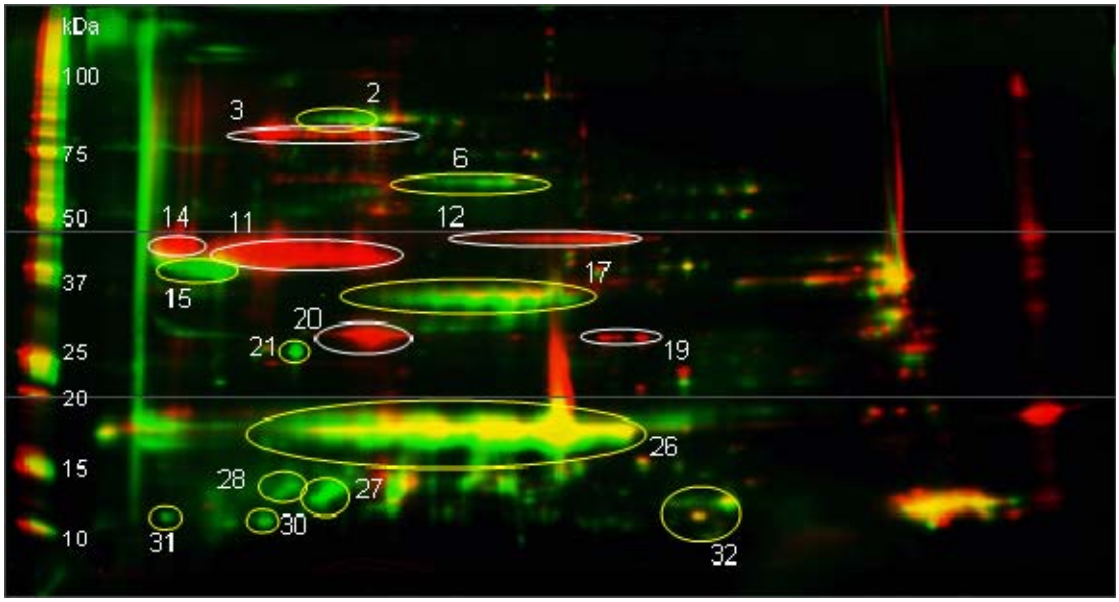

Fig 2.6. Image comparison of 2-D gels (pI 3-11NL and 10-20% PAGE) of extracellular proteins from GMI1266 (*sdpD*1*')* (red) and GMI1415 (Δ*sdpD*1) (green). White ovals indicate proteins that were more plentiful in GMI1266, than in GMI1415, whereas yellow ovals represent the reverse. Numbers identifying these regions correspond to the list in Table 2.2. Gray horizontal lines indicate points where images where digitally aligned.

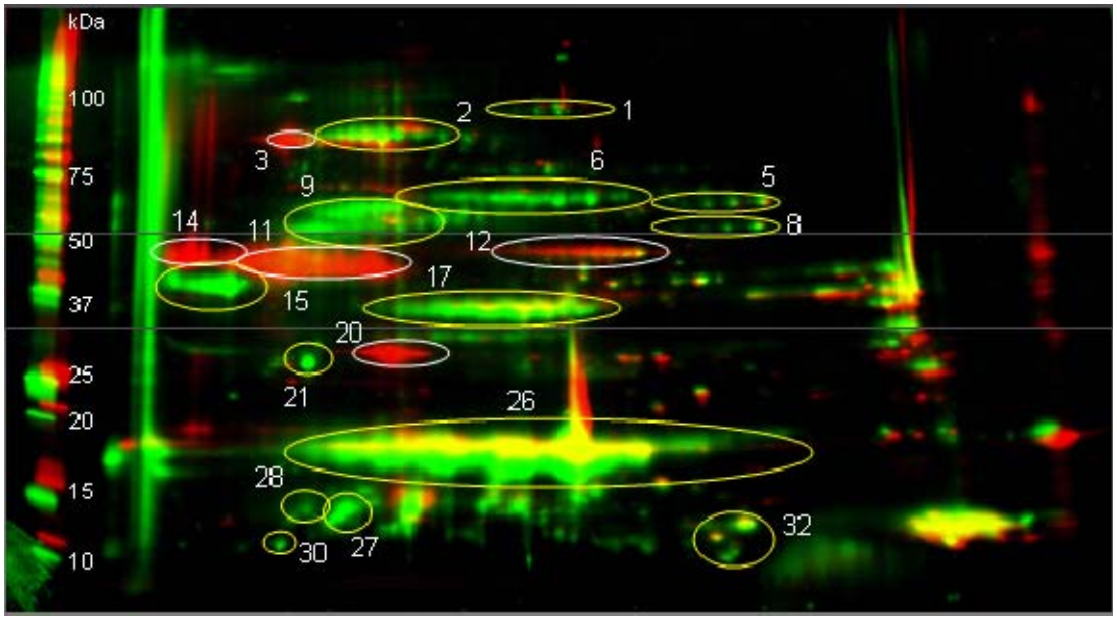

Fig 2.7. Image comparison of 2-D gels (pI 3-11NL and 10-20% PAGE) of extracellular proteins from GMI1266 (*sdpD*1') (red) and GMI1423 (4x*sdpD)* (green). Common proteins are indicated by yellowish areas. White ovals indicate proteins that were present in greater amounts in GMI1266 than in GMI1423, whereas yellow ovals represent the reverse. Numbers identifying these regions correspond to the list in Table 2.2. Gray horizontal lines indicate points where images where digitally aligned.

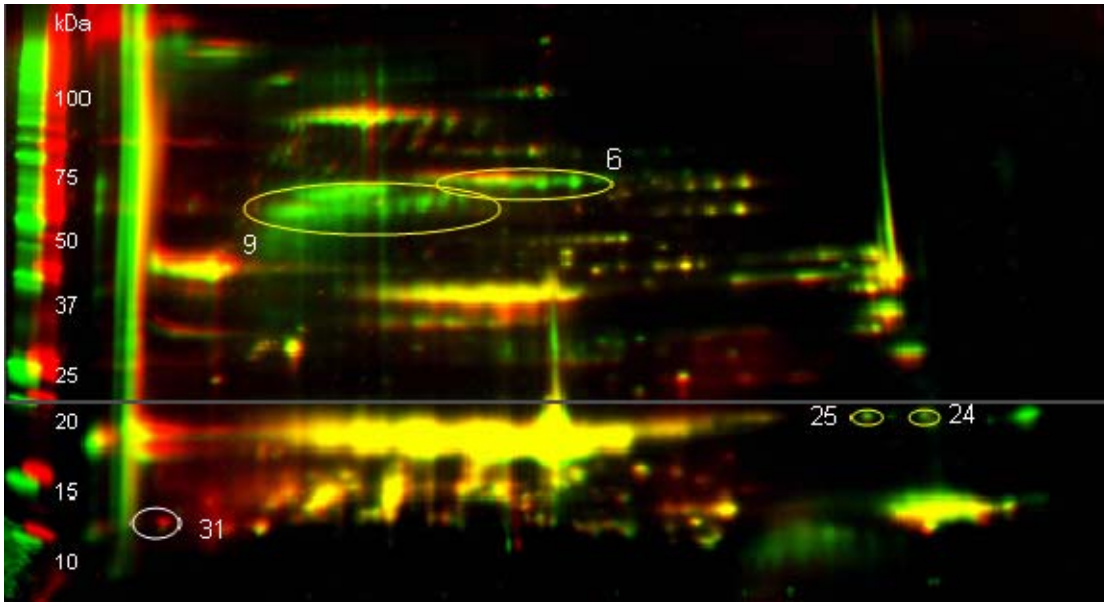

Fig 2.8. Image comparison of 2-D gels (pI 3-11NL and 10-20% PAGE) of extracellular proteins from GMI1415 (Δ*sdpD*1) (red) and GMI1423 (4x*sdpD)* (green). White oval indicates the area where the protein was more plentiful in GMI1266 mutant, yellow ovals indicate the area where proteins were more plentiful in GMI1388 mutant. Numbers identifying these regions correspond to the list in Table 2.2. Gray horizontal lines indicate points where images where digitally aligned.

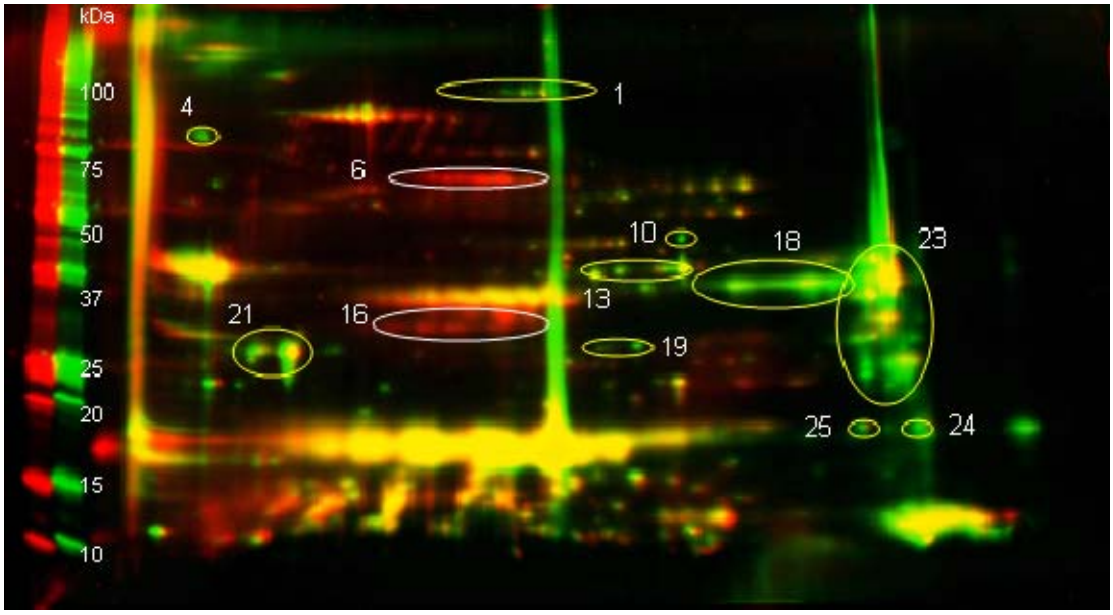

Fig 2.9. Image comparison of 2-D gels (pI 3-11NL and 10-20% PAGE) of extracellular proteins from GMI1415 (Δ*sdpD*1) (red) and GMI1388 (4x*sdpD')* (green). White ovals indicate proteins that were more plentiful in GMI1415 than in GMI1388, whereas yellow ovals represent the reverse. Numbers identifying these regions correspond to the list in Table 2.2.

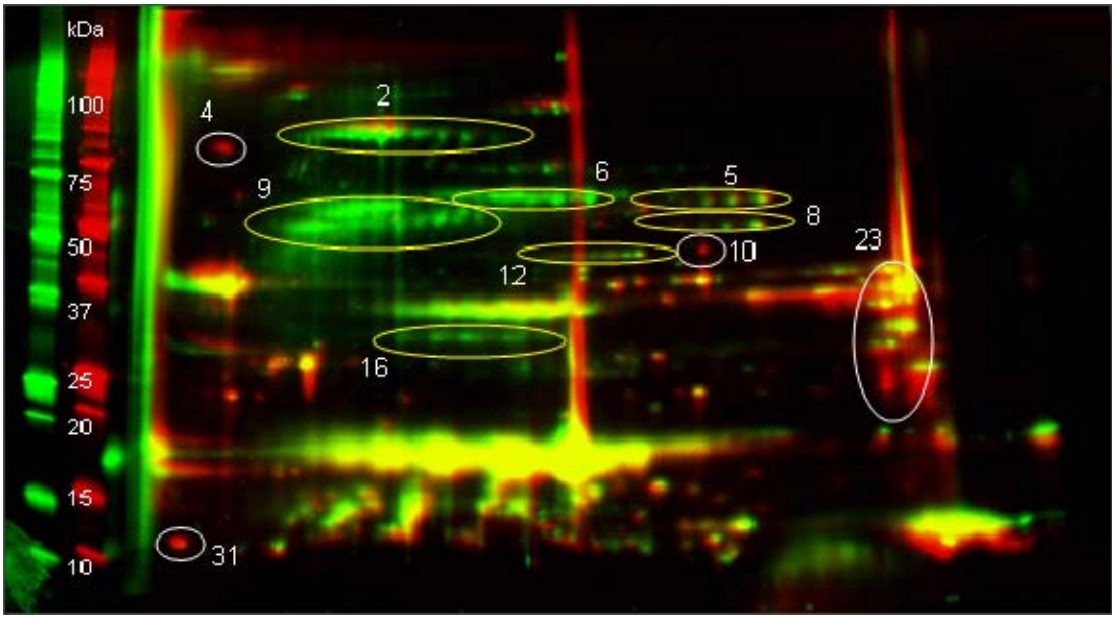

Fig 2.10. Image comparison of 2-D gels (pI 3-11NL and 10-20% PAGE) of extracellular proteins from GMI1388 (4x*sdpD')* (red) and GMI1423 (4x*sdpD)* (green). Common proteins are indicated by yellowish areas, white ovals indicate the area where proteins where just present on the GMI1388 mutant and yellow ovals for proteins present on GMI1423 non-polar mutant. Numbers identifying these regions correspond to the list in Table 2.2.

Table 2.2. Localization on 2-D gels of proteins secreted in major abundance by each of the *sdpD* mutants tested.

ID on gel	Mass (kDa)	pI	ID on gel	Mass (kDa)	pI
1	> 100	5.5 – 6.1	17	32	5.1 – 5.8
2	90	4.8 – 5.2	18	30	7.0 – 8.5
3	85	4.0 – 5.2	19	30	5.9 – 6.3
4	85	3.5	20	30	4.8 – 5.1
5	70	6.5 – 7.5	21	28	4.5
6	70	5.2 – 5.6	22	24	4.0
7	70	4.0 – 5.3	23	20 - 50	8.5 – 9.5
8	55	6.5 – 7.5	24	17	10.0
9	55 - 65	4.5 – 5.2	25	17	9.0
10	50	6.8	26	15 - 20	4.5 – 6.0
11	45	3.5 – 5.2	27	14	4.8
12	45	5.5 – 6.2	28	14	4.5
13	40	5.8 – 6.5	29	13	4.3
14	40	3.0 – 3.5	30	12	5.0
15	37	3.2 – 4.0	31	12	3.0
16	32	5.2 – 5.6	32	11 - 13	6.5 – 7.2

Table 2.3. Protein spot comparison between *sdpD* mutants.

Fig.	Mutant 1 vs. Mutant 2	Over produced in mutant 1	Over produced in mutant 2
2.5	GMI1266 (*sdpD*1') / GMI1388 (*4xsdpD*')	3, 7, 11, 12, 14, 17, 19, 20	1, 2, 5, 13, 15, 17, 18, 21, 22, 23, 24, 26, 27, 29, 30, 31, 32
2.6	GMI1266 (*sdpD*1') / GMI1415 (Δ*sdpD*1)	3, 11, 12, 14, 19, 20	2, 6, 15, 17, 21, 26, 27, 28, 30, 31, 32
2.7	GMI1266 (*sdpD*1') / GMI1423 (4x*sdpD*)	3, 11, 12, 14, 20	1, 2, 5, 6, 8, 9, 15, 17, 21, 26, 27, 28, 30, 32
2.8	GMI1415 (Δ*sdpD*1) / GMI1423 (4x*sdpD*)	31	6, 9, 24, 25
2.9	GMI1415 (Δ*sdpD*1 / GMI1388 (4x*sdpD*')	6, 16	1, 4, 10, 13, 18, 19, 21, 23, 24, 25
2.10	GMI1388 (4x*sdpD*') / GMI1423 (4x*sdpD*)	4, 10, 23, 31	2, 5, 6, 8, 9, 12, 16

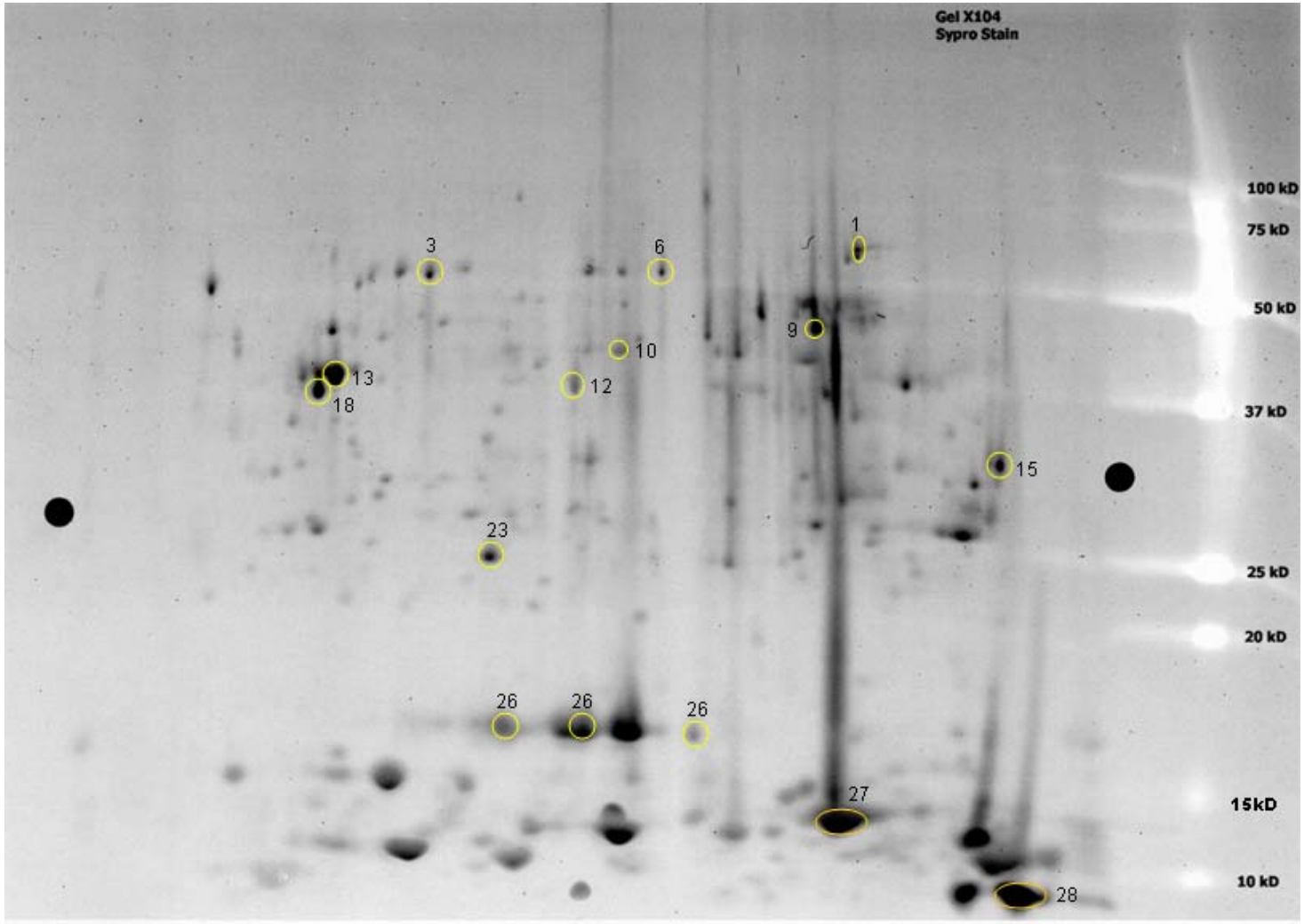

Fig 2.11. Large format 2-D gel analysis of exoproteins from GMI-7. The first dimension was an 18 cm, 3-11 IPG strip and the second dimension was an 8-16% polyacrylamide gel. The gel was stained with Sypro Ruby. Circled spots with numbers indicate the proteins identified (see Table 2.4).

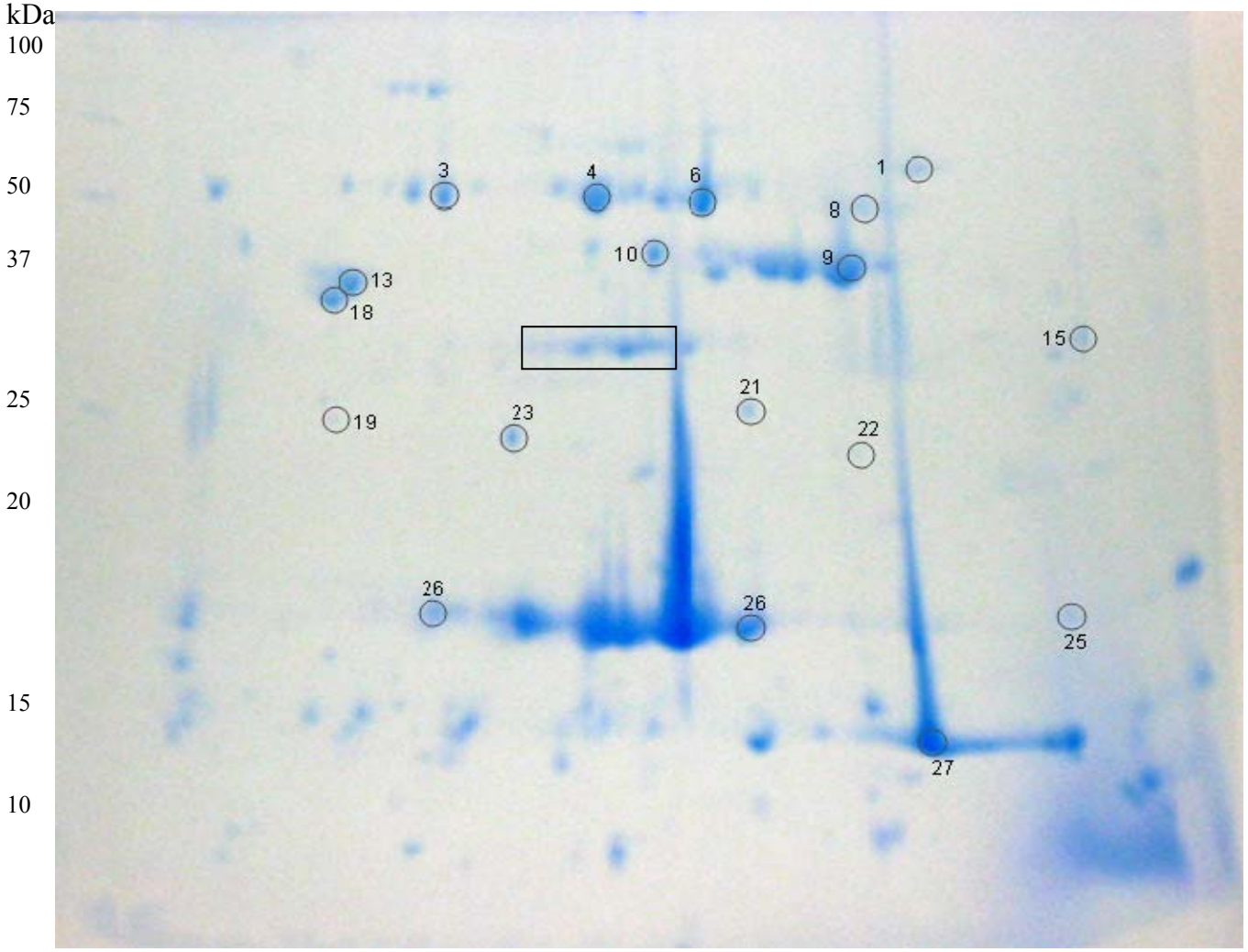

Fig 2.12. 2-D gel analysis of exoproteins from GMI-7. The first dimension was an 18 cm, 3 - 11 IPG strip and the second dimension was an 8-16% polyacrylamide gel. The gel was stained with colloidal Coomassie Blue. Circled spots with numbers indicate the proteins identified and box represents a non-annotated protein (see Table 2.4).

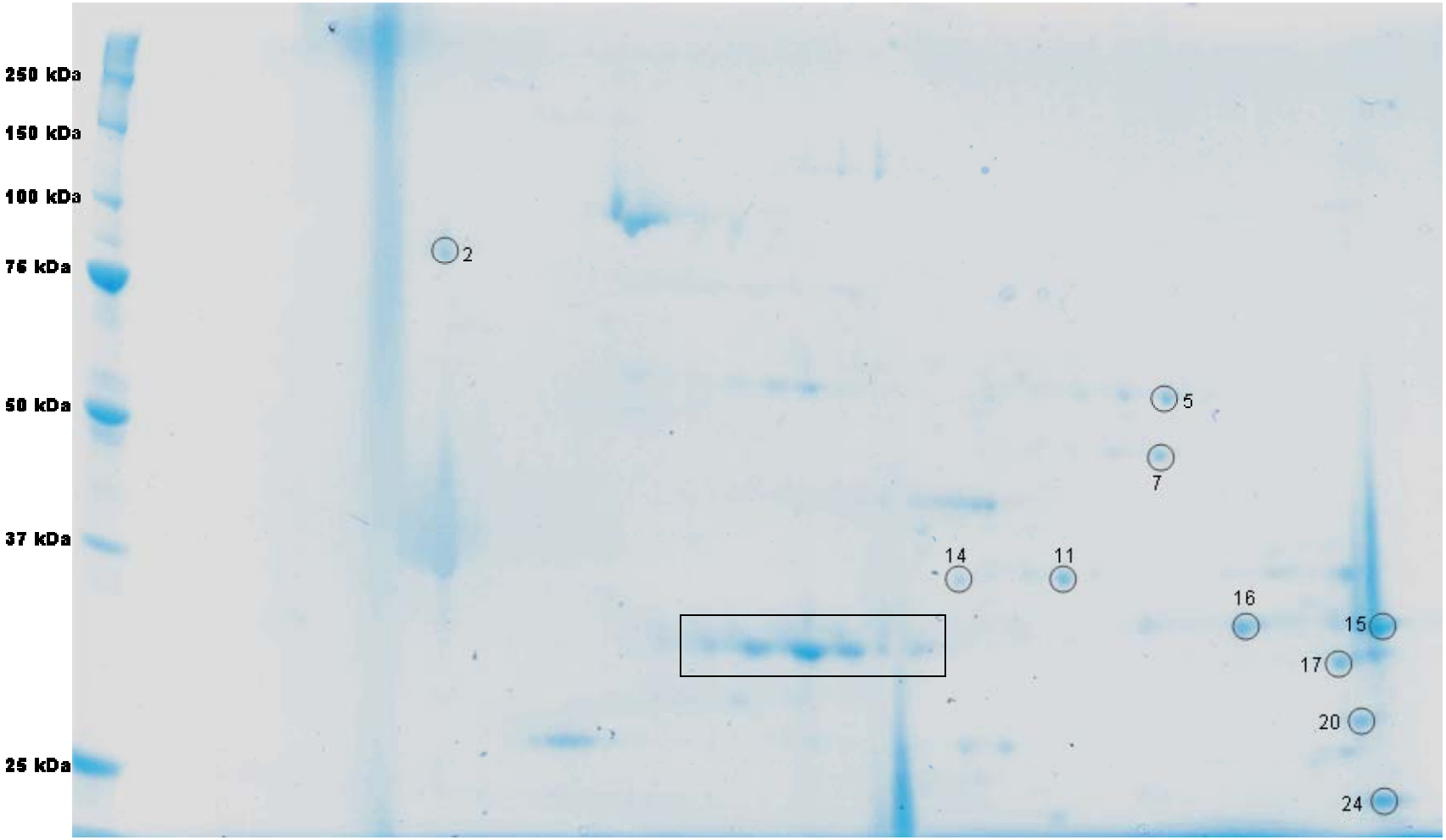

Fig. 2.13. 2-D gel analysis of exoproteins from GMI1266 (*sdpD*1'). The first dimension was an 11 cm 3 - 11 IPG strip and the second dimension was a 10% polyacrylamide gel. The gel was stained with colloidal Coomassie Blue. Circled spots with numbers indicate the proteins identified and box represents a non-annotated protein (see Table 2.4).

Table 2.4. Exoproteins identified from 2-D gel spots by FTICR-MS from supernatant of GMI-7 and GMI1266 cultured in MMP liquid medium.

				Predicted[a]		Log_{10} MOWSE score [b]		
Spot #	Locus tag	Gene	Protein identified	pI	Mass (kDa)	Fig. 2.11	Fig. 2.12	Fig. 2.13
1	RSc2547	*aac*	Probable aculeacin A acylase transmembrane protein	7.69	82.8	6.0334	7.6273	
2	RSp0295		Putative hemolysin-type protein	4.34	70.2			3.2174
3	RSc3101		Putative serine protease protein	6.05	70.2 [c]	2.1303	8.1072	
4	RSp0603		Putative serine protease	6.43	69.7		7.1673	
5	RSc3051		Hypothetical signal peptide protein	7.25	61.8			4.7315
6	RSp0277	*treA*	α, α-trehalase signal peptide protein	6.15	56	3.9030	10.8987	
7	RSp1581	*katE*	Probable catalase hydroperoxidase hpII oxidoreductase protein	7.34	53.9			4.2988
8	RSp0161		Putative transmembrane protein	7.84	51.4		7.1818	
9	RSp1610		Hypothetical protein	6.45	46.4	5.6148	5.3159	
10	Rsp1240		Putative trans-glycosylase protein	6.03	42.3	5.4712	10.6304	
11	RSc2855		Putative outer membrane porin signal peptide protein	7.09	39.3			5.1702
12	RSp0275		Probable hydrolase transmembrane protein	5.69	39.1	2.5105		
13	RSc3155		Putative antibiotic hydrolase signal peptide protein	4.9	38.8	4.4082	5.3979	
14	RSc3390		Probable porin signal peptide protein	6.5	37.7			4.0791
15	RSc2933		Putative porin signal peptide protein	9.19	37.6	3.8169	4.7379	4.6674

				Predicted[a]		Log_{10} MOWSE score [b]		
Spot #	Locus tag	Gene	Protein identified	pI	Mass (kDa)	Fig. 2.11	Fig. 2.12	Fig. 2.13
16	RSc3091		Probable outer membrane porin signal peptide	8.34	37.5			3.3636
17	RSc1336	*sbp*	Probable sulfate-binding precursor signal peptide	8.93	33.9			4.00
18	RSc2241		Conserved hypothetical protein	4.68	32.6	4.4329	4.4329	
19	RSc2238		Probable transmembrane protein	4.93	32.5		6.3159	
20	RSc0481	*PBPb*	Probable amino-acid-binding periplasmic ABC transporter protein	9.09	31.4			5.2355
21	RSc2495		Hypothetical hydrolase	6.15	30.5		3.3856	
22	RSc2093		Probable signal peptide protein	6.66	26.6		6.2576	
23	RSc0152		Probable lipoprotein	5.42	26.2	5.4608	3.8169	
24	RSc0900		Probable signal peptide protein	9.33	21.2			3.1335
26	RSp0745	*hcp*	Hemolysin corregulated protein	5.8	18.4	2.6541	3.5965	
25	RSc1165	*ppiA*	Probable peptidyl-prolyl cis-transisomerase A signal peptide protein	8.69	18.4		4.5171	
27	RSc2285	*virK*	Putative signal peptide protein	8	13.3	3.4281	3.0969	
28	RSp1461		Probable signal peptide protein	9.31	9.1	1.9294		

[a] pI and mass for mature protein after *in silico* removal of the predicted signal peptide.

[b] The MOWSE (Molecular weight search score) reported by MS-Fit is based on the system described by Pappin et al. (1993). Higher scores indicate greater likelihood of correct identification. In most cases, MS-Fit returned only a single protein identification.

[c] Red numbers indicate proteins with good MOWSE score but for which the predicted pI differed from that observed during 2-D gel analysis.

Table 2.5. Exoproteins identified from *sdpD* mutants using iTRAQ labeling and LC-MS/MS.

#	Gene	Locus Tag	Protein Identified	Relative Ratio [a] GMI1266/ GMI1388 [b]	GMI1415/ GMI1423 [c] Rep A	GMI1415/ GMI1423 [c] Rep B
1	*hrpJ*	RSp0866	HrpJ protein	4.4587	0.8943	1.2275
2	*popB*	RSp0876	PopB protein	3.6702	1.0842	1.3467
3		RSp0304	Probable AvrPphD-related protein	3.1497		
4		RSc0293	Hypothetical signal peptide protein	2.7047		
5		RSp1415	Hypothetical protein	2.4656	0.9427	1.0901
6	*fliE*	RSp0389	Flagellar hook-basal body protein	2.2255		
7		RSc3051	Hypothetical signal peptide protein	1.8133		
8	*flgM*	RSp0340	Anti- σ-28 factor protein	1.7917	0.8749	1.1296
9	*hupB2*	RSc2521	Probable DNA-binding protein Hu-β	1.534		
10		RSc0895	Hypothetical protein	1.5157	1.3182	1.2383
11	*ppiA*	RSc1165	Probable peptidyl-prolyl cis-trans isomerase A signal peptide protein	1.4873		

#	Gene	Locus Tag	Protein Identified	Relative Ratio [a] GMI1266/ GMI1388 [b]	GMI1415/ GMI1423 [c] Rep A	GMI1415/ GMI1423 [c] Rep B
12		RSc2675	Putative type 4 fimbrial biogenesis PilY1-related protein signal peptide	1.4104	0.9281	1.2444
13		RSc3290	Conserved hypothetical protein	1.3991		
14	*hrpY*	RSp0855	Hrp pilus subunit HrpY protein	1.3768	0.926	1.1607
15	*PilY1*	RSc0724	Putative type-4 fimbrial biogenesis PilY1-related signal peptide protein	1.3756		
16	*cspD3*	RSp0002	Probable cold shock-like transcription regulator protein	1.3519		
17		RSc2353	Probable signal peptide protein	1.3476		
18		RSp1461	Probable signal peptide protein	1.3435	1.155	0.9598
19		RSc3386	Putative outer membrane signal peptide	1.3191		
20		RSc3204	Hypothetical protein	1.3075		
21		RSc2933	Putative porin signal peptide protein	1.2671	0.7087	0.7213
22		RSc2652	Probable lipoprotein	1.2441		
23	*avrA*	RSc0608	AvrA protein	1.2383		
24		RSp1466	Probable signal peptide protein	1.2058	1.0984	1.2201

#	Gene	Locus Tag	Protein Identified	Relative Ratio [a] GMI1266/ GMI1388 [b]	GMI1415/ GMI1423 [c] Rep A	GMI1415/ GMI1423 [c] Rep B
25	*hcp*	RSp0745	Hemolysin corregulated protein	1.1972	1.2318	1.0572
26		RSp0197	Chorismate mutase	1.151		
27	*virK*	RSc2285	Putative signal peptide protein	1.1435	0.5171	0.218
28		RSc0900	Probable signal peptide protein	1.1189		
29		RSc0617	Probable signal peptide protein	1.1069	1.1717	1.0185
30		RSc2257	Probable amino-acid-binding periplasmic ABC transporter protein	1.0845		
31		RSc0902	Probable signal peptide protein	1.0665		
32	*sbp*	RSc1336	Probable sulfate-binding precursor signal peptide protein	1.0642	0.9651	0.9218
33		RSc0254	Hypothetical transmembrane protein	1.0568		
34	*PBPb*	RSc0481	Probable amino-acid-binding periplasmic abc transporter protein	1.0432	0.8242	0.9762
35		RSc0532	Hypothetical transmembrane protein	1.0163	0.9025	1.0119

#	Gene	Locus Tag	Protein Identified	Relative Ratio [a] GMI1266/ GMI1388 [b]	GMI1415/ GMI1423 [c] Rep A	GMI1415/ GMI1423 [c] Rep B
36		RSc3426	Probable transmembrane protein	1.0093	0.8765	1.3595
37		RSc3091	Probable outer membrane porin signal peptide protein	0.9907		
38		RSc2855	Putative outer membrane porin signal peptide protein	0.9853		
39		RSc1878	Putative lipoprotein	0.978		
40	*copC*	RSp0658	Probable copper resistance c signal peptide protein	0.9735		
41		RSp0213	Hypothetical protein	0.9522	1.0403	0.8807
42		RSc1737	Putative transmembrane outer membrane porin signal peptide protein	0.9513	0.9747	1.0566
43		RSc3300	Putative amino-acid transport signal peptide protein	0.9222	0.8876	0.6448
44		RSp0742	Putative lipoprotein	0.9058		
45		RSp0572	Hypothetical protein	0.8915		
46	*PilA*	RSc0558	Type 4 fimbrial pilin signal peptide	0.8388	1.1132	0.8339
47		RSc3430	Putative Vgr-related protein	0.8381		

#	Gene	Locus Tag	Protein Identified	Relative Ratio [a] GMI1266/ GMI1388 [b]	GMI1415/ GMI1423 [c] Rep A	GMI1415/ GMI1423 [c] Rep B
48	*sodC*	RSc2368	Probable superoxide dismutase Cu-Zn precursor protein	0.8364		
49		RSc1259	Hypothetical signal peptide protein	0.8274		
50		RSc2792	Putative outer membrane lipoprotein transmembrane	0.8035		
51	*fliC*	RSp0382	Flagellin protein	0.7643	1.0713	0.6981
52		RSc2380	Probable transmembrane protein	0.7574		1.2131
53		RSc2958	Probable signal peptide protein	0.7493		
54		RSc3272	Hypothetical protein	0.7109	0.7706	0.874
55		RSp0879	Hypothetical protein	0.697		
56	*groES*	RSc0641	Probable 10 kDa chaperonin	0.6801		
57		RSc1206	Probable lipoprotein NlpD/LppB homolog	0.6385		
58		RSp1073	Probable hemagglutinin-related protein	0.568	1.3774	1.0498
59	*popA*	RSp0877	PopA protein	0.496	0.8964	0.6617
60		RSp0603	Putative serine protease protein	0.4956		
61		RSc2888	Hypothetical protein	0.4758		

#	Gene	Locus Tag	Protein Identified	Relative Ratio [a] GMI1266/ GMI1388 [b]	GMI1415/ GMI1423 [c] Rep A	GMI1415/ GMI1423 [c] Rep B
62		RSc0038	Putative transmembrane protein	0.454		
63		RSp0295	Putative hemolysin-type protein	0.4325	0.5522	1.0389
64		RSc1475	Probable transmembrane protein	0.413		
65	*Tek*	RSp1002	Tek signal peptide protein	0.3256		
66	*popF1*	RSp1555	Secreted protein PopF1	0.2706		
67	*popW*	RSc2775	Probable harpin-related protein	0.2576	1.8035	0.6926
68		RSp0161	Putative transmembrane protein	0.2503		
69		RSp1130	Hypothetical protein	0.2482		
70		RSp0294	Putative hemolysin-type calcium-binding protein	0.1238		
71	*dsbA1*	RSc0285	Probable thiol:disulfide interchange signal peptide prot.			
72		RSc0824	Conserved hypothetical protein			
73		RSc0894	Probable signal peptide protein			
74	*rpsB*	RSc1404	Probable 30s ribosomal protein s2			

#	Gene	Locus Tag	Protein Identified	Relative Ratio [a] GMI1266/ GMI1388 [b]	GMI1415/ GMI1423 [c] Rep A	GMI1415/ GMI1423 [c] Rep B
75		RSc1707	Putative transmembrane protein		0.9969	1.5711
76	*accB1*	RSc2786	Probable biotin carboxyl carrier protein of acetyl-CoA carboxylase			
77	*tuf*	RSc3041	Probable elongation factor Tu			
78		RSc3260	Probable cytochrome c transmembrane protein			
79		RSp1137	Putative Rhs-related transmembrane protein			
80		RSp1201	Probable signal peptide protein			

[a] Yellow cells indicate values with Pval <0.05 and error factor (EF) <2. Gray cells indicate proteins identified but not quantified. Empty cells indicate proteins not identified in the pair tested. Tan cells indicate proteins previously identified (T. Denny, personal communication)

[b] Ratios were bias corrected (117/114=2.0281)

[c] Ratios were not bias corrected

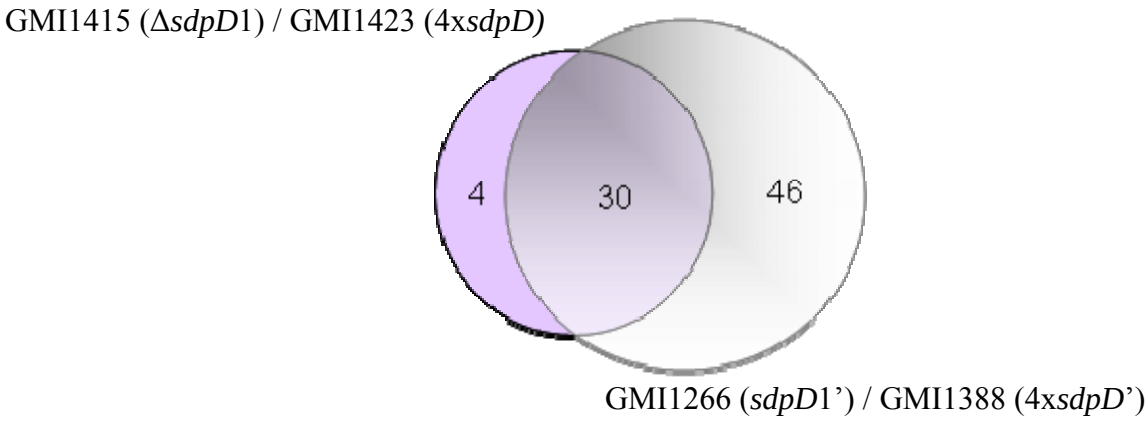

Fig 2.14. Venn diagram of proteins identified using iTRAQ labeling and LC-MS/MS analysis in comparisons of GMI1415 (Δ*sdpD*1) / GMI1423 (4x*sdpD)* and GMI1266 (*sdpD*1') / GMI1388 (4x*sdpD*').

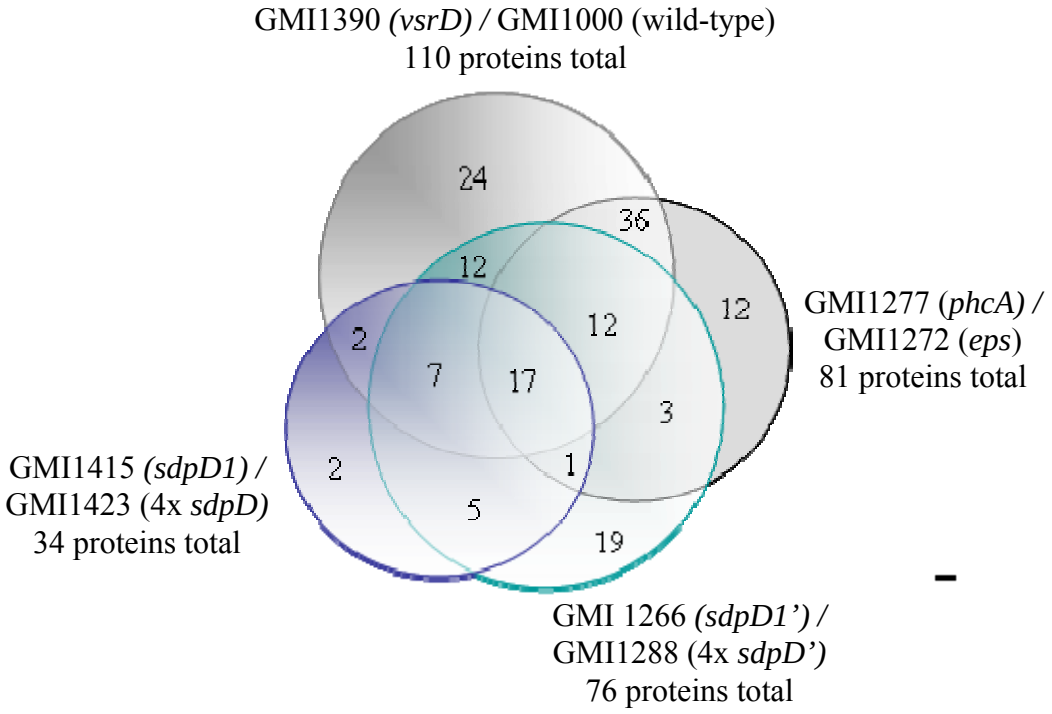

Fig 2.15. Venn diagram of proteins identified using iTRAQ labeling and LC-MS/MS analysis in comparisons of GMI1390 (*vsrD)* / GMI1000 (wild type) and GMI1277 (*phcA)* /GMI1272 (EPS^-) GMI1415 (Δ*sdpD*1) / GMI1423 (4x*sdpD)* and GMI1266 (*sdpD*1') / GMI1388 (4x*sdpD*').

Table 2.6. Classifications of the proteins present in strains with a functional T2SS and absent in *sdpD* mutants.

Classification	Gene	Locus tag [a]	Protein function
T1SS		RSc3101	Putative serine protease protein
T2SS Known function	*pehB*	RSc1756	Exo-polygalacturonase
	pme	RSp0138	Pectin methylesterase protein
	pqaA	RSp0161	PhoP/Q-regulated protein PqaA
	egl	RSp0162	Endoglucanase (endo-1,4-β-glucanase)
	treA	RSp0277	α, α-trehalase signal peptide protein
	cbhA	RSp0583	Exo-glucanase A (1,4-β-cellobiosidase)
	pehC	RSp0833	Exo-polygalacturonase
	pglA	RSp0880	Endo-polygalacturonase
	tek2	RSp1000	Tek-related protein
	tek	RSp1002	Tek signal peptide protein
T2SS Hypothetical proteins with putative function		RSc0769	Putative hydrolase glycosidase protein
		RSc0818	Putative endoglucanase protein
		RSc1003	Probable carboxypeptidase protein
		RSc1334	Probable D-3-hydroxybutyrate oligomer hydrolase lipoprotein
		RSc1777	Putative lipoprotein protein
		RSc2452	Putative endonuclease protein
		RSc2495	Probable arylsulfatase precursor hydrolase

Classification	Gene	Locus tag [a]	Protein function
T2SS Hypothetical proteins with putative function	*aac*	RSc2547	Probable aculeacin A acylase transmembrane protein
		RSc2653	Putative extracellular protease signal peptide protein
		RSc2654	Probable serine protease protein
		RSc3155	Putative antibiotic hydrolase signal peptide protein
		RSp0275	Probable glycosyl hydrolase transmembrane protein
		RSp0532	Putative aminopeptidase transmembrane prot .
		RSp0758	Conserved hypothetical protein
		RSp0780	Hypothetical hydrolase protein
	acpA	RSp1174	AcpA - Putative acid phosphatase protein
		RSp1240	Putative membrane-bound lytic murein transglycosylase protein
T2SS Hypothetical proteins with unknown function		RSc0019	Hypothetical protein
		RSc0152	Probable lipoprotein
		RSc0336	Probable signal peptide protein
		RSc0616	Hypothetical protein
		RSc1740	Hypothetical signal peptide protein
		RSc2180	Putative transmembrane protein
		RSc2178	Hypothetical protein

Classification	Gene	Locus tag [a]	Protein function
T2SS Hypothetical proteins with unknown function		RSc2238	Probable transmembrane protein
		RSc2241	Conserved hypothetical protein
		RSc2494	Hypothetical signal peptide protein
		RSc2718	Probable signal peptide protein
		RSp0261	Putative transmembrane protein
		RSp0602	Probable signal peptide protein
		RSp0758	Conserved hypothetical protein
		RSp1526	Hypothetical protein
		RSp1610	Hypothetical protein
		RSp1673	Hypothetical lipoprotein transmembrane
T3SS	*popP*	RSc0826	PopP protein
	popP2	RSc0868	Probable YopP/AvrRxv family protein
		RSc1357	Gala protein 5
		RSp0028	Lrr-gala family type III effector protein Gala 3
		RSp0845	Putative type III effector protein
	popC	RSp0875	PopC protein
	popF2	RSp0900	Secreted protein PopF2
		RSp1212	Type III effector protein
T4SS		RSc2601	Putative type IV secretory pathway VirD2 related protein

Classification	Gene	Locus tag [a]	Protein function
Flagella proteins	*flgB*	RSp0342	Probable flagellar basal-body rod protein
	flgC	RSp0343	Probable flagellar basal-body rod protein
	flgE	RSp0345	Flagellar hook-associated protein
	flgF	RSp0346	Probable flagellar basal-body rod protein
	flgG	RSp0347	Probable flagellar basal-body rod protein
	flgJ	RSp0350	Probable flagellar protein
	flgK	RSp0351	Flagellar hook-associated protein
	flgL	RSp0352	Probable flagellar hook-associated protein
	fliD	RSp0383	Probable flagellar hook-associated protein
	fliK	RSp0395	Probable flagellar hook-length control protein
Other proteins	*ugpB*	RSc1264[b]	Probable glycerol-3-phosphate-binding periplasmic lipoprotein signal peptide
	dnaK	RSc2635	Chaperone protein (hsp70)
		RSc2937	Putative periplasmic iron-binding signal peptide protein
		RSp1139	Probable Vgr-related protein

[a]Tan cells indicate proteins previously identified as candidates for T2SS from 2-D gel FTICR-MS (Zuleta and Denny) or LC-MS/MS (Liu and Denny).

[b]Gray cells indicate proteins that have a predicted signal peptide but not included as T2SS candidates.

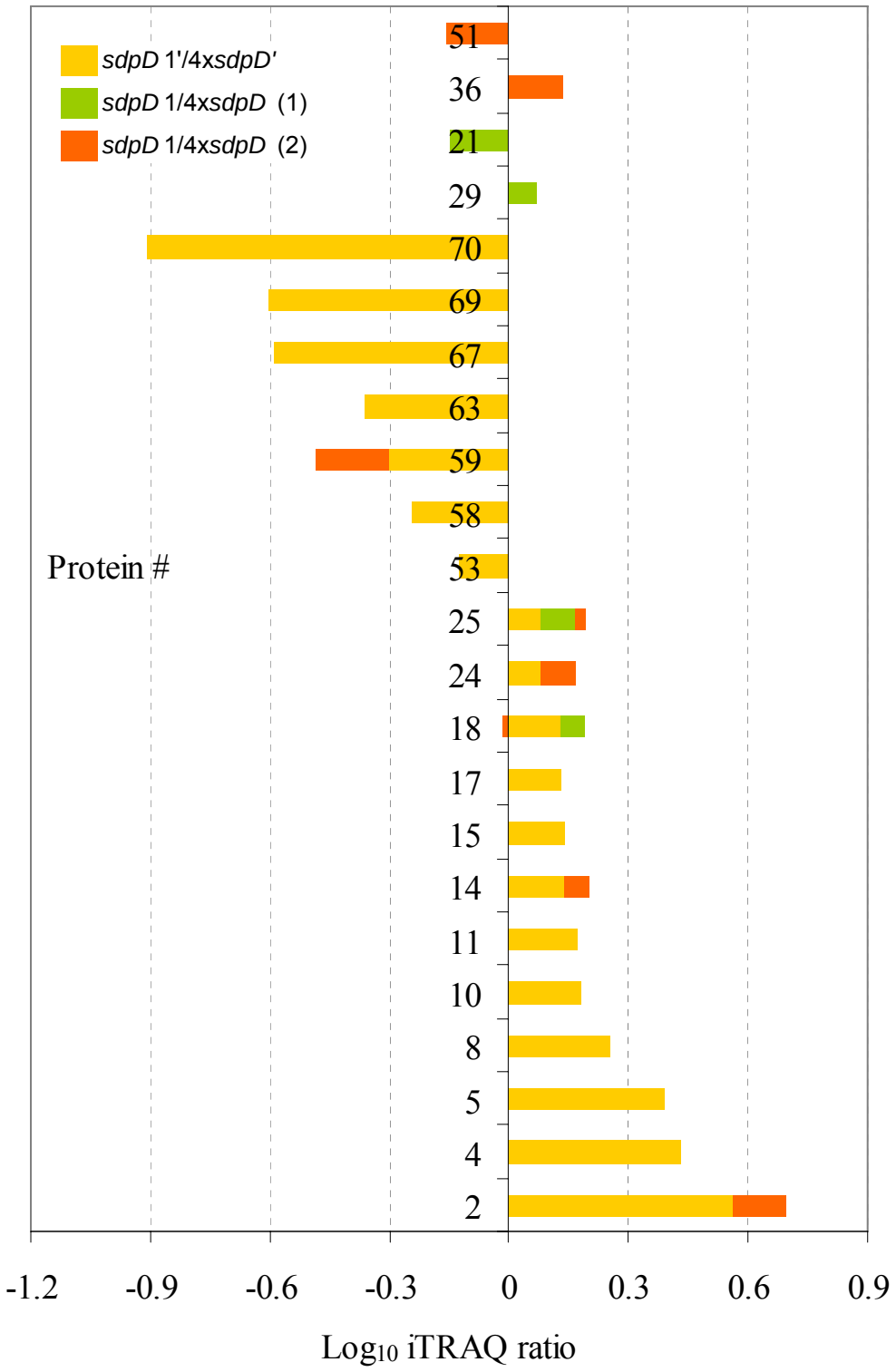

Fig 2.16. Protein production ratio in *sdpD*/4x*sdpD* pairs. Logarithmic scale $Log_{10} \pm 0.3$ indicates a 2-fold increase or decrease in protein production. Data are listed in Table 2.5.

Table 2.7. Strains and plasmids used on this study.

Strain	Characteristics[a]	Source
R. solanacearum		
GMI1000	Wild type, race 1, biovar 3, phylotype I, Tfp^+ Twt^+ Pil^+ HR^+	(Salanoubat et al. 2002)
GMI1266	GMI1000 *sdpD*1::pTOK2, $T2SS^-$, Tc^r	(Liu et al. 2005)
GMI-7	GMI1000 Δ *pglA pglB pglC egl pme tek, cbhA*::*aphA*3, Km^r	Tim Denny lab
GMI1367	GMI1000 Δ *sdpD*2, missing nucleotides RSc-2505225-2501839, -949 and + 38	This study
GMI1369	GMI1000 Δ *sdpD*3, missing nucleotides RSp-166098-164095	This study
GMI1370	GMI1000 Δ *sdpD*4, missing nucleotides RSp-591164-587368	This study
GMI1374	GMI1000 Δ *sdpD*2 *sdpD*3 *sdpD*4	This study
GMI1388	GMI1000 *sdpD1*::pTOK2 Δ *sdpD*2 *sdpD*3 *sdpD*4, Tc^r	This study
GMI1415	GMI1000 Δ *sdpD*1, missing nucleotides RSc-3350858-3351764	This study
GMI1423	GMI1000 Δ *sdpD*1 *sdpD*2 *sdpD*3 *sdpD*4	This study
Escherichia coli		
DH5α	Φ80*dlacZ*ΔM15 *recA*1 *endA*1 *gyrA*96 *thi*-1 *hsdR*17 (rk^- mk^+) *supE*44 *relA*1 *deoR* Δ(*lacZYA*-*argF*)U169	Invitrogen

Strain	Characteristics[a]	Source
Plasmids		
pEX18Tc	gene-replacement vector, *oriT sacB*, Tc^r	(Hoang et al. 1998)
pCR2.1	T-A cloning vector for PCR fragments, Km^r	Invitrogen
pS3114	1 kb *sdpD*1 deletion allele in pEX18Tc, Tc^r	This study
pS2303	1 kb *sdpD*2 deletion allele in pEX18Tc, Tc^r	This study
pS0143	1 kb *sdpD*3 deletion allele in pEX18Tc, Tc^r	This study
pS0474	1 kb *sdpD*4 deletion allele in pEX18Tc, Tc^r	This study

[a] Twt = twitching motility, Tfp = type IV pili, Pil = Hrp pili, HR= hypersensitive response on tobacco, EPS = exopolysacharide, PC-type = phenotype conversion type, T2SS = type II secretion system, Km^r, Tc^r, Sp^r = kanamycin, tetracycline and spectinomycin resistant, respectively.

Table 2.8. Primers used in unmarked mutagenesis.

Gene target		Primer Sequence (5' -> 3')[a]	Restriction site
Rsc3114	SOE1	GAC***GGTACC***CGCTGACCTGGA	*Kpn*I
	SOE2	GTTCTTGACCGCAATCA	
	SOE3	GATTGCGCTGAAGAAC***ACTAGT***	
		CCTGGGCGCGATCCT	*Spe*I
	SOE4	GAC***TCTAGA***GGTCTTCTTGCGCGTC	*Xba*I
	DIAG	GATTGCGCTGAAGAACACT	
RSc2303	SOE1	GAC***AAGCTT***CGCCGCGCTGTCCTATT	*Hin*dIII
	SOE2	GGTTGAGCGGCAGGTAGGTA	
	SOE3	ACCTACCTGCCGCTCAACC***ACTAGT***	
		GCCTGGTCATGCTT	*Spe*I
	SOE4	GAC***TCTAGA***GGCTTCCGACATGGGTCAAC	*Xba*I
	DIAG	ACCTACCTGCCGCTCAACCACT	
RSp0143	SOE1	GAC***AAGCTT***GTACCTGCGGAGCGA	*Hin*dIII
	SOE2	CAATGCCTGTCCGGTGTTCA	
	SOE3	TGAACACCGGACAGGCATTG***ACTAGT***	
		GCCTGAGTATCCGCGAACGAG	*Spe*I
	SOE4	GAC***TCTAGA***CTTCATCGCCGGCACGTTTG	*Xba*I
	DIAG	ACACCGGACAGGCATTGACTA	

Continued Table

Gene target		Primer Sequence (5' -> 3')[a]	Restriction site
RSp0474	SOE1	GAC***AAGCTT***GAAGCGGAGCCAACCAAATA	*Hin*dIII
	SOE2	CCGGTATGCGATGGTGTCCT	
	SOE3	AGGACACCATCGCAGACCGG***ACTAGT***	*Spe*I
		TAGAAAACCGCACCGAACCTG	
	SOE4	GAC***TCTAGA***TTCAGCGGCGATTCC	*Xba*I
	DIAG	ACACCATCGCAGACCGGACTA	

[a]SOE= splice overlap extension, DIAG= diagnostic primer, italic-bold letters = restriction site added. Primer pair SOE1 and SOE2 and pair SOE3 and SOE4 amplify upstream and downstream fragments, respectively.

CHAPTER 3

IDENTIFICATION OF EXOPROTEINS ASSOCIATED WITH PLANT COLONIZATION USING iTRAQ LABELING AND LIQUID CHROMATOGRAPHY-TANDEM MASS SPECTOMETRY[2]

[2] Zuleta, M. C., Schell, M. A. and Denny, T. P. To be submitted to *Molecular Plant-Microbe Interaction.*

Introduction

Ralstonia solanacearum is vascular pathogen that causes lethal wilting diseases on a variety of crop plants and weeds (Denny 2006). The pathogen initiates root infection through wounds caused by machinery or soil inhabitants such as nematodes and insects. Invasion is also possible through the colonization of unwounded roots starting at exudation sites in the extremities and axils of secondary roots. Infection of the inner cortex and the vascular parenchyma ensues, and bacteria soon invade the protoxylem vessels by degrading cell walls (Vasse et al. 1995). Bacteria then move throughout the xylem and accumulate to high cell densities. Initial wilt symptoms in young tomato plants occur only after the pathogen has colonized at least one xylem vessel bundle from root to shoot apex.

R. solanacearum needs multiple virulence factors to colonize plants effectively. These factors include high molecular mass exopolysaccharide (EPS) and several plant cell wall degrading enzymes (CWDE) secreted by the type II secretion system (T2SS) (Denny 2006). EPS promotes rapid systemic colonization of tomato plants because mutants lacking EPS rarely wilt or kill plants, mostly colonizing the roots and lower stem of susceptible plants even when introduced directly into stem wounds (Saile et al. 1997). A mutant lacking both endo- and exo-glucanase CWDE is significantly less virulent than wild type, but inactivation of the T2SS results in a mutant that is almost non-pathogenic on tomato plants and generally is unable to migrate out of roots to colonize the stem (Liu et al. 2005).

The confinement sensing system in *R. solanacearum* is a regulatory network that controls expression of many genes, including those for virulence and pathogenicity factors. Central to this system is PhcA, a global-acting LysR-type transcriptional regulator. PhcA positively regulates production of EPS, and the Egl endo-glucanase and Pme pectin methylesterase CWDE. It also

increases expression of *xpsR*, a intermediary regulator of the *eps* operon, competence for natural transformation by DNA, and the acyl-homoserine lactone mediated quorum-sensing system. PhcA negatively regulates production of PehA endo-polygalacturonase CWDE, staphyloferrin B siderophore, type IV pili (necessary for twitching motility, autoaggregation and biofilm formation), flagellar motility, salt tolerance, and activity of the HrpG transcriptional regulator (Denny 2006). PhcA function is controlled by a unique quorum-sensing system encoded by the products of the *phcBSR* operon. The confinement sensing system allows *R. solanacearum* to switch from one phenotypical state to another in response to nutrient availability and cell density (Denny 2006). At low cell densities the activity of PhcA also is low, which results in reduced expression of genes not required *in planta* and enhanced expression of genes that promote survival as a saprophyte. Expression of these genes is reversed at high cell densities when activity of PhcA increases, which enhances pathogenesis and colonization of plant tissues.

PhcA is not the only regulator of virulence, colonization and EPS production. In particular, the *vsrB/C* and *vsrA/D* two-component systems also play important roles. The *vsrA* and *vsrB* genes encode sensor kinases, and their corresponding response regulators are encoded by *vsrC* and *vsrD* (Schell et al. 1994; Huang et al. 1995). Inactivation of *vsrB* or *vsrC* reduces EPS production, because VsrC (along with XpsR) must bind to the *eps* promoter to induce transcription (Garg et al. 2000). Inactivation of either *vsrA* or *vsrD* reduces EPS production and also the ability to grow *in planta* but not in culture media (Schell et al. 1994). VsrD functions by working with PhcA to induce expression of *xpsR* (Huang et al. 1995). Constitutive expression of *xpsR* restores EPS production to a *vsrD* mutant, but not the ability to colonize tomato plants (McGarvey 1999a). This observation suggests that additional, as yet unidentified VsrD-regulated genes are required for wild type growth *in planta* and production of disease symptoms.

Production of the CbhA exo-glucanase CWDE is one factor that is positively regulated by VsrD (McGarvey and Schell, personal communication), whereas swimming motility is negatively regulated by VsrD (C. Allen, personal communication).

Modern proteomic techniques should help to elucidate the role of PhcA and VsrD in colonization of susceptible plants by identifying exoproteins made by the wild type but not by the mutants. In this study, we used a iTRAQ isobaric tag labeling, a technique that allows proteins to be identified and quantified at the same time by liquid chromatography-tandem mass spectrometry (LC-MS/MS) is. This approach revealed which extracellular proteins were over or under produced when mutants lacking the global regulator *phcA* or the two-component system *vsrD* genes were compared with the wild type. Similar to the better characterized PhcA regulon, the *vsrA/D* two-component system was found to be an important global regulator of many traits that are known or suspected to be involved in virulence and plant colonization.

Results

vsrD mutant confirmation and characterization

A *R. solanacearum* GMI1000 *vsrD* mutant was created by homologous recombination. As expected, the resulting mutant was EPS reduced, and it also exhibited greater swimming motility than its wild-type parent 48 hours after they were stabbed into motility media plates (Fig. 3.1). This mutant also was more twitching motile than the wild-type, a characteristic clearly observed on the surface of BG agar plates 12 to 24 hours after streaking (not shown). These characteristics agree with the phenotype exhibited by a *R. solanacearum* strain AW *vsrD* mutant that has reduced *eps* transcription and EPS production, as well being reduced virulence and colonization ability (Huang et al. 1995).

LC-MS/MS protein identification and quantification

One hundred and twenty-six proteins were identified using iTRAQ labeling and LC-MS/MS to examine exoproteins from the pairs GMI1390 (*vsrD)*/GMI1000 (wild type) and GMI1277 (*phcA)*/GMI1272 (*eps*). One hundred and ten proteins were identified in the *vsrD*/wild-type pair; 104 proteins were quantified and the ratio of relative abundance was statistically different from 1.0 for 58 of these proteins (Table 3.1, Fig 3.2). However, we used a 2-fold change in expression as the threshold for biological significance. Thirty-seven proteins were secreted in 2-fold greater quantity by the *vsrD* mutant, suggesting that VsrD negatively regulates these genes. Ten proteins were 10- to 70-fold more plentiful in the supernatant of the *vsrD* mutant. This group included the flagella components (FliC, FlgC, FlgM, FlgL, FlgB), two putative type IV fimbrial biogenesis proteins (PilY1-related), and a probable sulfate-binding precursor signal peptide protein (Sbp). Twenty-seven proteins were 2- to 10-fold more plentiful in the *vsrD* mutant, including two flagella components (FlgE, FlgF), a probable thiol:disulfide interchange signal peptide protein (DsbA1), a putative iron binding signal peptide, a probable hemagglutinin-related protein, a putative hemolysin-type protein (RSp0295) and two ABC transporter components. This group also included a probable lipoprotein, a probable serine protease, five probable transmembrane proteins, four probable signal peptides and three hypothetical proteins with unknown functions. The *vsrD* mutant also over produced by 2-fold CbhA, which exits via the T2SS, and by 3-fold PopF1, which exits via the Hrp type III secretion system (T3SS).

Positive regulation of *vsrD* was observed for the PehA endo-polygalacturonase and Tek, which exit via the T2SS, a putative aminopeptidase transmembrane protein, two probable signal peptide proteins. GMI1390 secreted significantly less of the pectinolytic enzymes Pme pectin methylesterase and PehB exo-polygalacturonase, but did not meet the two-fold threshold for

biological significance. Although not statistically significant, the Egl endo-glucanase, and TreA α, α-trehalase, which exit via the T2SS, were also reduced in comparison with the wild type.

Among the 81 proteins identified in the global regulator *phcA*/*eps* pair, 23 quantified proteins were statistically significant and met the 2-fold change for biological significance (Table 3.1, Fig 3.2). Seventeen proteins were more plentiful in the supernatant of the *phcA* mutant. Proteins over produced by 10-fold included PehA and PopF2. Fifteen proteins were over produced between 2- and 5.4-fold, including a PehC exo-polygalacturonase, two T3SS effectors (PopF1 and PopW), two flagella components (FlgG and FlgK) and two putative type IV fimbrial biogenesis proteins (PilY1-related). A putative antibiotic-hydrolase signal peptide protein, a putative trans-glycosylase protein, a putative transmembrane protein, a hypothetical protein and three probable signal peptide proteins also doubled in production. Six proteins were less plentiful in the supernatant of the *phcA* mutant (Table 3.1, Fig. 3.2): TreA, Pme, and a putative lipoprotein (RSc1878) were 4-fold decreased, and amounts of VirK, a putative hemolysin-type calcium binding protein (RSp0294) and a probable signal peptide protein (RSc0602) were reduced by half.

Twenty-two proteins quantified were common in the two pairs tested (Fig. 3.2). The two putative type IV fimbrial biogenesis proteins (PilY1-related), the T3SS protein PopF1 and a signal peptide protein (RSc0900) were >2-fold over produced by both GMI1390 and GMI1277. In contrast, a signal peptide protein (RSp0602) was produced in half the normal amount in both mutants. Only the PehA and a probable signal peptide protein (RSc0617) were over produced > 2-fold in the *phcA* mutant but reduced by half in the *vsrD* mutant (Table 3.1). No proteins were over produced by GMI1390 but under produced by GMI1277.

Discussion

A total of 126 *R. solanacearum* exoproteins were identified using iTRAQ labeling and LC-MS/MS. In the *vsrD*/wild-type pair, 104 proteins were quantified and 43 of them were differentially produced at statistically and biologically significant levels. Among the 77 proteins quantified in the *phcA*/*eps* pair, 23 were both statistically and biologically significant. These were much better results than we could have achieved using 2- dimensional polyacrylamide gel electrophoresis (2-D gels) in several ways. It was substantially faster to iTRAQ label and process a pair of samples for LC-MS/MS analysis than to run comparable samples on 2-D gels and prepare many protein spots for MS. LC-MS/MS analysis itself was also faster than MS analysis of many individual protein digests. More importantly, many more exoproteins were identified in our samples using the iTRAQ approach than on gels, which also reduced the cost per protein identified. In addition, iTRAQ labeling simultaneously provided quantitative relative ratios of protein abundance, which is impossible with standard 2-D gels. There are gel-based methods to quantitatively compare two samples (e.g., fluorescence 2-D difference gel electrophoresis), but they are not simple and require post-processing of individual protein spots to identify the differentially produced proteins.

iTRAQ labeling is a relatively new method than can reliably quantify the relative abundances of proteins in artificial mixtures with known ratios(Wiese et al. 2007). To evaluate whether this method was reliable with *R. solanacearum* exoproteins, our very first sample paired a *phcA* mutant with a wild type ($PhcA^+$, EPS^-) strain, because prior knowledge allowed us to predict many of the proteins that be differentially produced. For example, iTRAQ analysis showed that Pme protein was about 5-fold reduced in the *phcA* mutant compared to the observed 30-fold decrease in Pme enzyme activity seen previously in a K60 *phcA* mutant (Tans-Kersten et

al. 1998). Similarly, although the ratio was not statistically significant, iTRAQ found the Egl protein was about 10-fold reduced in the *phcA* mutant compared to the observed 20 to 50-fold decrease in Egl enzyme activity seen previously (Brumbley et al. 1993; Clough et al. 1997). Conversely, PehA activity increases in a *phcA* mutant between 2 and 3-fold (Tans-Kersten et al. 1998; Brumbley and Denny 1990), and we observed a 10-fold increase in PehA protein using iTRAQ. Although we could not predict their change, we also observed a small increase in PehC, but no change in PehB, by the *phcA* mutant. There was also a very large, although not statistically significant, decrease in ChbA production.

Given the hypermotile phenotype observed in a *phcA* mutant (Fig. 3.1) and the existing regulation model (Denny, 2006), we were happy to see that iTRAQ analysis detected an over production of flagella. The increase in two flagellar components was biologically significant, and although not statistically significant, five other Flg or Fli proteins increased > 2-fold. The 89-fold increase FliC, the major flagellin, may not have been statistically significant because there was too little of this protein in the wild type sample for comparison. Thus, the iTRAQ results are consistent with phcA cells being hyperflagellated and/or having shed flagella into the supernatant. Although flagellar swimming motility has an important role in invasion or infection of tomato roots (Tans-Kersten et al. 2001), over production of flagella could be detrimental. For instance, in *E. coli,* FliC over expression negatively affects attachment and biofilm formation in solid surfaces (Landini and Zehnder 2002)

Colonies of *phcA* mutants also remain twitching motile long after the confinement sensing system has turned off this and other negatively regulated traits in wild-type colonies (Kang et al. 2002). iTRAQ analysis detected significant over production of two PilY1 proteins and a slight increase in PilA pilin protein. Reports in *Neisseria meningitidis* indicate that PilC

(PilY1) upregulation is required during the initial localized adhesion process, but the maintenance of *pilC1 (pilY1)* expression in adhering bacteria leads to the persistence of abundant tfp expression that prevents pilus retraction. Downregulation of *pilC* transcription is required to allow efficient PilT-driven retraction(Morand et al. 2004). Retraction of type IV pili mediates intimate attachment to and signaling in host cells, surface motility, biofilm formation, natural transformation(Aukema et al. 2005). Based on observations of hyper twitching motility on solid media and strong virulence reduction, we supposed that inability to have pilus retraction is the reason to have this effect.

Genin et al. (2005) found that PhcA negatively regulates the T3SS, repressing the *hrp* genes at high cell density when PhcA is activated. The PhcA-dependent repression of *hrp* genes is best observed during growth in complex nitrogen sources and probably occurs by controlling the activity of HrpG. Therefore, the T3SS should be more active at low cell density or in a *phcA* mutant. As expected, our iTRAQ analysis detected almost 2- to 10-fold over production of the known T3SS PopB, PopF1, PopF2, and PopW. The overproduction of PopF1 and F2 is particularly interesting, because these proteins are about 50% homologous to HrpF, which in *Xanthomonas campestris* pv. vesicatoria appears to play a role at the bacteria-plant interface by mediating effector protein delivery across the host cell membrane (Buttner et al. 2002). Contrary to expectations, iTRAQ analysis detected a decrease in HrpY protein, which is the main constituent of the Hrp pilus through which the other Hrp effectors move on their way to host cells.

In summary, because the results of iTRAQ analysis correlated well with known phenotypic changes of *phcA* mutants, we conclude that it is a reliable method for analyzing *R. solanacearum* exoproteins. It is evident that PhcA controls production of numerous additional

exoproteins besides CWDEs, and resulted in a more detailed model of functions regulated by PhcA (Fig. 3.4). Given that a mutant lacking all six CWDE remains colonization proficient (Liu et al. 2005), even though reduced in virulence, it seems likely that it is these other traits regulated by PhcA that contribute to the greatly reduced virulence and colonization ability of a *phcA* mutant.

The two-component regulatory system *vsrA/vsrD* controls genes associated with EPS production and bacterial growth *in planta*, negatively and positively regulate production of some exoproteins (Huang et al. 1995). iTRAQ analysis correctly identified many traits regulated by the VsrA/VsrD system. Even more than PhcA, VsrD negatively regulated many proteins in flagella biosynthesis (i.e., up to 70-fold changes in FliC, FlgC, FlgM, FlgL, FlgB, FlgE and FlgF were statistically and biologically significant, but those in FliD, FliK, FlgK and FlgG were not), which correlated with the *vsrD* mutant being even more motile than the *phcA* mutant (Fig. 3.1). Not surprisingly, given its enhanced twitching motility, the *vsrD* mutant also over produced the same two PilY1-related proteins negatively regulated by PhcA. However, the *vsrD* mutation had relatively little effect on production of the T3SS effectors. Unexpectedly, our iTRAQ results indicated that CbhA production is negatively regulated by this two-component system in GMI1000, contrary to what was observed in strain AW (McGarvey and Schell, personal communication). Although it is possible the iTRAQ data are incorrect, these differences could also be due to experimental factors such as strain, culture stage and culture medium. Initial reports used a *R. solanacearum* AW *vsrA* mutant grown to stationary phase in rich medium in contrast with our GMI100 *vsrD* mutant grown to late logarithmic phase in minimal medium. Further research is required to confirm the role of this system in *cbhA* regulation.

Other proteins negatively regulated by VsrA/D included a probable sulfate-binding precursor signal peptide protein and a probable thiol:disulfide interchange signal peptide protein (DsbA1), this protein is involved in folding of membrane or secreted proteins as well as expression of the T3SS and twitching motility (Sinha et al. 2004). This role is supported by the involvement of *Pseudomonas aeruginosa* DsbA in protein folding, intracellular survival, expression of the T3SS and twitching motility (Ha et al. 2003). Although this protein was over produced in the *vsrA/D* mutant we do not have enough evidence to include this protein as responsible for colonization deficiency. Other negatively regulated proteins include a probable hemagglutinin-related protein that has been suggested to be important for adhesion to plant surfaces and host specificity (Guidot et al. 2007).

T2SS candidates positively regulated by VsrD between 2- and 4-fold included PehA, Tek, and two probable signal peptide proteins. Pme and PehB were statistically significant but did not meet the two-fold threshold for biological significance. Although not statistically significant, Egl and TreA were also reduced in comparison with the wild type. As for a *phcA* mutant, these changes in CWDE cannot alone account for the reduced ability of *vsrA*/*D* mutants to multiply in planta. On the other hand, we found 4 putative proteins with a signal peptide that could be T2SS candidates were increased in *vsrD* mutant. The role of these and other proteins in colonization remain unclear.

This study successfully implemented the use of iTRAQ and LC-MS/MS to identify and quantify PhcA and VsrD regulated exoproteins. This method identified new proteins in these regulatory pathways, generating a more detailed model supported by quantitative data (Fig. 3.4). Our results show that the regulon controlled by VsrA/D is larger than previously envisioned, and this two-component system could be a global regulator as important as PhcA. Although we

identified a large number of exoproteins that directly or indirectly might contribute to colonization, more work is required to determine which are functional. We realize, however, that our efforts focused on the identification of exoproteins affected by VsrA/D and PhcA, but these global regulators presumably also control production of may cell-associated proteins that also could affect the pathogen's ability to colonize plants.

Materials and methods

Bacterial strains and gene targets

Existing strains GMI1000 (wild type, race 1, biovar 3, phylotype I, Tfp^+ Twt^+ Pil^+ HR^+), GMI1272 (GMI1000 *epsB*::pCR2.1, EPS^-, Km^r) and GMI1277 (GMI1000 *phcA*::Ω, PC-type, Sp^r) were used in this study. *R. solanacearum* mutants and *E. coli* DH5α (Invitrogen) strains with the plasmids carrying the deletion alleles were stored at -80^{o}C after PCR and restriction enzyme digestion confirmation. Swimming motility was tested in media containing 1% tryptone and 0.3% agar. Media and growth conditions, DNA manipulation and transformation, PCR conditions protein precipitation, protein identification using iTRAQ and LC-MS/MS are described in Chapter 2.

Marked mutant creation

A *vsrD* mutant was created by site-specific, marked mutagenesis. A 303-bp internal fragment of *vsrD* was amplified using primers *vsrD*-forward (5'-GGAATTCGCGCTTGGAC-3') and *vsrD*-reverse (5'-ACATCTCCATGCCCGACC-3'). The resulting fragment was gel purified (Qiagen), ligated to pCR2.1 (Invitrogen), and the mixture used to transform *E. coli* DH5α. Selected kanamycin-resistant colonies were confirmed to carry the *vsrD* fragment by PCR, and one clone with pCR2.1::*vsrD*' was retained. *R. solanacearum* GMI1000 competent cells were transformed

with pCR2.1::*vsrD*' DNA by electroporation, and a resulting EPS-deficient, kanamycin-resistant colony was retained as GMI1390 (GMI1000 *vsrD*::pCR2.1, Km^r).

References

Aukema, K. G., Kron, E. M., Herdendorf, T. J., and Forest, K. T. 2005. Functional dissection of a conserved motif within the pilus retraction protein PilT. J. Bacteriol. 187:611-618.

Brumbley, S. M., Carney, B. F., and Denny, T. P. 1993. Phenotype conversion in *Pseudomonas solanacearum* due to spontaneous inactivation of PhcA, a putative LysR transcriptional activator. J. Bacteriol. 175:5477-5487.

Brumbley, S. M., and Denny, T. P. 1990. Cloning of *phcA* from wild-type *Pseudomonas solanacearum*, a gene that when mutated alters expression of multiple traits that contribute to virulence. J. Bacteriol. 172:5677-5685.

Buttner, D., Nennstiel, D., Klusener, B., and Bonas, U. 2002. Functional Analysis of HrpF, a Putative Type III Translocon Protein from *Xanthomonas campestris* pv. vesicatoria. J. Bacteriol. 184:2389-2398.

Clough, S. J., Flavier, A. B., Schell, M. A., and Denny, T. P. 1997. Differential expression of virulence genes and motility in *Ralstonia* (*Pseudomonas*) *solanacearum* during exponential growth. Appl. Environ. Microbiol. 63:844-850.

Denny, T. P. 2006. Plant pathogenic *Ralstonia* species. Pages 573-644 in: Plant-Associated Bacteria. S. S. Gnanamanickam, ed. Springer, Dordrecht, The Netherlands.

Garg, R. P., Huang, J., Yindeeyoungyeon, W., Denny, T. P., and Schell, M. A. 2000. Multicomponent transcriptional regulation at the complex promoter of the exopolysaccharide I biosynthetic operon of *Ralstonia solanacearum*. J. Bacteriol. 182:6659-6666.

Genin, S., Brito, B., Denny, T. P., and Boucher, C. 2005. Control of the *Ralstonia solanacearum* type III secretion system (Hrp) genes by the global virulence regulator PhcA. FEBS Lett. 579:2077-2081.

Guidot, A., Prior, P., Schoenfeld, J., Carrere, S., Genin, S., and Boucher, C. 2007. Genomic structure and phylogeny of the plant pathogen *Ralstonia solanacearum* inferred from gene distribution analysis. J. Bacteriol. 189:377-387.

Ha, U.-H., Wang, Y., and Jin, S. 2003. DsbA of *Pseudomonas aeruginosa* is essential for multiple virulence factors. Infection. Immunity 71:1590-1595.

Huang, J., Carney, B. F., Denny, T. P., Weissinger, A. K., and Schell, M. A. 1995. A complex network regulates expression of *eps* and other virulence genes of *Pseudomonas solanacearum*. J. Bacteriol. 177:1259-1267.

Kang, Y., Liu, H., Genin, S., Schell, M. A., and Denny, T. P. 2002. *Ralstonia solanacearum* requires type 4 pili to adhere to multiple surfaces, and for natural transformation and virulence. Mol. Microbiol. 46:427-437.

Landini, P., and Zehnder, A. J. B. 2002. The global regulatory *hns* gene negatively affects adhesion to solid surfaces by anaerobically grown *Escherichia coli* by modulating expression of flagellar genes and lipopolysaccharide production. J. Bacteriol. 184:1522-1529.

Liu, H., Zhang, S., Schell, M. A., and Denny, T. P. 2005. Pyramiding unmarked mutations in *Ralstonia solanacearum* shows that secreted proteins in addition to plant cell wall degrading enzymes contribute to virulence. Mol. Plant-Microbe Interact. 18:1296-1305.

McGarvey, J. A. (1999). In vivo and in vitro growth and virulence factor production by *Ralstonia solanacearum*. (Abstract)

Morand, P. C., Bille, E., Morelle, S., Eugène, E., Beretti, J.-L., Wolfang, M., Meyer, T. F., Koomey, M., and Nassif, X. 2004. Type IV pilus retraction in pathogenic *Neisseria* is regulated by the PilC proteins. EMBO J. 23:2009-2017.

Saile, E., Schell, M. A., and Denny, T. P. 1997. Role of extracellular polysaccharide and endoglucanase in root invasion and colonization of tomato plants by *Ralstonia solanacearum*. Phytopathology 87:1264-1271.

Schell, M. A., Denny, T. P., and Huang, J. 1994. VsrA, a second two-component system regulating virulence genes of *Pseudomonas solanacearum*. Mol. Microbiol. 11:489-500.

Sinha, S., Langford, P. R., and Kroll, J. S. 2004. Functional diversity of three different DsbA proteins from *Neisseria meningitidis*. Microbiology 150:2993-3000.

Tans-Kersten, J., Guan, Y. F., and Allen, C. 1998. *Ralstonia solanacearum* pectin methylesterase is required for growth on methylated pectin but not for bacterial wilt virulence. Appl. Environ. Microbiol. 64:4918-4923.

Tans-Kersten, J., Huang, H. Y., and Allen, C. 2001. *Ralstonia solanacearum* needs motility for invasive virulence on tomato. J. Bacteriol. 183:3597-3605.

Vasse, J., Frey, P., and Trigalet, A. 1995. Microscopic studies of intercellular infection and protoxylem invasion of tomato roots by *Pseudomonas solanacearum*. Mol. Plant-Microbe Interact. 8:241-251.

Wiese, S., Reidegeld, K. A., Meyer, H. E., and Warscheid, B. 2007. Protein labeling by iTRAQ: A new tool for quantitative mass spectrometry in proteome research. Proteomics 7:340-350.

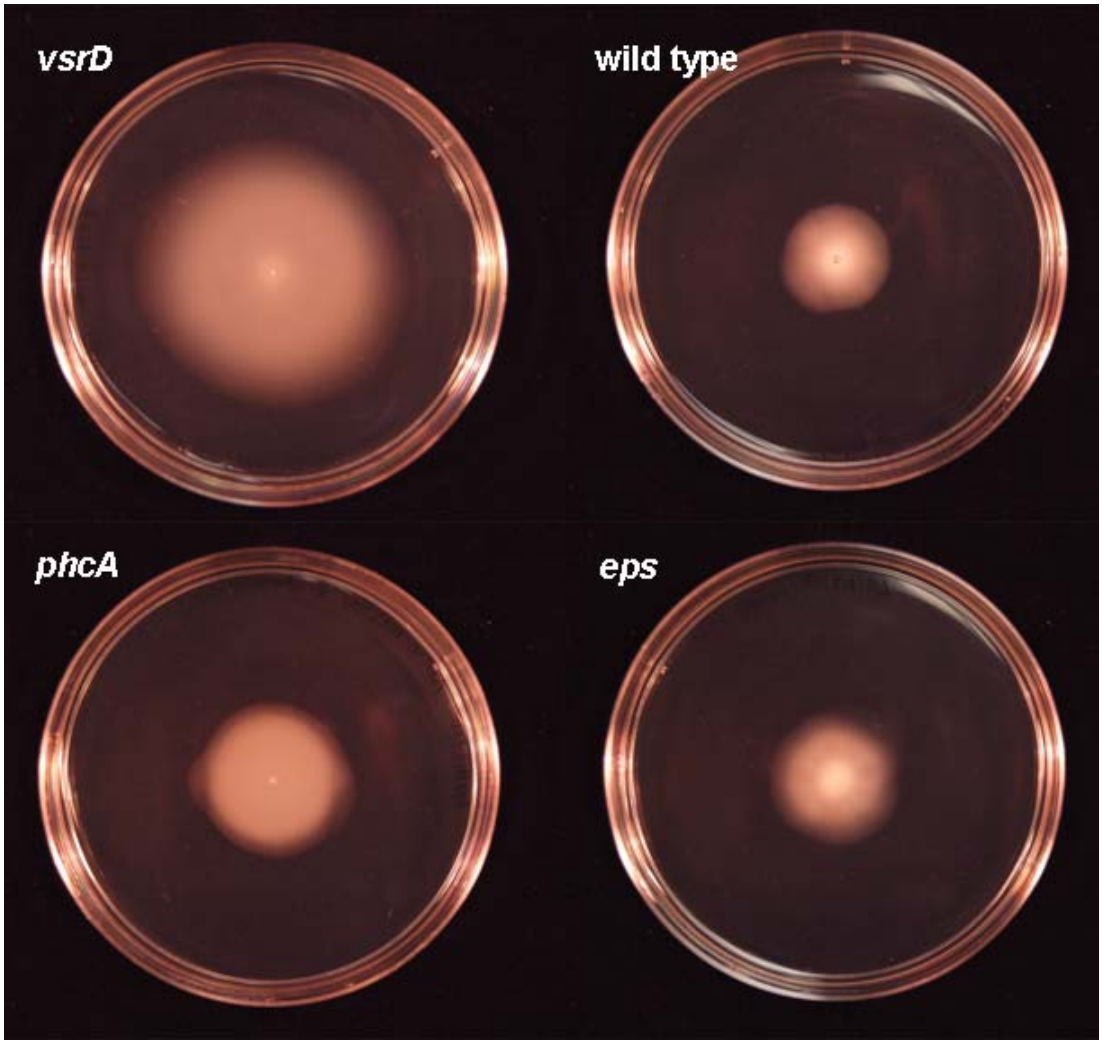

Fig. 3.1. Swimming motility of wild-type GMI1000 and its *vsrD, phcA* and *eps* mutants.

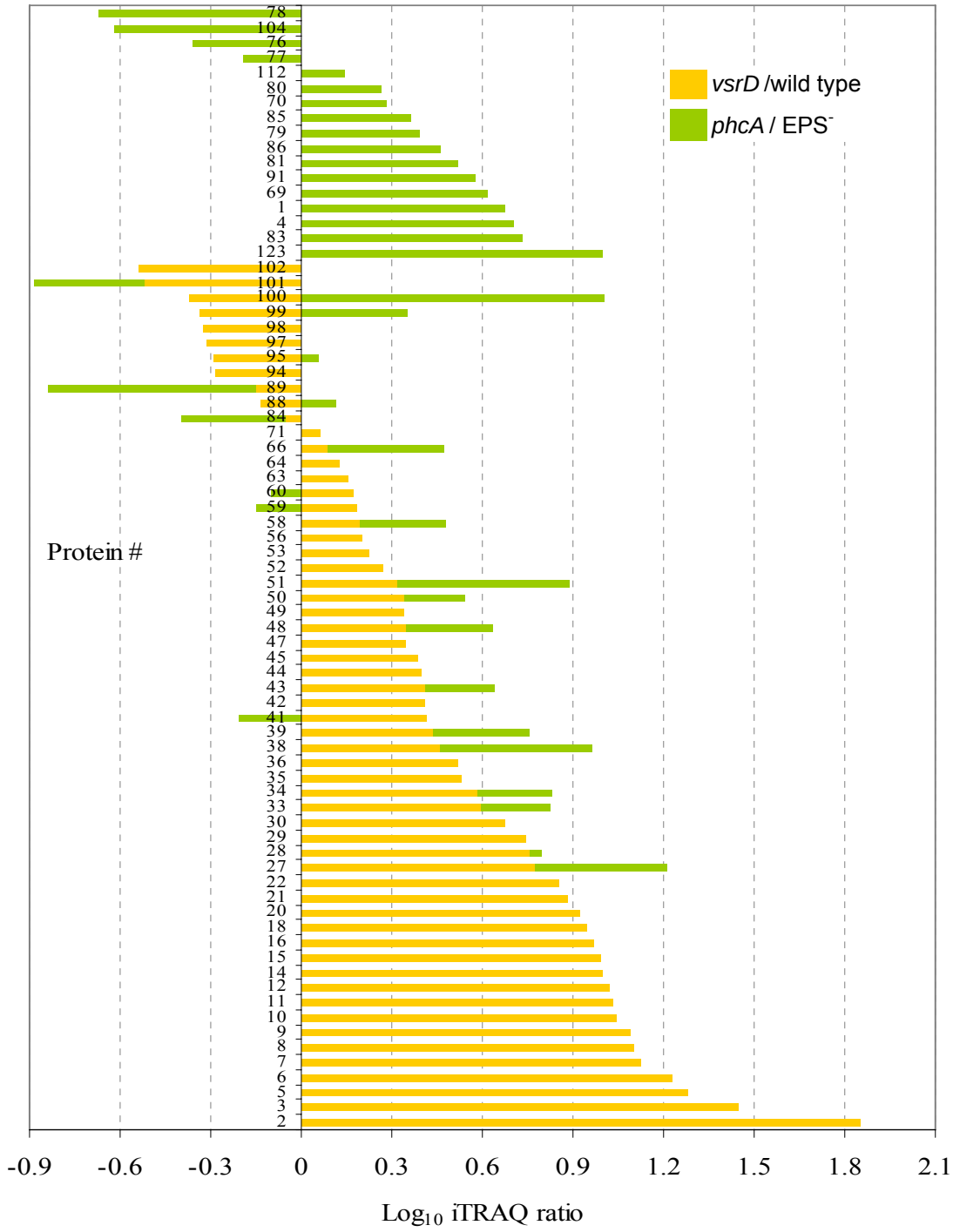

Fig. 3.2. Protein production ratio in GMI1390 (*vsrD)*/GMI1000 (wild type) and GMI1277 (*phcA)*/GMI1272 (*eps*) pairs. An iTRAQ ratio of $Log_{10} \pm 0.3$ indicates a 2-fold increase or decrease in protein production. Proteins and ratio data are listed in Table 3.1.

GMI1390 (*vsrD*)/GMI1000 (wild type

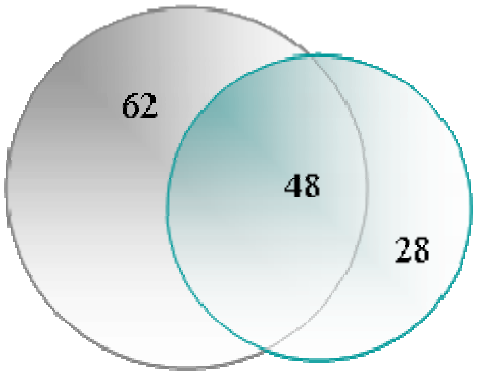

GMI1277 (*phcA*)/GMI1272 (*eps*)

Fig 3.3. Venn diagram of proteins identified using iTRAQ labeling and LC-MS/MS in comparisons of GMI1390 (*vsrD)*/GMI1000 (wild type) and GMI1277 (*phcA)*/GMI1272 (*eps*).

Table 3.1. Proteins identified using iTRAQ labeling and LC-MS/MS in comparisons of GMI1390 (*vsrD)*/GMI1000 (wild type) and GMI1277 (*phcA)*/GMI1272 (*eps*).

#	Gene	Locus tag	Protein identified	Relative ratio[a]	
				vsrD/ wt	*phcA*/ *eps*
1	*flgK*	RSp0351	Flagellar hook-associated protein	81.8225	4.7591
2	*fliC*	RSp0382	Flagellin protein	70.7893	88.989
3	*flgC*	RSp0343	Probable flagellar basal-body rod protein	28.0166	
4	*flgG*	RSp0347	Probable flagellar basal-body rod protein	20.8944	5.0789
5	*flgM*	RSp0340	Probable negative regulator of flagellin synthesis	19.0102	
6	*flgL*	RSp0352	Probable flagellar hook-associated protein 3	16.9451	2.9444
7	*flgB*	RSp0342	Probable flagellar basal-body rod protein	13.2471	
8		RSc2353	Probable signal peptide protein	12.6005	
9		RSc0293	Hypothetical signal peptide protein	12.2542	
10		RSp1415	Hypothetical protein	11.0742	
11	*sbp*	RSc1336	Probable sulfate-binding precursor signal peptide protein	10.7432	2.4901
12	*flgE*	RSp0345	Flagellar hook protein	10.4776	3.3122
13		RSc3342	Putative substrate-binding ABC transporter protein	10.1999	
14		RSc2937	Putative iron-binding signal peptide	9.8929	
15	*dsbA1*	RSc0285	Probable thiol:disulfide interchange	9.8438	

#	Gene	Locus tag	Protein identified	Relative ratio[a]	
				vsrD/ wt	*phcA*/ *eps*
			signal peptide protein		
16	*flgF*	RSp0346	Probable flagellar basal-body rod protein	9.3105	2.6696
17		RSc3300	Putative amino-acid transport signal peptide protein	9.0274	
18		RSc2257	Probable amino-acid-binding ABC transporter protein	8.8461	
19	*copC*	RSp0658	Probable copper resistance c signal peptide protein	8.4334	1.669
20		RSc3386	Putative signal peptide protein	8.394	
21	*PBPb*	RSc0481	Probable amino-acid-binding (pbp) ABC transporter protein	7.6392	
22		RSp1073	Probable hemagglutinin-related protein	7.1177	0.4311
23		RSp1137	Putative Rhs-related transmembrane protein	6.8048	
24	*fliD*	RSp0383	Probable flagellar hook-associated protein 2	6.1	2.5371
25		RSp0808	Probable hemagglutinin-related transmembrane protein	6.0282	
26	*fliK*	RSp0395	Probable flagellar hook-length control protein	6.0135	
27		RSc2675	Putative type 4 fimbrial biogenesis	5.9487	2.7242

#	Gene	Locus tag	Protein identified	Relative ratio[a]	
				vsrD/ wt	*phcA*/ *eps*
			PilY1-related protein signal peptide		
28		RSp0295	Putative hemolysin-type protein	5.7072	1.1001
29		RSc2958	Probable signal peptide protein	5.5662	
30		RSp1139	Probable Vgr-related protein	4.7561	0.2252
31	*dnaK*	RSc2635	Probable heat shock protein 70 (hsp70) chaperone	4.4905	
32	*hcp*	RSp0745	Hemolysin corregulated protein	3.9696	0.0017
33		RSc3051	Hypothetical signal peptide protein	3.9366	1.7078
34		RSc2241	Conserved hypothetical protein	3.8106	1.7754
35		RSc2494	Hypothetical signal peptide protein	3.3853	
36		RSc2654	Probable serine protease protein	3.2933	
37		RSp0572	Hypothetical protein	3.2066	
38	*popF1*	RSp1555	Secreted protein PopF1	2.909	3.1414
39		RSc0900	Probable signal peptide protein	2.7606	2.0676
40		RSc0902	Probable signal peptide protein	2.6351	
41		RSp0275	Probable hydrolase transmembrane protein	2.6017	0.6224
42		RSc2380	Probable transmembrane protein	2.5778	
43		RSc0532	Hypothetical transmembrane protein	2.5645	1.7069
44		RSp0732	Putative transmembrane protein	2.4916	
45		RSp0261	Putative transmembrane protein	2.4233	

#	Gene	Locus tag	Protein identified	Relative ratio[a]	
				vsrD/ wt	*phcA*/ *eps*
46		RSc2470	Probable Rhs-related protein	2.2397	0.0692
47		RSp0178	Hypothetical protein	2.229	
48		RSc0152	Probable lipoprotein	2.2067	1.9633
49	*cbhA*	RSp0583	Exoglucanase A (1,4-β-cellobiosidase)	2.1975	0.0028
50		RSp0758	Hypothetical protein	2.1963	1.5865
51		RSc0724	Putative type-4 fimbrial biogenesis PilY1-related signal peptide protein	2.067	3.729
52		RSc2495	Hypothetical hydrolase protein	1.8592	1.3017
53		RSc1357	Gala protein 5	1.6699	1.0445
54		RSp1071	Putative hemagglutinin-related protein	1.6659	
55		RSc3290	Conserved hypothetical protein	1.5949	
56		RSp0780	Hypothetical protein	1.5944	0.0618
57		RSc0254	Hypothetical transmembrane protein	1.5905	
58		RSc3091	Probable outer membrane porin signal peptide protein	1.5701	1.9135
59	*hrpY*	RSp0855	Hrp pilus subunit HrpY protein	1.5351	0.7069
60		RSc2653	Putative protease signal peptide protein	1.482	0.7998
61		RSp1130	Hypothetical protein	1.4757	
62		RSc1334	Probable D-3-hydroxy butyrate oligomer hydrolase lipoprotein transmembrane	1.4652	1.8273
63		RSc1475	Probable transmembrane protein	1.4321	1.6547

#	Gene	Locus tag	Protein identified	Relative ratio[a]	
				vsrD/ wt	*phcA*/ *eps*
64	*aac*	RSc2547	Probable aculeacin A acylase transmembrane protein	1.3378	0.8956
65	*popA*	RSp0877	PopA protein	1.2548	2.0401
66		RSc3101	Putative serine protease protein	1.2269	2.415
67	*popC*	RSp0875	PopC protein	1.2188	
68	*popP2*	RSc0868	Probable YopP/AvrRxv family protein	1.2173	
69		RSp0881	Putative transmembrane protein	1.1977	4.1167
70		RSc2933	Putative porin signal peptide protein	1.1816	1.9286
71		RSc2180	Putative transmembrane protein	1.1535	
72		RSp0603	Putative serine protease protein	1.1532	0.9306
73		RSc0769	Putative hydrolase glycosidase protein	1.1274	0.9252
74	*avrA*	RSc0608	AvrA protein	1.0917	
75	*popP1*	RSc0826	PopP1 protein	1.0719	
76		RSp0294	Putative hemolysin-type calcium-binding protein	1.0526	0.4405
77		RSp1610	Hypothetical protein	1.0422	0.642
78		RSc1878	Putative lipoprotein	1.0395	0.2141
79		RSp1240	Putative transglycosylase protein	1.0181	2.467
80	*popB*	RSp0876	PopB protein	1.0059	1.8425
81		RSc3155	Putative antibiotic hydrolase signal peptide protein	1.0027	3.2927

#	Gene	Locus tag	Protein identified	Relative ratio[a]	
				vsrD/ wt	*phcA*/ *eps*
82		RSp0304	Probable AvrPphD-related protein	0.9508	
83	*popW*	RSc2775	Probable harpin-related protein	0.902	5.4063
84	*virK*	RSc2285	Putative signal peptide protein	0.8831	0.4551
85	*pehC*	RSp0833	Exo-polygalacturonase	0.8713	2.3188
86		RSp1466	Probable signal peptide protein	0.8554	2.881
87		RSp0028	Probable gala protein	0.7558	
88		RSp1461	Probable signal peptide protein	0.7396	1.3056
89	*pme*	RSp0138	Pectin methylesterase protein	0.7083	0.2049
90		RSc0336	Probable signal peptide protein	0.6755	0.0755
91		RSc0616	Hypothetical protein	0.6672	3.7628
92		RSp0879	Hypothetical protein	0.6449	
93		RSp0845	Hypothetical protein	0.5491	
94		RSp0161	Putative transmembrane protein	0.5215	0.9598
95	*pehB*	RSc1756	Exo-polygalacturonase	0.5143	1.1488
96	*pilA*	RSc0558	Type 4 fimbrial pilin	0.5112	1.3828
97		RSp1526	Hypothetical protein	0.4891	0.0497
98		RSp0532	Putative aminopeptidase transmembrane protein	0.4736	0.0256
99		RSc0617	Probable signal peptide protein	0.4606	2.2535
100	*pehA*	RSp0880	Endo-polygalacturonase	0.4291	10.0478
101		RSp0602	Probable signal peptide protein	0.3045	0.4293

#	Gene	Locus tag	Protein identified	Relative ratio[a]	
				vsrD/ wt	*phcA*/ *eps*
102	*tek*	RSp1002	Tek signal peptide protein	0.2899	0.022
103	*egl*	RSp0162	Endoglucanase (endo-1,4-β-glucanase)	0.1938	0.1187
104	*treA*	RSp0277	α, α-trehalase signal peptide protein	0.0156	0.2425
105		RSc0019	Hypothetical protein		0.2055
106		RSc0818	Putative endoglucanase protein		0.2009
107		RSc1003	Probable carboxypeptidase protein		
108	*ppiA*	RSc1165	Probable peptidyl-prolyl cis-trans isomerase A signal peptide protein		
109	*ugpB*	RSc1264	Probable glycerol-3-phosphate-binding lipoprotein signal peptide		
110		RSc1740	Hypothetical signal peptide protein		
111		RSc2238	Probable transmembrane protein		3.2728
112		RSc2441	Putative amino acid-binding ABC transporter protein		1.3899
113		RSc2452	Putative endonuclease protein		1.7684
114		RSc2601	Hypothetical protein		1.0134
115		RSc2718	Probable signal peptide protein		
116		RSc2855	Putative outer membrane porin signal peptide protein		1.1074
117	*tuf*	RSc3041	Probable elongation factor Tu		
118		RSc3272	Hypothetical protein		1.3841

#	Gene	Locus tag	Protein identified	Relative ratio[a]	
				vsrD/ wt	*phcA*/ *eps*
119		RSc3430	Putative Vgr-related protein		0.0004
120	*flgJ*	RSp0350	Probable flagellar protein		
121	*copA*	RSp0656	Probable copper resistance transmembrane protein		2.1756
122		RSp0693	Hypothetical protein		2.0084
123	*popF2*	RSp0900	Secreted protein PopF2		10.0044
124	*tek2*	RSp1000	Probable Tek-related protein		
125		RSp1212	Hypothetical protein		
126		RSp1673	Hypothetical lipoprotein transmembrane		

[a] Ratios are not bias corrected. Yellow cells indicate values with Pval <0.05 and an error factor (EF) <2. Empty cells indicate proteins not identified in the pair tested. Gray cells indicate proteins identified but not quantified.

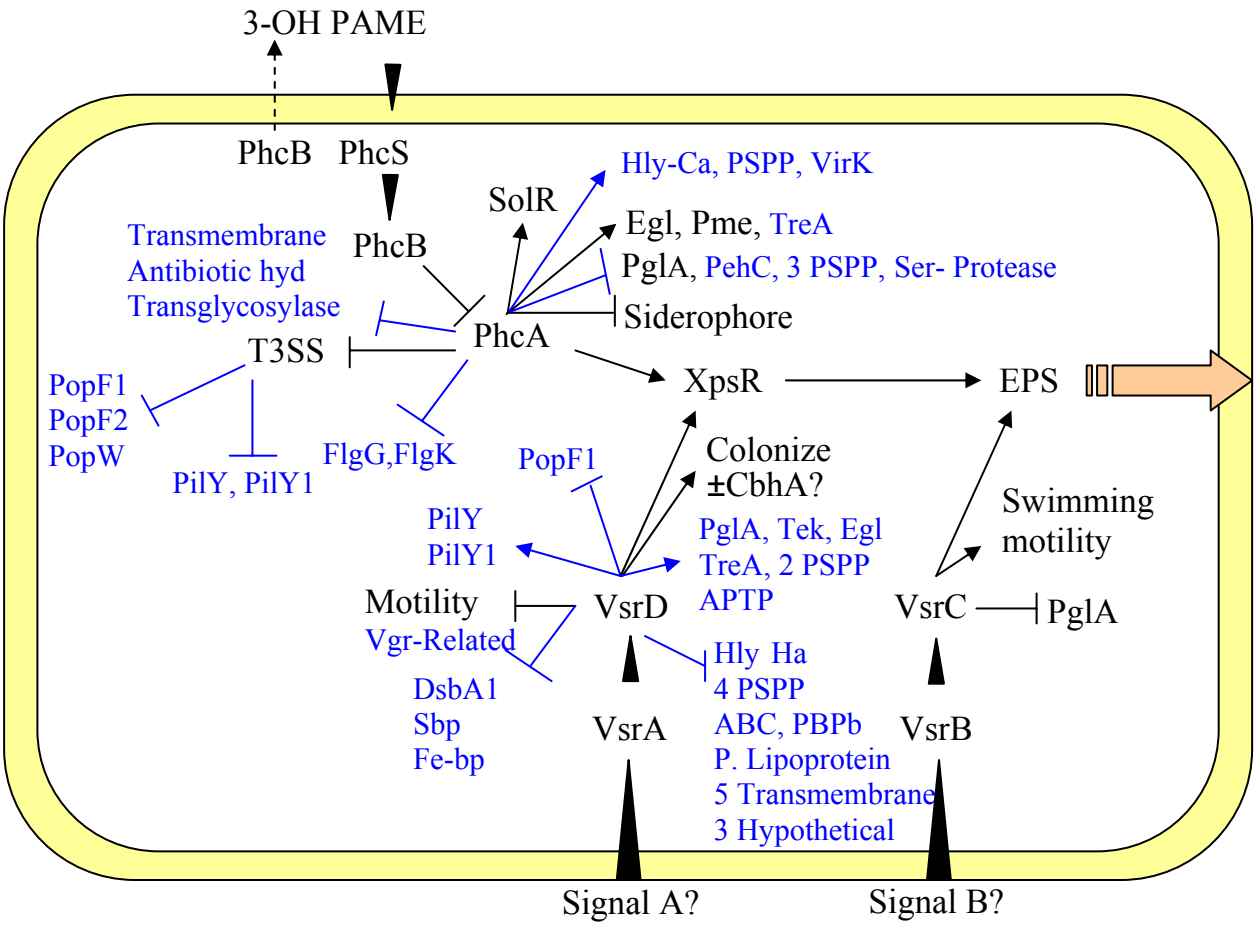

Fig 3.4. Regulatory pathway model based on iTRAQ LC-MS/MS information.

PSPP, probable signal peptide protein
Hly, putative hemolysin-type protein
Ha, probable hemagglutinin-related protein
Sbp, probable sulfate binding precursor signal peptide protein
Fe-bp, putative iron-binding signal peptide
DsbA1, probable thiol:disulfide interchange signal peptide protein
APTP, putative aminopeptidase transmembrane protein
PBPb, probable amino-acid-binding ABC transporter protein

CHAPTER 4

CONCLUSIONS

The role of the *Ralstonia solanacearum* type II secretion system (T2SS) in producing extracellular plant cell wall degrading enzymes (CWDEs) and in virulence has been recognized using different genetic techniques, such pyramidal gene mutagenesis, allowed the exploration of its components. This has led to a better understanding of the function of these virulence factors and to the conclusion that other proteins secreted by the type II system are important for systemic colonization of tomato plants.

The first objective of this project was to identify the exoproteins secreted through the conserved T2SS and possibly through the three alternative T2SS present in strain GMI1000. I first created mutants lacking either the primary SdpD1 secretin or one of the three SdpD-like proteins. I also made a mutant lacking all three SdpD-like proteins and one lacking all four SdpD proteins. The sdpD1 mutant could not make the secretin pore in the outer membrane, but should have retained functionality of "core" components of the conserved T2SS, which might be used by the SdpD-like proteins to secrete some proteins. As in previous reports where "core" genes essential for T2SS function were inactivated (Kang et al. 1994; Liu et al. 2005), I found that the sdpD1 deletion mutant secreted many fewer proteins in culture and was severely defective in its ability to colonized tomato plants and cause disease. Consequently, it seems that SdpD1 is required for functionality of the principle T2SS and that the SdpD-like proteins cannot replace it.

By using proteomic techniques, such as 2-dimensional polyacrylamide (2-D PAGE) and iTRAQ labeling combined with mass spectrometry, I identified a total of 126 proteins. Of these, 44 proteins were probably secreted by the T2SS based on quantitative information on their relative abundance in wild type and T2SS mutants. No other bacterium has been reported to have this many type II-secreted proteins. Some of the additional exoproteins were probably secreted by type I or type III systems, but other proteins presumably reached the supernatant due to cell

leakage or lysis. I found that 2-D PAGE was more time consuming and identified many fewer proteins than did iTRAQ labeling. Image analysis of 2-D gels of various *sdpD* mutants revealed visual differences between mutants, but it was difficult to identity of the proteins.

I could not confirm the functionality of the alternative T2SS using iTRAQ, because an unexpectedly low number of proteins was identified in the samples analyzed and none of the proteins exceeded the 2-fold change threshold necessary for biological significance. However, it is still possible that SdpD3 is functional, based on this mutant's slightly reduced symptom production in virulence assays. This aspect requires more exploration though iTRAQ labeling and more virulence assays.

The second objective of this project was to identify the exoproteins associated with colonization that are regulated by PhcA and VsrD, components of the *R. solanacearum* phenotype conversion system. I first used iTRAQ labeling and mass spectrometry to identify and quantify proteins regulated by the global regulator PhcA, and the results were in almost total agreement with predicted changes based on years of previous work with *phcA* mutants (Denny 2006). Therefore, I concluded that the iTRAQ technique reliably reports relative protein abundance for *R. solanacearum* exoproteins. I also found that VsrD regulates as many virulence and colonization traits as PhcA. Similar to PhcA, VsrD negatively regulated at least 10 proteins associated with swimming and twitching motility. Unlike PhcA, VsrD did not have an effect on secretion of type III effector proteins. I also found some proteins (especially CbhA) that did not change as predicted, but this discrepancy could be due to differences in the strain, the culture medium, or the culture stage used during protein production. To date this is the most complete information about protein regulation in the phenotype conversion system in *R. solanacearum* and provides new insights into this regulatory pathway.

References

Denny, T. P. 2006. Plant pathogenic *Ralstonia* species. Pages 573-644 in: Plant-Associated Bacteria. S. S. Gnanamanickam, ed. Springer, Dordrecht, The Netherlands.

Kang, Y., Huang, J. Z., Mao, G. Z., He, L. Y., and Schell, M. A. 1994. Dramatically reduced virulence of mutants of *Pseudomonas solanacearum* defective in export of extracellular proteins across the outer membrane. Mol. Plant-Microbe Interact. 7:370-377.

Liu, H., Zhang, S., Schell, M. A., and Denny, T. P. 2005. Pyramiding unmarked mutations in *Ralstonia solanacearum* shows that secreted proteins in addition to plant cell wall degrading enzymes contribute to virulence. Mol. Plant-Microbe Interact. 18:1296-1305.

APPENDIX

APPENDIX 1. Natural color images of 2-D gels.

GMI1000. pI 3-11NL; 10% SDS-PAGE; run 06-22-05

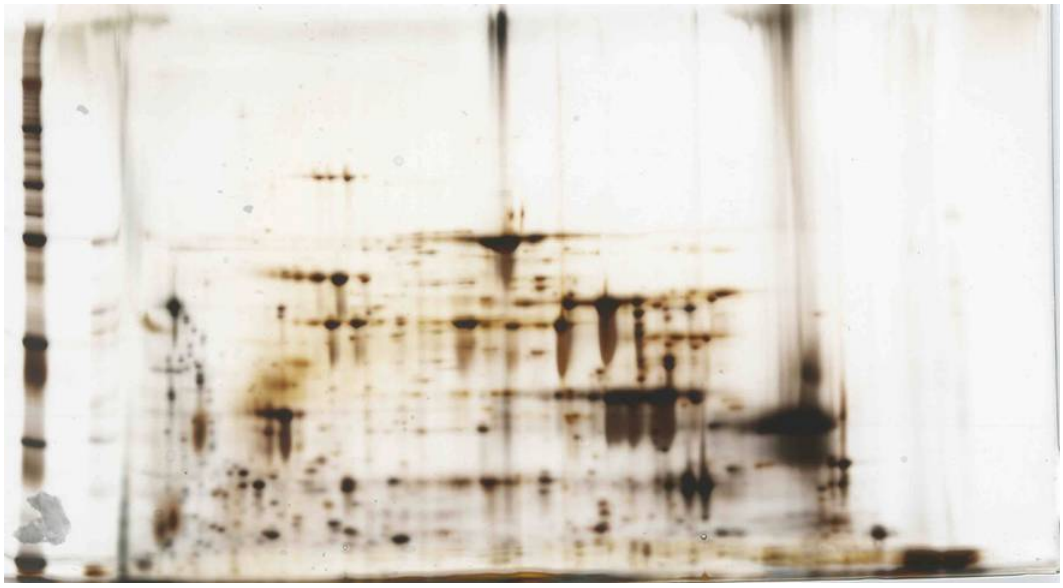

GMI1000. pI 3-11NL; 10% SDS-PAGE; run 06-24-05:

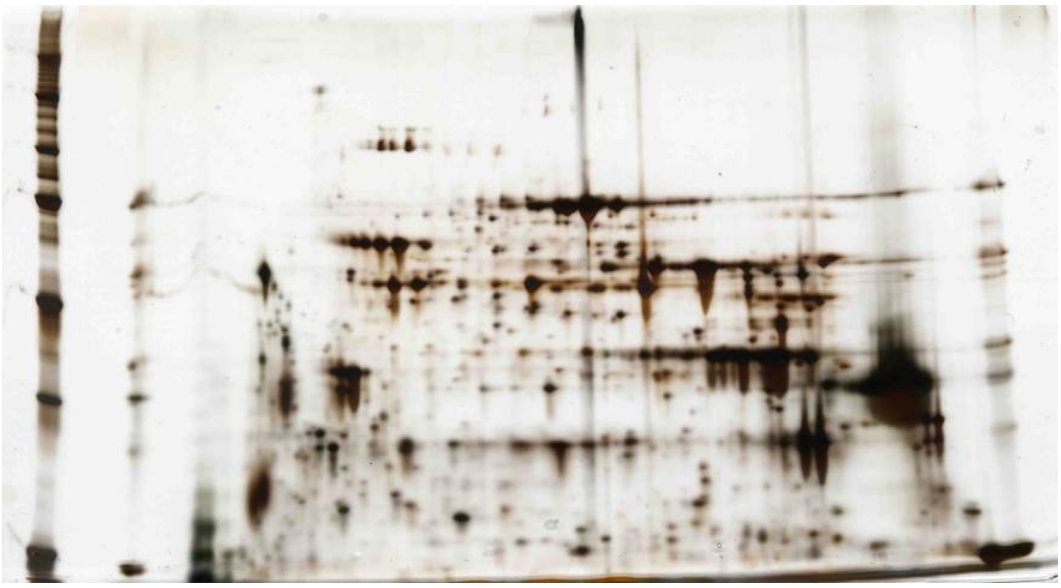

GMI1000. pI 3-10NL; 10% SDS-PAGE; run 06-27-05:

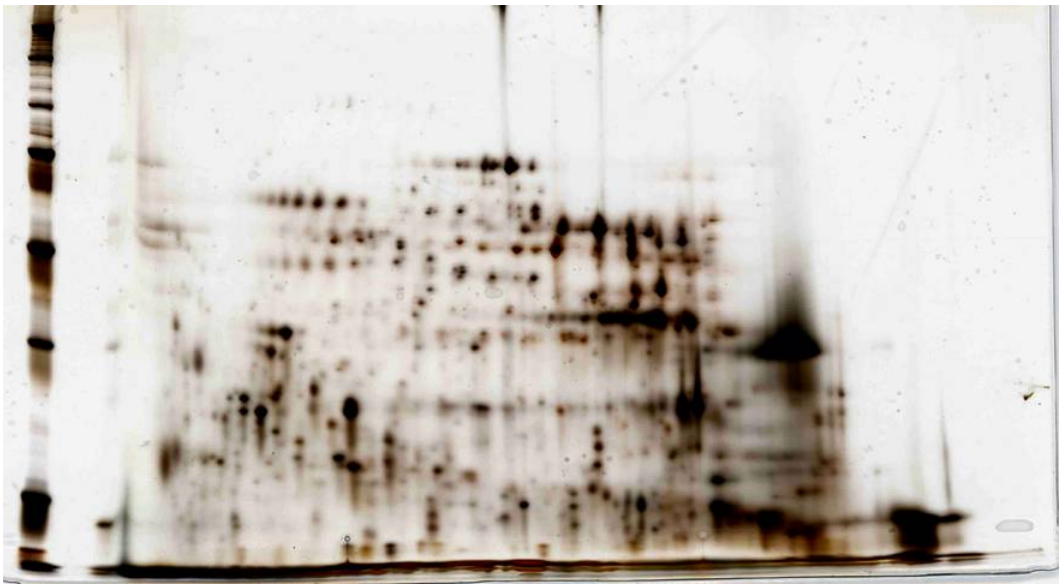

GMI1000. pI 3-10NL; 10% SDS-PAGE; run 09-02-05

GMI1266 (*sdp*D1'). pI 3-10NL; 10% SDS-PAGE; run 07-07-05

GMI1266 (*sdp*D1'). pI 3-10NL; 10% SDS-PAGE; run 06-14-05; Fig. 2.5.

GMI1266 (*sdp*D1'). pI 3-11NL; 10% SDS-PAGE; run 03-06-06

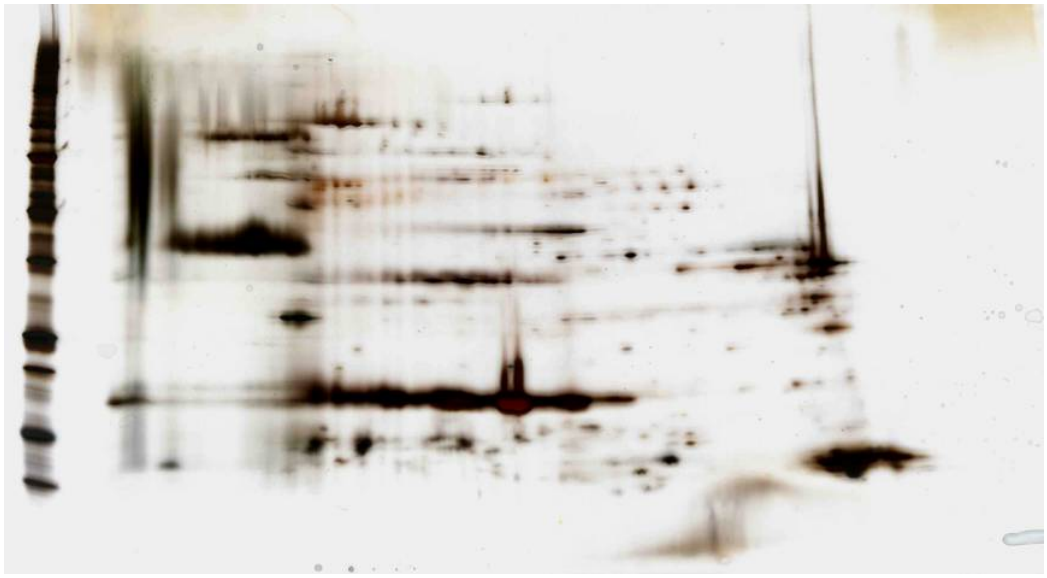

GMI1266 (*sdp*D1'). pI 3-11 NL; 10-20% SDS-PAGE; run 04-20-06

GMI1266 (*sdp*D1'). pI 3-11 NL; 10-20% SDS-PAGE; run 06-29-06

GMI1266 (*sdp*D1'). pI 3-11 NL; 10-20% SDS-PAGE; run 08-14-06; Fig. 2.5, 26 and 2.7.

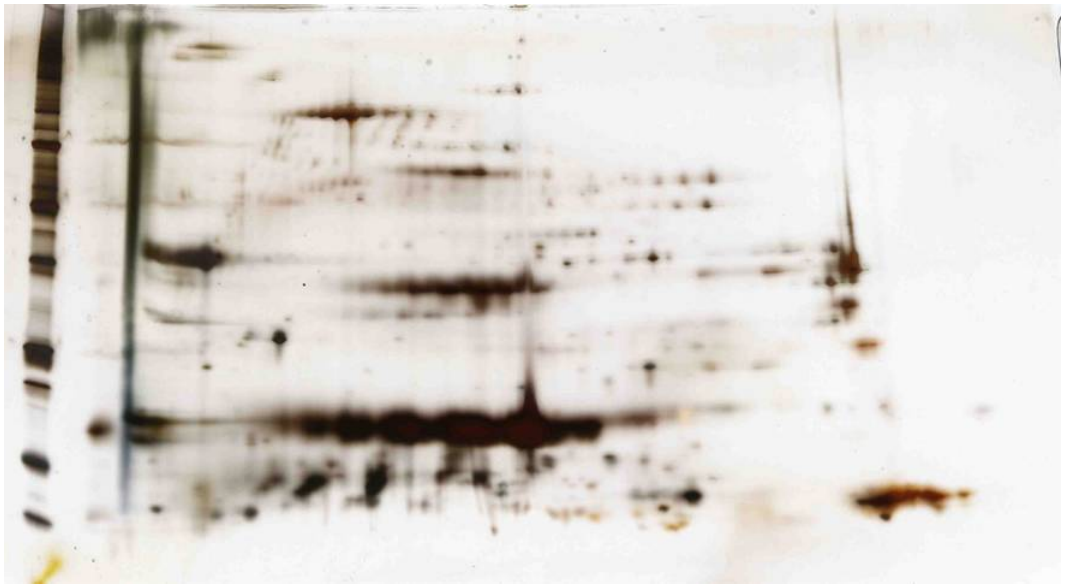

GMI1415 (Δ *sdp*D1). pI 3-11 NL; 10-20% SDS-PAGE; run 01-18-07; Fig. 2.6, 2.8 and 2.9.

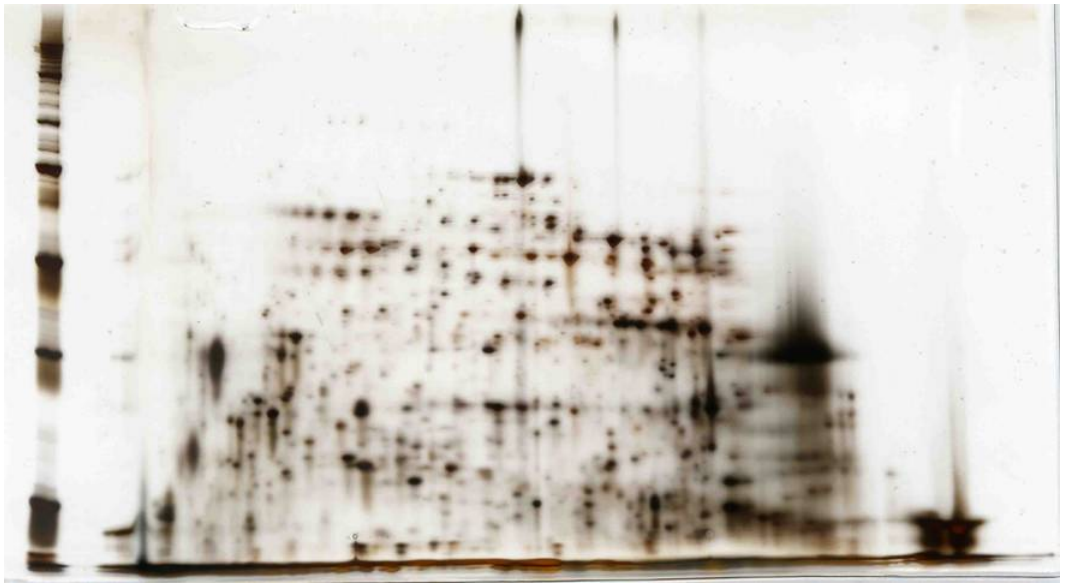

GMI1367 (Δ *sdp*D2). pI 3-10 NL; 10% SDS-PAGE; run 09-01-05

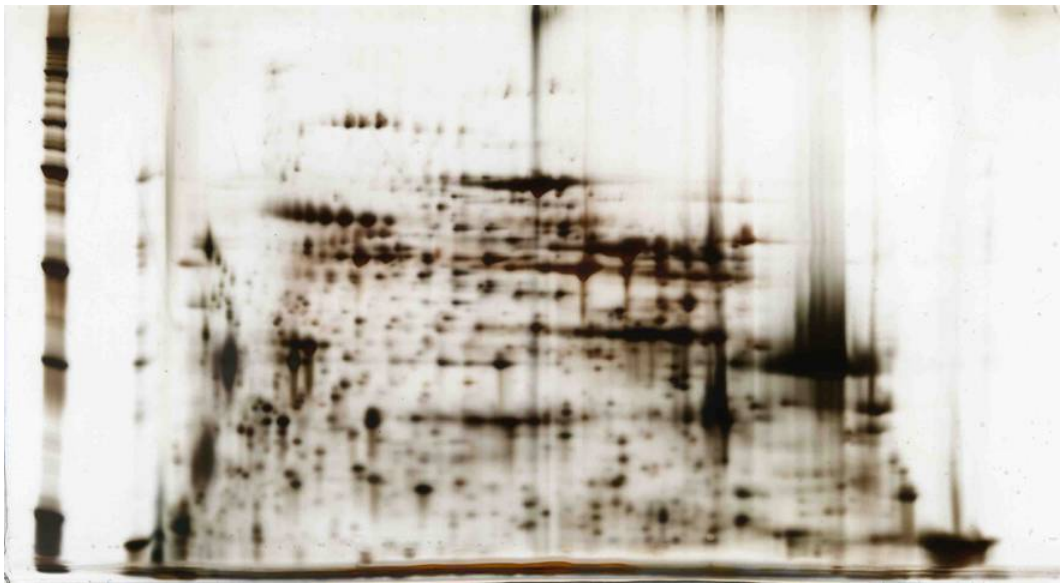

GMI1369 (Δ *sdp*D3). pI 3-10 NL;10% SDS-PAGE; run 09-06-05

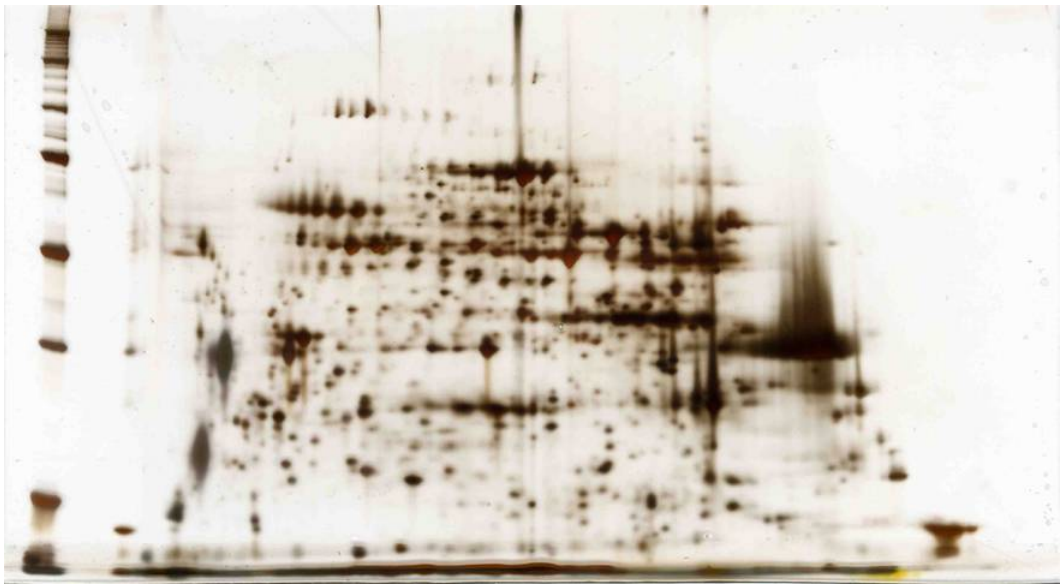

GMI1370 (Δ *sdp*D4). pI 3-10 NL; 10% SDS-PAGE; run 09-06-05

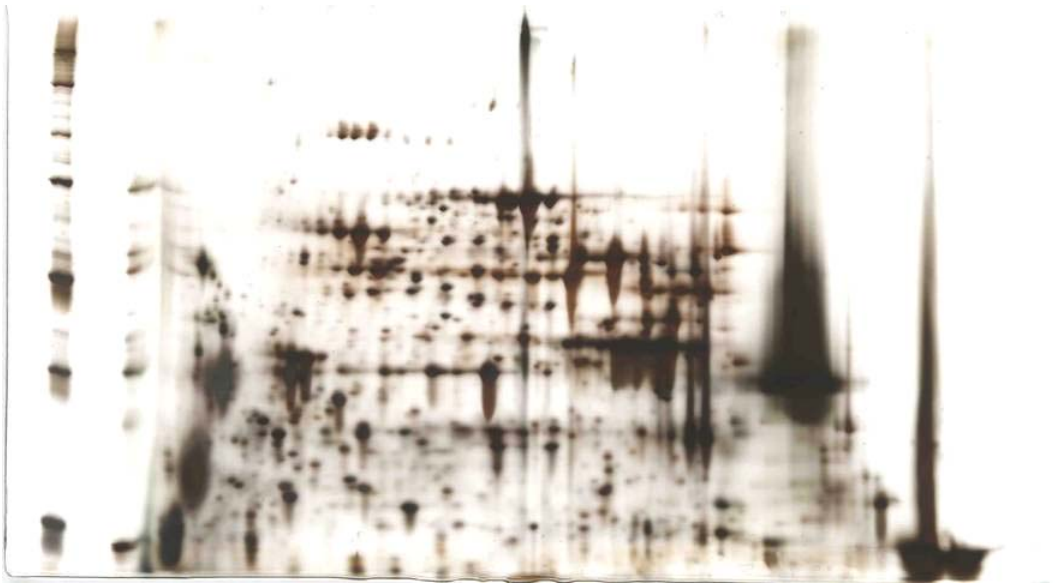

GMI1374 (Δ *sdp*D2-3-4). pI 3-11 NL; 10% SDS-PAGE; run 11-17-05

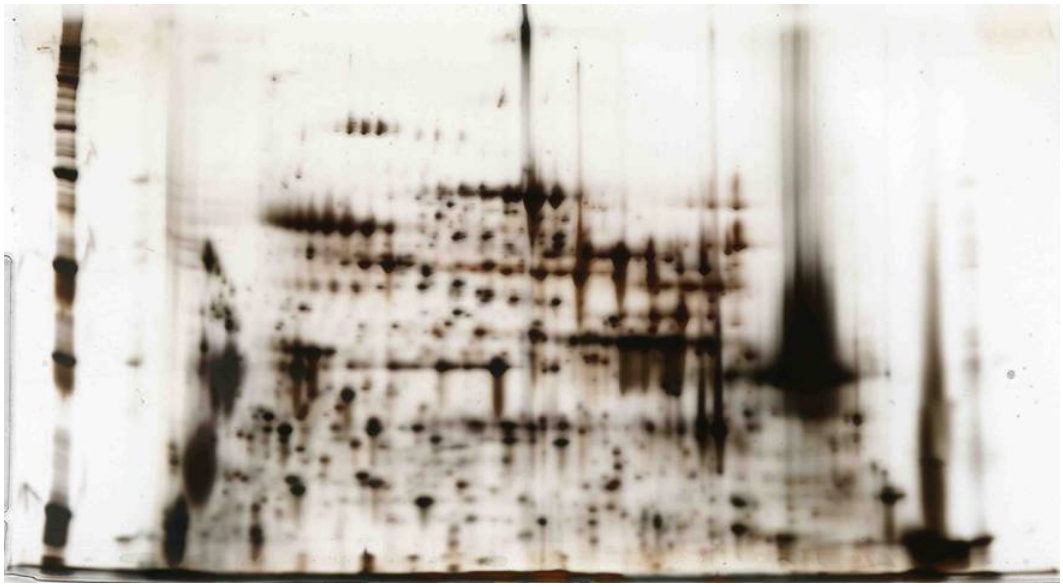

GMI1374 (Δ *sdp*D2-3-4). pI 3-11 NL; 10% SDS-PAGE; run 12-01-05

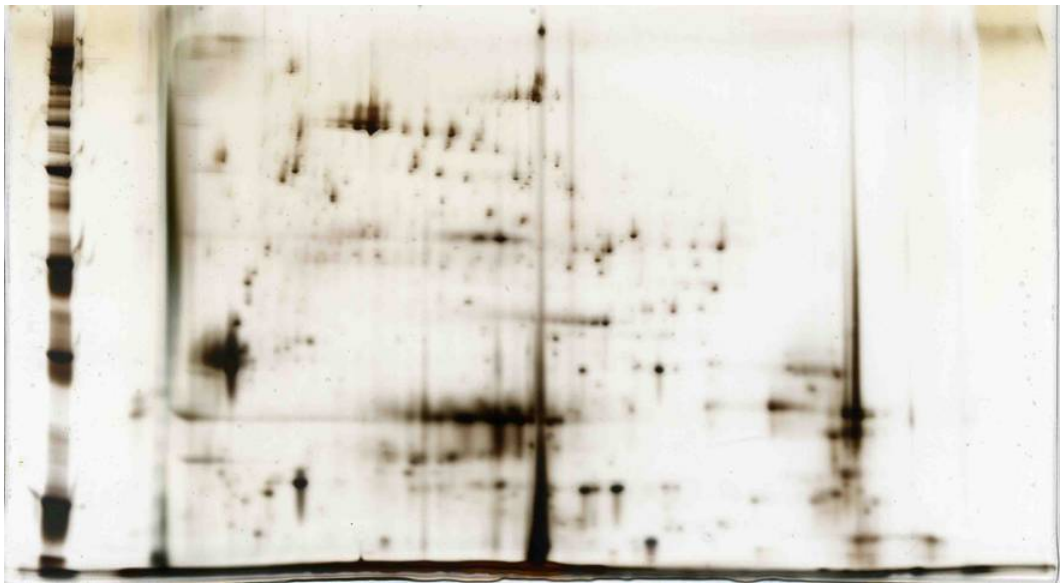

GMI1388 (4x*sdpD*'). pI 3-11 NL; 10% SDS-PAGE; run 12-01-06; Fig. 2.5.

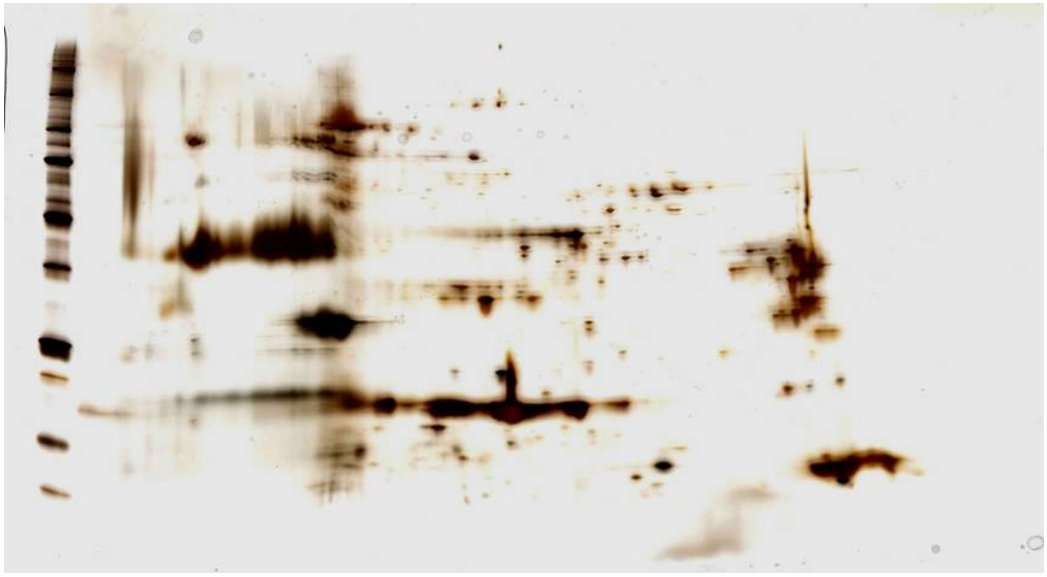

GMI1388 (4x*sdpD*'). pI 3-11 NL; 10-20% SDS-PAGE; run 04-20-06

GMI1388 (4x*sdpD*'). pI 3-11 NL; 10-20% SDS-PAGE; run 06-29-06

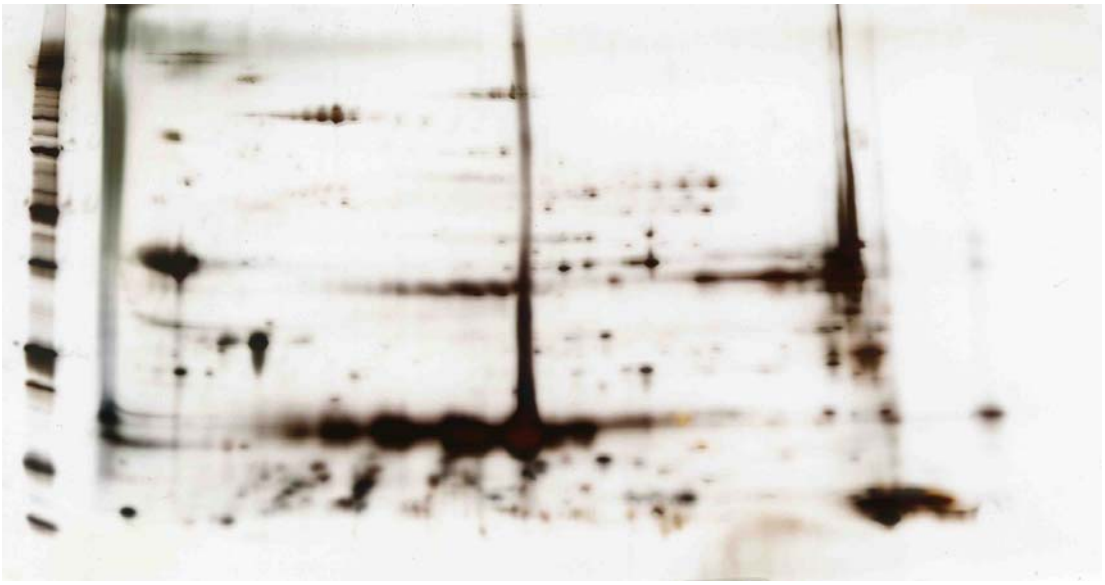

GMI1388 (4x*sdpD*'). pI 3-11 NL; 10-20% SDS-PAGE; run 01-24-07; Fig. 2.5, 2.9 and 2.10.

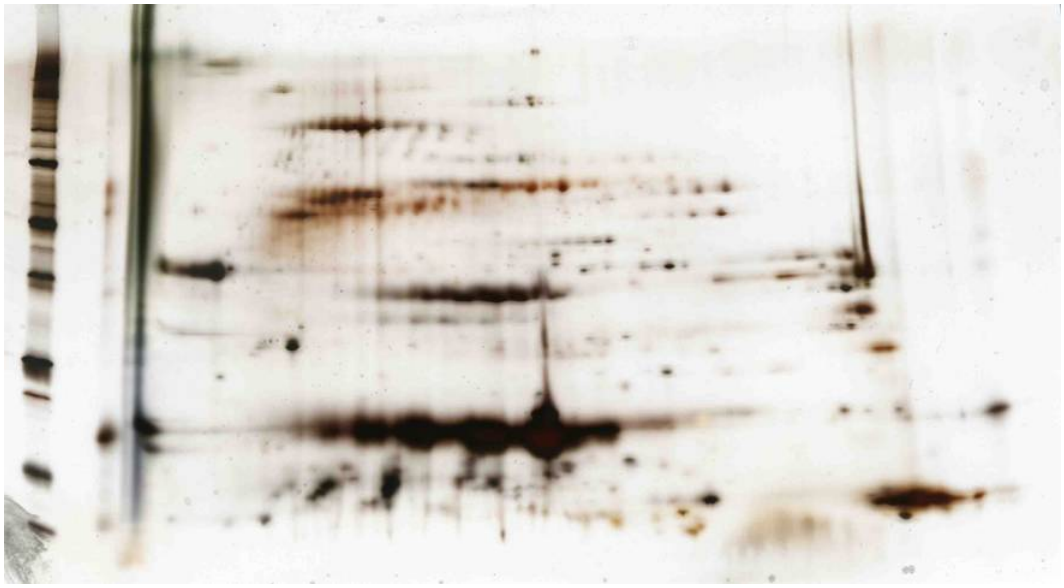

GMI1423 (4x*sdpD*). pI 3-11 NL and 10-20% SDS-PAGE; run 01-18-07; Fig. 2.7, 2.8 and 2.10.

GMI1272 (EPS^-). pI 3-11 NL; 10% SDS-PAGE; run 03-28-06

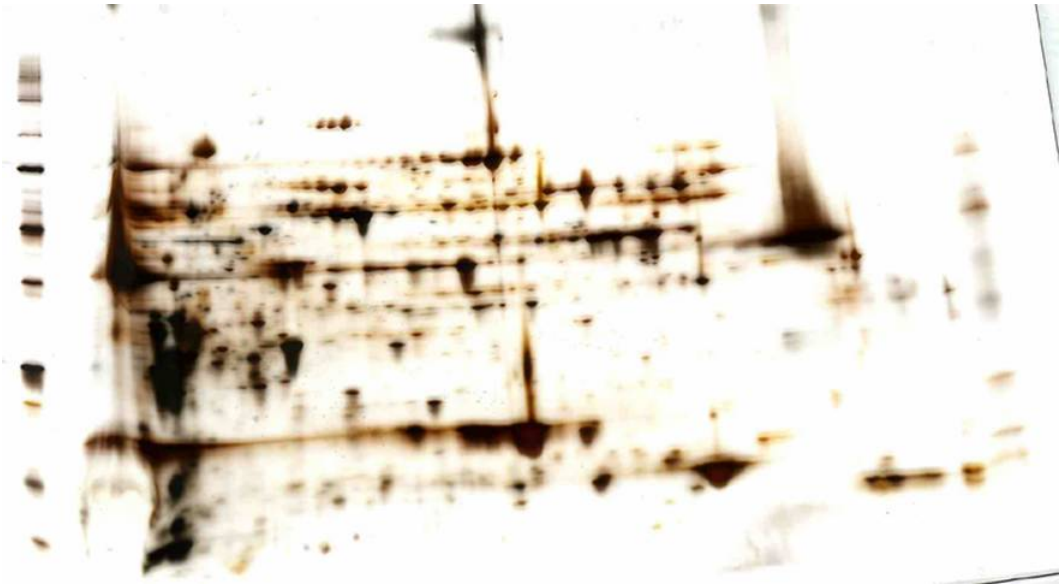

GMI1272 (EPS$^-$). pI 3-11 NL; 10-20% SDS-PAGE; run 08-14-06

GMI1277 (*phcA*). pI 3-11 NL; 10% SDS-PAGE; run 03-07-06

GMI1277 (*phcA*). pI 3-11 NL; 10% SDS-PAGE; run 03-28-06

GMI1277 (*phcA*). pI 3-11 NL; 10-20% SDS-PAGE; run 09-21-06

GMI1390 (*vsrD*). pI 3-11 NL; 10% SDS-PAGE; run 04-28-06